CFD BASED SIMULATION AND ANALYSIS OF TAR-GAS CRACKING IN A PACKED BED REACTOR

By

SANDEEPAN GOSWAMI

R70209021/500007417

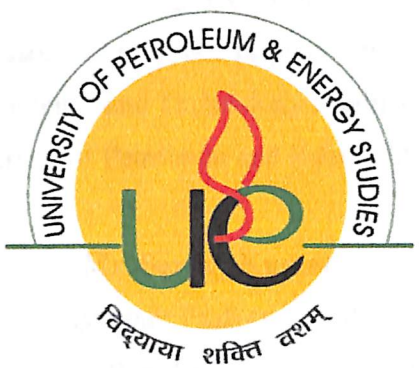

College of Engineering

University of Petroleum & Energy Studies

Dehradun

May, 2011

"CFD Based Simulation And Analysis Of Tar-Gas Cracking In A Packed Bed Reactor"

A thesis submitted in partial fulfillment of the requirements for the award of the degree of Master of Technology in Process Design Engineering

By

Sandeepan Goswami

(R1670209021/500007417)

Under the guidance of

Dr. Ugur Guven

Professor of Aerospace Engineering (P.hD)

Nuclear Science and Technology Engineer (M.Sc)

University of Petroleum and Energy Studies.

Mr. Sanjay Kumar

Assistant Professor (SS)

University of Petroleum and Energy Studies

Approved

Dean

College of Engineering Studies

University of Petroleum and Energy Studies

Dehradun

May, 2011

CERTIFICATE

This is to certify that the thesis entitled "**CFD Based Simulation And Analysis Of Tar-Gas Cracking In A Packed Bed Reactor**" submitted by Mr. Sandeepan Goswami (Roll no: R670209021, SAP-id: 500007417) to College of Engineering Studies, University of Petroleum and Energy studies, Dehradun in partial fulfillment of the requirements for the award of the degree of Master of Technology in Process Design Engineering is an authentic work carried under our supervision and guidance.

To the best of our knowledge, the matter embodied in the thesis has not been submitted to any other University/Institute for the award of any Degree/Diploma.

Dr. Ugur Guven
Professor
Aerospace Engineer (P.hD)
Nuclear Technology Specialist (M.Sc)
University of Petroleum and Energy Studies
Dehradun.

Mr. Sanjay Kumar
Asst. Professor (SS)
University of Petroleum and Energy Studies
Dehradun.

ACKNOWLEDGEMENT

In pursuit of this academic endeavor, I feel I have been singularly fortunate; inspiration, direction, guidance, co-operation, love and care all came in my way in abundance and it seems almost an impossible task for me to acknowledge the same in adequate terms. Yes, I shall be failing in my duty if I do not record my profound sense of indebtedness and heartfelt gratitude to my supervisors **Dr. Ugur Guven** (Aerospace Engineer / Nuclear Technology Specialist (PhD), COES, UPES) and **Mr. Sanjay Kumar** (Asst. Professor (SS), COES, UPES) who guided and inspired me in pursuance of this work. Their association will always remain a beacon of light to me throughout my career.

I owe a depth of gratitude to **Dr. Vasudev Singh**, HOD Department of Chemical Engineering and Dean **Dr. Srihari**, COES, UPES. I am thankful to **Dr. Alok Saxena** for acting as project coordinator and his valuable suggestions.

I would like to thank the entire faculty of Chemical engineering for their continuous support through the course work. I want to acknowledge the support of all the staff members of Chemical Engineering UPES, Dehradun and graduating and under graduates' students of Aerospace department for allowing to supervise their CFD related projects which in return helped me gain better understanding of CFD.

I thank to encouragement, support and best wishes of my parents and family members without which this thesis would never have been completed.

Last but not the least; I would like to thank **Mr. Bill Gates** and **Microsoft Corporation** for inventing this wonderful tool "MS-Office" without which this thesis would never had a "wordly" existence.

Sandeepan Goswami

CHAPTER 01. ABSTRACT

Biomass is in trend now-a-days as an alternate energy source because of reduced CO_2 emissions, abundance and cost effectivity. Gasification of biomass is the first activity done in order to obtain bio-syn-gas, which is processed downstream to produce motor fuels, but the products from biomass gasifier contain tar. The work presented here is concerned to tar and its removal by means of cracking to improve carbon conversion efficiency. Volatiles obtained from biomass gasification require further processing to justify biomass usage as an alternate; it is then, when tar comes to picture. Processes downstream to gasification use catalysts like Fischer- Tropsch process, in such processes tar poisons the catalysts, i.e., the carbon blocks the active sites in the catalysts. Also tar in raw gas causes corrosion and blockage in pipes. So, tar removal is of prime interest and it done by means of two processes thermal cracking and catalytic cracking.

The work presented here is analysis of tar cracking using CFD, i.e., to analyze the hydrodynamics along with chemical kinetics in a packed bed reactor. The analysis is done in 2D as well as 3D. The 2D model is simple model with consideration of a single homogeneous phase of gas and catalysts. The reactor has dimensions of 12" X 2" with a mass flow rate of 0.138e-04 kg/s (5 mg min^{-1}). The analysis of 2D model was done to get a proper hydrodynamic and reaction profile occurring inside the reactor. On validation of the trends in the 2D model the input conditions were applied on the 3D model. In the 3D model two separate phases' gas and solid were considered so as to obtain correct trends of hydrodynamics and reaction profile. A simple first order reaction was taken into consideration but it was an overall reaction. The activation energy and rate exponent was used in accordance with literature (Rath et al, 2001). The reactor is 6" long and 2" diameter and the catalysts used in the study are spherical dolomite particles of 0.5inch diameter and are stacked in structured manner.

The vital factor in the study was tar characterization. As we know that tar is a complex mixture of PAH's (Polycyclic Aromatic Hydrocarbons) and consists of numerous compounds. In this study model compound toluene C_6H_5-CH_3 was used in feed either than actual tar. Moreover, in the exit stream products with maximum concentration were accounted for as Fluent Solver requires detailed chemical kinetics along with balanced chemical reactions for apt results. The feed was fed at 700^0C (923.15 K). The reaction taking place is an endothermic reaction. Products obtained are CO_2, CO, H_2, H_2O and CH_4.

Analysis in 3D was done at steady state to understand the effect of rate exponent (n) on the reaction kinetics as well as on hydrodynamics. Finally, contour plots for pressure, temperature distribution, and mass fraction of components engaged in the reaction and velocity vectors were plotted.

Work cited here is a nascent one, flaws may be embedded in the system but the study was focused to analyze the affect of reaction on hydrodynamics in packed bed reactor. Simplicity in - design and parameters fed to Fluent solver, was done to make the work feasible in all possible manners and minimize errors in the output.

It is tried that the work cited below may thus act and serve as the road for CFD to enter into analysis of intense chemical phenomena.

TABLE OF CONTENT

LIST OF FIGURES

LIST OF TABLES

NOMENCLATURE

ρ is the density of gas.

ε_k is volume fraction of solids.

$\bar{u}$ is superficial velocity of the gas.

C_p, $C_{p,s}$ are specific heat capacity of fluid and solids respectively.

k, k_s are thermal conductivity of fluid and solids respectively.

q, q_s are heat for fluid and solid phases respectively.

κ is turbulent kinetic energy.

ε is turbulent energy dissipation rate.

μ is effective viscosity of the fluid.

d_p is diameter of the catalysts particles.

u_x is the velocity in X-direction.

G_κ represents the generation of turbulent kinetic energy due to mean velocity gradients.

G_b is the generation of turbulent kinetic energy due to buoyancy.

Y_M represents the contribution of fluctuation dilatation in compressible turbulence to the overall dissipation rate.

$C_{1\varepsilon}$, $C_{2\varepsilon}$ and $C_{3\varepsilon}$ are constants.

σ_κ and σ_ε are the turbulent Prandtl numbers for turbulent kinetic energy and dissipation rate respectively.

S_κ and S_ε are user defined source terms.

C_μ is a constant.

μ_t is turbulent viscosity.

CHAPTER 02. INTRODUCTION

2.1 PACKED BED REACTOR

In chemical processing, a packed bed is a hollow tube, pipe, or other vessel that is filled with a packing material. The packing can be randomly filled with small objects like Raschig rings or else it can be a specifically designed structured packing.

The purpose of a packed bed is typically to improve contact between two phases in a chemical or similar process. Packed beds can be used in a chemical reactor, a distillation process, or a scrubber, but packed beds have also been used to store heat in chemical plants. In this case, hot gases are allowed to escape through a vessel that is packed with a refractory material until the packing is hot. Air or other cool gas is then fed back to the plant through the hot bed, thereby pre-heating the air or gas feed.

2.1.1 Applications

In industry, a packed column is a type of packed bed used to perform separation processes, such as absorption, stripping, and distillation. A packed column is a pressure vessel that has a packed section. The column can be filled with random dumped packing or structured packing sections, which are arranged or stacked. In the column, liquids tend to wet the surface of the packing and the vapors pass across this wetted surface, where mass transfer takes place. Packing material can be used instead of trays to improve separation in distillation columns. Packing offers the advantage of a lower pressure drop across the column (when compared to plates or trays), which is beneficial while operating under vacuum. Differently shaped packing materials have different surface areas and void space between the packing. Both of these factors affect packing performance.

Another factor in performance, in addition to the packing shape and surface area, is the liquid and vapor distribution that enters the packed bed. The number of theoretical stages required to make a given separation is calculated using a specific vapor to liquid ratio. If the liquid and vapor are not evenly distributed across the superficial tower area as it enters the packed bed, the liquid to vapor ratio will not be correct and the required separation will not be achieved. The packing will appear to not be working properly. The height equivalent to a

theoretical plate (HETP) will be greater than expected. The problem is not the packing itself but the mal-distribution of the fluids entering the packed bed. These columns can contain liquid distributors and redistributors which help to distribute the liquid evenly over a section of packing, increasing the efficiency of the mass transfer. The design of the liquid distributors used to introduce the feed and reflux to a packed bed is critical to making the packing perform at maximum efficiency.

Packed columns have a continuous vapor-equilibrium curve, unlike conventional tray distillation in which every tray represents a separate point of vapor-liquid equilibrium. However, when modeling packed columns it is useful to compute a number of theoretical plates to denote the separation efficiency of the packed column with respect to more traditional trays. In design, the number of necessary theoretical equilibrium stages is first determined and then the packing height equivalent to a theoretical equilibrium stage, known as the "height equivalent to a theoretical plate" (HETP), is also determined. The total packing height required is the number theoretical stages multiplied by the HETP.

Columns used in certain types of chromatography consisting of a tube filled with packing material can also be called packed columns and their structure has similarities to packed beds.

Packed bed reactors can be used in chemical reaction. These reactors are tubular and are filled with solid catalyst particles, most often used to catalyze gas reactions. The chemical reaction takes place on the surface of the catalyst. The advantage of using a packed bed reactor is the higher conversion per weight of catalyst than other catalytic reactors. The reaction rate is based on the amount of the solid catalyst rather than the volume of the reactor.

2.2 CATALYSIS

Catalysis is the change in rate of a chemical reaction due to the participation of a substance called a catalyst. Unlike other reagents that participate in the chemical reaction, a catalyst is not consumed by the reaction itself. A catalyst may participate in multiple chemical transformations. Catalysts that speed the reaction are called positive catalysts. Substances that interact with catalysts to slow the reaction are called inhibitors (or negative catalysts). Substances that increase the activity of catalysts are called promoters, and substances that deactivate catalysts are called catalytic poisons.

Catalytic reactions have a lower rate-limiting free energy of activation than the corresponding uncatalyzed reaction, resulting in higher reaction rate at the same temperature. However, the mechanistic explanation of catalysis is complex. Catalysts may affect the reaction environment favorably, or bind to the reagents to polarize bonds, e.g. acid catalysts for reactions of carbonyl compounds, or form specific intermediates that are not produced naturally, such as osmate esters in osmium tetroxide-catalyzed dihydroxylation of alkenes, or cause lysis of reagents to reactive forms, such as atomic hydrogen in catalytic hydrogenation.
Kinetically, catalytic reactions are typical chemical reactions; i.e. the reaction rate depends on the frequency of contact of the reactants in the rate-determining step. Usually, the catalyst participates in this slowest step, and rates are limited by amount of catalyst and its "activity".
In heterogeneous catalysis, the diffusion of reagents to the surface and diffusion of products from the surface can be rate determining. Analogous events associated with substrate binding and product dissociation apply to homogeneous catalysts.
Although catalysts are not consumed by the reaction itself, they may be inhibited, deactivated, or destroyed by secondary processes. In heterogeneous catalysis, typical secondary processes include coking where the catalyst becomes covered by polymeric side products. Additionally, heterogeneous catalysts can dissolve into the solution in a solid-liquid system or evaporate in a solid-gas system.

2.2.1 Background

The production of most industrially important chemicals involves catalysis. Similarly, most biochemically significant processes are catalysed. Research into catalysis is a major field in applied science and involves many areas of chemistry, notably in organometallic chemistry and materials science. Catalysis is relevant to many aspects of environmental science, e.g. the catalytic converter in automobiles and the dynamics of the ozone hole. Catalytic reactions are preferred in environmentally friendly green chemistry due to the reduced amount of waste generated, as opposed to stoichiometric reactions in which all reactants are consumed and more side products are formed. The most common catalyst is the proton (H^+). Many transition metals and transition metal complexes are used in catalysis as well. Catalysts called enzymes are important in biology.
A catalyst works by providing an alternative reaction pathway to the reaction product. The rate of the reaction is increased as this alternative route has lower activation energy than the

reaction route not mediated by the catalyst. The disproportionation of hydrogen peroxide to give water and oxygen is a reaction that is strongly affected by catalysts:

$2\ H_2O_2 \rightarrow 2\ H_2O + O_2$

This reaction is favoured in the sense that reaction products are more stable than the starting material, however the uncatalysed reaction is slow. The decomposition of hydrogen peroxide is in fact so slow that hydrogen peroxide solutions are commercially available. Upon the addition of a small amount of manganese dioxide, the hydrogen peroxide rapidly reacts according to the above equation. This effect is readily seen by the effervescence of oxygen. The manganese dioxide may be recovered unchanged, and re-used indefinitely, and thus is not consumed in the reaction. Accordingly, manganese dioxide *catalyses* this reaction.

2.2.2 General principles of catalysis

2.2.2.1 Typical mechanism

Catalysts generally react with one or more reactants to form intermediates that subsequently give the final reaction product, in the process regenerating the catalyst. The following is a typical reaction scheme, where ***C*** represents the catalyst, X and Y are reactants, and Z is the product of the reaction of X and Y:

$X + \boldsymbol{C} \rightarrow X\boldsymbol{C}$ (1)

$Y + X\boldsymbol{C} \rightarrow XY\boldsymbol{C}$ (2)

$XY\boldsymbol{C} \rightarrow \boldsymbol{C}Z$ (3)

$\boldsymbol{C}Z \rightarrow \boldsymbol{C} + Z$ (4)

Although the catalyst is consumed by reaction 1, it is subsequently produced by reaction 4, so for the overall reaction:

$X + Y \rightarrow Z$

As a catalyst is regenerated in a reaction, often only small amounts are needed to increase the rate of the reaction. In practice, however, catalysts are sometimes consumed in secondary processes.

As an example of this process, in 2008 Danish researchers first revealed the sequence of events when oxygen and hydrogen combine on the surface of titanium dioxide (TiO_2, or titania) to produce water. With a time-lapse series of scanning tunneling microscopy images, they determined the molecules undergo adsorption, dissociation and diffusion before reacting. The intermediate reaction states were: HO_2, H_2O_2, then H_3O_2 and the final reaction product (water molecule dimers), after which the water molecule desorbs from the catalyst surface.

2.2.2.2 Catalysis and reaction energetics

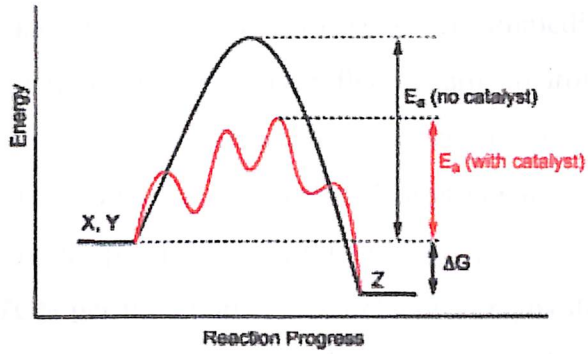

Figure 02-1: Change in activation energy using catalysts.

Source: www.wikipedia.com/packedbed

Generic potential energy diagram showing the effect of a catalyst in a hypothetical exothermic chemical reaction X + Y to give Z. The presence of the catalyst opens a different reaction pathway (shown in red) with lower activation energy. The final result and the overall thermodynamics are the same.

Catalysts work by providing an (alternative) mechanism involving a different transition state and lower activation energy. Consequently, more molecular collisions have the energy needed to reach the transition state. Hence, catalysts can enable reactions that would otherwise be blocked or slowed by a kinetic barrier. The catalyst may increase reaction rate or selectivity, or enable the reaction at lower temperatures. This effect can be illustrated with a Boltzmann distribution and energy profile diagram.

In the catalyzed elementary reaction, catalysts do not change the extent of a reaction: they have no effect on the chemical equilibrium of a reaction because the rate of both the forward and the reverse reaction are both affected (see also thermodynamics). The fact that a catalyst does not change the equilibrium is a consequence of the second law of thermodynamics. Suppose there was such a catalyst that shifted equilibrium. Introducing the catalyst to the system would result in reaction to move to the new equilibrium, producing energy. Production of energy is a necessary result since reactions are spontaneous if and only if Gibbs free energy is produced, and if there is no energy barrier, there is no need for a catalyst. Then, removing the catalyst would also result in reaction, producing energy; i.e. the addition and its reverse process, removal, would both produce energy. Thus, a catalyst that could change the equilibrium would be a perpetual motion machine, a contradiction to the laws of thermodynamics.

If a catalyst does change the equilibrium, then it must be consumed as the reaction proceeds, and thus it is also a reactant. Illustrative is the base-catalyzed hydrolysis of esters, where the produced carboxylic acid immediately reacts with the base catalyst and thus the reaction equilibrium is shifted towards hydrolysis.

The SI derived unit for measuring the catalytic activity of a catalyst is the "katal", which is moles per second. The productivity of a catalyst can be described by the turn over number (or TON) and the catalytic activity by the turn over frequency (TOF), which is the TON per time unit. The biochemical equivalent is the enzyme unit. For more information on the efficiency of enzymatic catalysis, see the article on Enzymes.

The catalyst stabilizes the transition state more than it stabilizes the starting material. It decreases the kinetic barrier by decreasing the difference in energy between starting material and transition state.

2.2.3 Typical catalytic materials

The chemical nature of catalysts is as diverse as catalysis itself, although some generalizations can be made. Proton acids are probably the most widely used catalysts, especially for the many reactions involving water, including hydrolysis and its reverse. Multifunctional solids often are catalytically active, e.g. zeolites, alumina, higher-order oxides, graphitic carbon, nanoparticles, nanodots, and facets of bulk materials. Transition metals are often used to catalyze redox reactions (oxidation, hydrogenation). Many catalytic processes, especially those used in organic synthesis, require so called "late transition metals", which include palladium, platinum, gold, ruthenium, rhodium, and iridium.

Some so-called catalysts are really precatalysts. Precatalysts convert to catalysts in the reaction. For example, Wilkinson's catalyst $RhCl(PPh_3)_3$ loses one triphenylphosphine ligand before entering the true catalytic cycle. Precatalysts are easier to store but are easily activated in situ. Because of this preactivation step, many catalytic reactions involve an induction period.

Chemical species that improve catalytic activity are called co-catalysts or promoters in cooperative catalysis.

2.2.4 Types of catalysis

C atalysts can be either heterogeneous or homogeneous, depending on whether a catalyst exists in the same phase as the substrate. Biocatalysts (enzymes) are often seen as a separate group.

2.2.4.1 Heterogeneous catalysts

Heterogeneous catalysts act in a different phase than the reactants. Most heterogeneous catalysts are solids that act on substrates in a liquid or gaseous reaction mixture. Diverse mechanisms for reactions on surfaces are known, depending on how the adsorption takes place (Langmuir-Hinshelwood, Eley-Rideal, and Mars-van Krevelen). The total surface area of solid has an important effect on the reaction rate. The smaller the catalyst particle size, the larger the surface area for a given mass of particles. For example, in the Haber process, finely divided iron serves as a catalyst for the synthesis of ammonia from nitrogen and hydrogen. The reacting gases adsorb onto "active sites" on the iron particles. Once adsorbed, the bonds within the reacting molecules are weakened, and new bonds between the resulting fragments form in part due to their close proximity. In this way the particularly strong triple bond in nitrogen is weakened and the hydrogen and nitrogen atoms combine faster than would be the case in the gas phase, so the rate of reaction increases. Another place where an Heterogeneous Catalyst is applied is in Contact Process. Heterogeneous catalysts are typically "supported," which means that the catalyst is dispersed on a second material that enhances the effectiveness or minimizes their cost. Sometimes the support is merely a surface on which the catalyst is spread to increase the surface area. More often, the support and the catalyst interact, affecting the catalytic reaction. Supports are porous materials with a high surface area, most commonly alumina or various kinds of carbon. Specialized supports include silicon dioxide, titanium dioxide, calcium carbonate, and barium sulfate.

2.2.4.2 Homogeneous catalysts

Homogeneous catalysts function in the same phase as the reactants, but the mechanistic principles invoked in heterogeneous catalysis are generally applicable. Typically homogeneous catalysts are dissolved in a solvent with the substrates. One example of homogeneous catalysis involves the influence of H^+ on the esterification of esters, e.g. methyl acetate from acetic acid and methanol. For inorganic chemists, homogeneous catalysis is often synonymous with organometallic catalysts.

2.2.4.3 Electrocatalysts

In the context of electrochemistry, specifically in fuel cell engineering, various metal-containing catalysts are used to enhance the rates of the half reactions that comprise the fuel cell. One common type of fuel cell electrocatalyst is based upon nanoparticles of platinum that are supported on slightly larger carbon particles. When in contact with one of the

electrodes in a fuel cell, this platinum increases the rate of oxygen reduction to water, either to hydroxide or hydrogen peroxide.

2.2.2.4 Organocatalysis

Whereas transition metals sometimes attract most of the attention in the study of catalysis, small organic molecules without metals can also exhibit catalytic properties, as is apparent from the fact that many enzymes lack transition metals. Typically, organic catalysts require a higher loading (amount of catalyst per unit amount of reactant, expressed in mol% amount of substance) than transition metal(-ion)-based catalysts, but these catalysts are usually commercially available in bulk, helping to reduce costs. In the early 2000s, these organocatalysts were considered "new generation" and are competitive to traditional metal(-ion)-containing catalysts. Organocatalysts are supposed to operate akin to metal-free enzymes utilizing, e.g., non-covalent interactions such as hydrogen bonding. The discipline organocatalysis is divided in the application of covalent (e.g., proline, DMAP) and non-covalent (e.g., thiourea organocatalysis) organocatalysts referring to the preferred catalyst-substrate binding and interaction, respectively.

2.2.4 Significance of catalysis

Estimates are that 90% of all commercially produced chemical products involve catalysts at some stage in the process of their manufacture.[10] In 2005, catalytic processes generated about $900 billion in products worldwide.[11] Catalysis is so pervasive that subareas are not readily classified. Some areas of particular concentration are surveyed below.

2.2.4.1 Energy processing

Petroleum refining makes intensive use of catalysis for alkylation, catalytic cracking (breaking long-chain hydrocarbons into smaller pieces), naphtha reforming and steam reforming (conversion of hydrocarbons into synthesis gas). Even the exhaust from the burning of fossil fuels is treated via catalysis: Catalytic converters, typically composed of platinum and rhodium, break down some of the more harmful byproducts of automobile exhaust.

$2\ CO + 2\ NO \rightarrow 2\ CO_2 + N_2$

With regard to synthetic fuels, an old but still important process is the Fischer-Tropsch synthesis of hydrocarbons from synthesis gas, which itself is processed via water-gas shift

reactions, catalysed by iron. Biodiesel and related biofuels require processing via both inorganic and biocatalysts.

Fuel cells rely on catalysts for both the anodic and cathodic reactions.

2.2.4.2 Bulk chemicals

Some of the largest-scale chemicals are produced via catalytic oxidation, often using oxygen. Examples include nitric acid (from ammonia), sulfuric acid (from sulfur dioxide to sulfur trioxide by the chamber process), terephthalic acid from p-xylene, and acrylonitrile from propane and ammonia.

Many other chemical products are generated by large-scale reduction, often via hydrogenation. The largest-scale example is ammonia, which is prepared via the Haber process from nitrogen. Methanol is prepared from carbon monoxide.

Bulk polymers derived from ethylene and propylene are often prepared via Ziegler-Natta catalysis. Polyesters, polyamides, and isocyanates are derived via acid-base catalysis.

Most carbonylation processes require metal catalysts, examples include the Monsanto acetic acid process and hydroformylation.

2.2.4.3 Fine chemicals

Many fine chemicals are prepared via catalysis; methods include those of heavy industry as well as more specialized processes that would be prohibitively expensive on a large scale. Examples include olefin metathesis using Grubbs' catalyst, the Heck reaction, and Friedel-Crafts reactions. Because most bioactive compounds are chiral, many pharmaceuticals are produced by enantioselective catalysis (catalytic asymmetric synthesis).

2.2.4.4 Food processing

One of the most obvious applications of catalysis is the hydrogenation (reaction with hydrogen gas) of fats using nickel catalyst to produce margarine. Many other foodstuffs are prepared via biocatalysis (see below).

2.2.4.5 Biology

In nature, enzymes are catalysts in metabolism and catabolism. Most biocatalysts are protein-based, i.e. enzymes, but other classes of biomolecules also exhibit catalytic properties including ribozymes, and synthetic deoxyribozymes.

Biocatalysts can be thought of as intermediate between homogenous and heterogeneous catalysts, although strictly speaking soluble enzymes are homogeneous catalysts and

membrane-bound enzymes are heterogeneous. Several factors affect the activity of enzymes (and other catalysts) including temperature, pH, concentration of enzyme, substrate, and products. A particularly important reagent in enzymatic reactions is water, which is the product of many bond-forming reactions and a reactant in many bond-breaking processes. Enzymes are employed to prepare many commodity chemicals including high-fructose corn syrup and acrylamide.

2.2.4.6 In the environment

Catalysis impacts the environment by increasing the efficiency of industrial processes, but catalysis also plays a direct role in the environment. A notable example is the catalytic role of chlorine free radicals in the breakdown of ozone. These radicals are formed by the action of ultraviolet radiation on chlorofluorocarbons (CFCs).

$Cl^{\cdot} + O_3 \rightarrow ClO^{\cdot} + O_2$

$ClO^{\cdot} + O^{\cdot} \rightarrow Cl^{\cdot} + O_2$

2.2.5 History

In a general sense, anything that increases the rate of a process is a "catalyst", a term derived from Greek "καταλύειν", meaning "to annul," or "to untie," or "to pick up." The phrase catalysed processes was coined by Jöns Jakob Berzelius in 1836[14] to describe reactions that are accelerated by substances that remain unchanged after the reaction. Other early chemists involved in catalysis were Alexander Mitscherlich who referred to contact processes and Johann Wolfgang Döbereiner who spoke of contact action and whose lighter based on hydrogen and a platinum sponge became a huge commercial success in the 1820s. Humphry Davy discovered the use of platinum in catalysis. In the 1880s, Wilhelm Ostwald at Leipzig University started a systematic investigation into reactions that were catalyzed by the presence of acids and bases, and found that chemical reactions occur at finite rates and that these rates can be used to determine the strengths of acids and bases. For this work, Ostwald was awarded the 1909 Nobel Prize in Chemistry.

2.2.6 Inhibitors, poisons and promoters

Substances that reduce the action of catalysts are called catalyst inhibitors if reversible, and catalyst poisons if irreversible. Promoters are substances that increase the catalytic activity, even though they are not catalysts by themselves.

Inhibitors are sometimes referred to as "negative catalysts" since they decrease the reaction rate. However they do not work by introducing a reaction path with higher activation energy, as this term might suggest; this would not reduce the rate since the reaction would continue to occur by the non-catalyzed path. Instead they act either by inactivating catalysts, or by removing reaction intermediates such as free radicals.

The inhibitor may modify selectivity in addition to rate. For instance, in the reduction of ethyne to ethene, the catalyst is palladium (Pd) partly "poisoned" with lead (II) acetate ($Pb(CH_3COO)_2$). Without the deactivation of the catalyst, the ethene produced will be further reduced to ethane.

The inhibitor can produce this effect by e.g. selectively poisoning only certain types of active sites. Another mechanism is the modification of surface geometry. For instance, in hydrogenation operations, large planes of metal surface function as sites of hydrogenolysis catalysis while sites catalyzing hydrogenation of unsaturated are smaller. Thus, a poison that covers surface randomly will tend to reduce the number of uncontaminated large planes but leave proportionally smaller sites free, thus changing the hydrogenation vs. hydrogenolysis selectivity. Many other mechanisms are also possible.

Promoters can cover up surface to prevent production of a mat of coke, or even actively remove such material (e.g. rhenium on platinum in plat forming). They can aid the dispersion of the catalytic material or bind to reagents.

2.2.7 Current market

The global demand on catalysts in 2007 was estimated at approximately 850 thousand tonnes. The market in volume is expected to grow by 3.5-4% annually through 2012, while the market in value will develop much faster. Surging price of precious metals (e.g. platinum and rhodium) is a main contributor to the rapidly growing catalysts market in value. The market is experiencing influences from environmental regulations, rising raw material prices, call for green chemistry, etc. It is a dramatically changing market with opportunities and risks.

2.3 CATALYSTS

In petroleum geology and chemistry, cracking is the process whereby complex organic molecules such as kerogens or heavy hydrocarbons are broken down into simpler molecules such as light hydrocarbons, by the breaking of carbon-carbon bonds in the precursors. The

rate of cracking and the end products are strongly dependent on the temperature and presence of catalysts. Cracking is the breakdown of a large alkane into smaller, more useful alkanes and an alkene. Simply put, hydrocarbon cracking is the process of breaking long-chain hydrocarbons into short ones.

2.3.1 History and patents

The thermal cracking method (also known as "Shukhov cracking process") was invented by Russian engineer Vladimir Shukhov and patented in 1891 in the Russian empire, patent no. 12926, November 27, 1891. This process was modified by the American engineer William Merriam Burton and patented as U.S. patent 1,049,667 on June 8, 1908. In 1924, the delegation of the American "Sinckler Oil" paid a visit to Shukhov. The "Sinckler Oil" firm protested the personal right appropriated by the Rockefeller "Standard Oil" concern on the discovery of oil cracking. It indicated that Burton's patent used by the "Standard Oil" concern was the modified patent of Shukhov. Shukhov proved to the Americans that the Burton's method was just the slightly changed modification of his 1891 patents. However, an agreement between the American companies finally was made not to buy the patent from Soviet Russia.

2.3.2 Applications

Oil refinery cracking processes allow the production of "light" products such as liquified petroleum gas (LPG) and gasoline from heavier crude oil distillation fractions such as gas oils and residues. Fluid catalytic cracking produces a high yield of gasoline and LPG, while hydrocracking is a major source of jet fuel, diesel, naphtha, and LPG.

Thermal cracking is currently used to "upgrade" very heavy fractions ("upgrading", "visbreaking"), or to produce light fractions or distillates, burner fuel and/or petroleum coke. Two extremes of the thermal cracking in terms of product range are represented by the high-temperature process called "steam cracking" or pyrolysis (ca. 750 °C to 900 °C or more) which produces valuable ethylene and other feedstocks for the petrochemical industry, and the milder-temperature delayed coking (ca. 500 °C) which can produce, under the right conditions, valuable needle coke, a highly crystalline petroleum coke used in the production of electrodes for the steel and aluminium industries.

2.3.2.1 Fluid catalytic cracking

Fluid catalytic cracking is a commonly used process, and a modern oil refinery will typically include a cat cracker, particularly at refineries in the U.S., due to the high demand for gasoline. The process was first used in around 1942 and employs a powdered catalyst. During the Second World War, in contrast to the Axis Forces which suffered severe shortages of gasoline and artificial rubber, the Allied Forces were supplied with plentiful supplies of the materials. Initial process implementations were based on low activity alumina catalyst and a reactor where the catalyst particles were suspended in a rising flow of feed hydrocarbons in a fluidized bed.

Aluminum-catalyzed cracking systems are still in use in high school and university laboratories in experiments concerning alkanes and alkenes. The catalyst is usually obtained by crushing pumice stones, which contain mainly aluminium oxide and silica into small, porous pieces. In the laboratory, aluminium oxide (or porous pot) must be heated.

In newer designs, cracking takes place using a very active zeolite-based catalyst in a short-contact time vertical or upward sloped pipe called the "riser". Pre-heated feed is sprayed into the base of the riser via feed nozzles where it contacts extremely hot fluidized catalyst at 1230 °F to 1400 °F (665 °C to 760 °C). The hot catalyst vaporizes the feed and catalyzes the cracking reactions that break down the high molecular weight oil into lighter components including LPG, gasoline, and diesel. The catalyst-hydrocarbon mixture flows upward through the riser for just a few seconds and then the mixture is separated via cyclones. The catalyst-free hydrocarbons are routed to a main fractionator for separation into fuel gas, LPG, gasoline, naphtha, light cycle oils used in diesel and jet fuel, and heavy fuel oil.

During the trip up the riser, the cracking catalyst is "spent" by reactions which deposit coke on the catalyst and greatly reduce activity and selectivity. The "spent" catalyst is disengaged from the cracked hydrocarbon vapors and sent to a stripper where it is contacted with steam to remove hydrocarbons remaining in the catalyst pores. The "spent" catalyst then flows into a fluidized-bed regenerator where air (or in some cases air plus oxygen) is used to burn off the coke to restore catalyst activity and also provide the necessary heat for the next reaction cycle, cracking being an endothermic reaction. The "regenerated" catalyst then flows to the base of the riser, repeating the cycle.

The gasoline produced in the FCC unit has an elevated octane rating but is less chemically stable compared to other gasoline components due to its olefinic profile. Olefins in gasoline are responsible for the formation of polymeric deposits in storage tanks, fuel ducts

and injectors. The FCC LPG is an important source of C_3-C_4 olefins and isobutane that are essential feeds for the alkylation process and the production of polymers such as polypropylene.

2.3.2.2 Hydrocracking

In 1920, a plant for the commercial hydrogenation of brown coal was commissioned at Leuna in Germany. Hydrocracking is a catalytic cracking process assisted by the presence of an elevated partial pressure of hydrogen gas. Similar to the hydrotreater, the function of hydrogen is the purification of the hydrocarbon stream from sulfur and nitrogen hetero-atoms. The products of this process are saturated hydrocarbons; depending on the reaction conditions (temperature, pressure and catalyst activity) these products range from ethane, LPG to heavier hydrocarbons consisting mostly of isoparaffins. Hydrocracking is normally facilitated by a bifunctional catalyst that is capable of rearranging and breaking hydrocarbon chains as well as adding hydrogen to aromatics and olefins to produce naphthenes and alkanes.

Major products from hydrocracking are jet fuel and diesel, while also high octane rating gasoline fractions and LPG are produced. All these products have a very low content of sulfur and other contaminants.

It is very common in India, Europe and Asia because those regions have high demand for diesel and kerosene. In the US, Fluid Catalytic Cracking is more common because the demand for gasoline is higher.

2.3.2.3 Steam cracking

Steam cracking is a petrochemical process in which saturated hydrocarbons are broken down into smaller, often unsaturated, hydrocarbons. It is the principal industrial method for producing the lighter alkenes (or commonly olefins), including ethene (or ethylene) and propene (or propylene).

In steam cracking, a gaseous or liquid hydrocarbon feed like naphtha, LPG or ethane is diluted with steam and briefly heated in a furnace without the presence of oxygen. Typically, the reaction temperature is very high, at around 850°C, but the reaction is only allowed to take place very briefly. In modern cracking furnaces, the residence time is reduced to milliseconds to improve yield, resulting in gas velocities faster than the speed of sound. After the cracking temperature has been reached, the gas is quickly quenched to stop the reaction in a transfer line heat exchanger or inside a quenching header using quench oil.

The products produced in the reaction depend on the composition of the feed, the hydrocarbon to steam ratio and on the cracking temperature and furnace residence time.
Light hydrocarbon feeds such as ethane, LPGs or light naphtha give product streams rich in the lighter alkenes, including ethylene, propylene, and butadiene. Heavier hydrocarbon (full range and heavy naphthas as well as other refinery products) feeds give some of these, but also give products rich in aromatic hydrocarbons and hydrocarbons suitable for inclusion in gasoline or fuel oil. The higher cracking temperature (also referred to as severity) favours the production of ethene and benzene, whereas lower severity produces higher amounts of propene, C4-hydrocarbons and liquid products. The process also results in the slow deposition of coke, a form of carbon, on the reactor walls. This degrades the efficiency of the reactor, so reaction conditions are designed to minimize this. Nonetheless, a steam cracking furnace can usually only run for a few months at a time between de-cokings. Decokes require the furnace to be isolated from the process and then a flow of steam or a steam/air mixture is passed through the furnace coils. This converts the hard solid carbon layer to carbon monoxide and carbon dioxide. Once this reaction is complete, the furnace can be returned to service.

2.3.3 Chemistry

"Cracking" breaks larger molecules into smaller ones, through thermic or catalytic method. The thermal cracking process follows a homolytic mechanism, that is, bonds break symmetrically and thus pairs of free radicals are formed.

The catalytic cracking process involves the presence of acid catalysts (usually solid acids such as silica-alumina and zeolites) which promote a heterolytic (asymmetric) breakage of bonds yielding pairs of ions of opposite charges, usually a carbocation and the very unstable hydride anion. Carbon-localized free radicals and cations are both highly unstable and undergo processes of chain rearrangement, C-C scission in position beta as in cracking, and intra- and intermolecular hydrogen transfer or hydride transfer. In both types of processes, the corresponding reactive intermediates (radicals, ions) are permanently regenerated, and thus they proceed by a self-propagating chain mechanism. The chain of reactions is eventually terminated by radical or ion recombination.

2.3.4 Thermal cracking

The first thermal cracking method, the Shukhov cracking process, was invented by Russian engineer Vladimir Shukhov, in the Russian empire, Patent No. 12926, November 27,

1891. William Merriam Burton developed one of the earliest thermal cracking processes in 1912 which operated at 700 - 750 °F (370 - 400 °C) and an absolute pressure of 90 psi (620 kPa) and was known as the Burton process. Shortly thereafter, in 1921, C.P. Dubbs, an employee of the Universal Oil Products Company, developed a somewhat more advanced thermal cracking process which operated at 750°F -860 °F (400°C - 460 °C) and was known as the Dubbs process. The Dubbs process was used extensively by many refineries until the early 1940s when catalytic cracking came into use.

Modern high-pressure thermal cracking operates at absolute pressures of about 7,000 kPa. An overall process of disproportionation can be observed, where "light", hydrogen-rich products are formed at the expense of heavier molecules which condense and are depleted of hydrogen. The actual reaction is known as homolytic fission and produces alkenes, which are the basis for the economically important production of polymers.

A large number of chemical reactions take place during steam cracking, most of them based on free radicals. Computer simulations aimed at modeling what takes place during steam cracking have included hundreds or even thousands of reactions in their models. The main reactions that take place include:

Initiation reactions, where a single molecule breaks apart into two free radicals. Only a small fraction of the feed molecules actually undergo initiation, but these reactions are necessary to produce the free radicals that drive the rest of the reactions. In steam cracking, initiation usually involves breaking a chemical bond between two carbon atoms, rather than the bond between a carbon and a hydrogen atom.

$CH_3CH_3 \rightarrow 2\ CH_3\bullet$

Hydrogen abstraction occurs where a free radical removes a hydrogen atom from another molecule, turning the second molecule into a free radical.

$CH_3\bullet + CH_3CH_3 \rightarrow CH_4 + CH_3CH_2\bullet$

Radical decomposition occurs where a free radical breaks apart into two molecules, one an alkene, the other a free radical. This is the process that results in the alkene products of steam cracking.

$CH_3CH_2\bullet \rightarrow CH_2{=}CH_2 + H\bullet$

Radical addition, the reverse of radical decomposition, occurs where a radical reacts with an alkene to form a single, larger free radical. These processes are involved in forming the aromatic products that result when heavier feedstocks are used.

$CH_3CH_2\bullet + CH_2{=}CH_2 \rightarrow CH_3CH_2CH_2CH_2\bullet$

Termination reactions occur when two free radicals react with each other to produce products that are not free radicals. Two common forms of termination are recombination, where the two radicals combine to form one larger molecule, and disproportionation, where one radical transfers a hydrogen atom to the other, giving an alkene and an alkane.

$CH_3\bullet + CH_3CH_2\bullet \rightarrow CH_3CH_2CH_3$

$CH_3CH_2\bullet + CH_3CH_2\bullet \rightarrow CH_2{=}CH_2 + CH_3CH_3$

Thermal cracking is an example of a reaction whose energetics are dominated by entropy ($\Delta S°$) rather than by enthalpy ($\Delta H°$) in the Gibbs Free Energy equation $\Delta G°=\Delta H°-T\Delta S°$. Although the bond dissociation energy D for a carbon-carbon single bond is relatively high (about 375 kJ/mol) and cracking is highly endothermic, the large positive entropy change resulting from the fragmentation of one large molecule into several smaller pieces, together with the extremely high temperature, makes $T\Delta S°$ term larger than the $\Delta H°$ term, thereby favoring the cracking reaction.

Here is an example of cracking of butane CH_3-CH_2-CH_2-CH_3

- 1st possibility (48%): breaking is done on the CH_3-CH_2 bond.

CH_3* / *CH_2-CH_2-CH_3

After a certain number of steps, we will obtain an alkane and an alkene: $CH_4 + CH_2{=}CH\text{-}CH_3$

- 2nd possibility (38%): breaking is done on the CH_2-CH_2 bond.

CH_3-CH_2* / *CH_2-CH_3

After a certain number of steps, we will obtain an alkane and an alkene from different types: $CH_3\text{-}CH_3 + CH_2{=}CH_2$

- 3rd possibility (14%): breaking of a C-H bond

After a certain number of steps, we will obtain an alkene and hydrogen gas: $CH_2{=}CH\text{-}CH_2\text{-}CH_3 + H_2$ this is very useful since the catalyst can be recycled.

CHAPTER 03. LITERATURE REVIEW

3.1 KINETICS REVIEW

Kinetics for catalytic cracking of tar was analyzed by Faundez et al, 2001. The model proposed was based on gas-oil cracking and was validated by using three types of tars used by Weekman .V et al, 1970. The catalyst used is calcined limestone ($11 m^2/g$). The reactions were carried out in a stainless steel cylindrical catalytic fixed bed reactor of 30mm diameter with 1.5cm catalyst bed-height with tar feed rate as 5.04 mg/min. The work was concentrated on: 1) The proposal of a mechanism and a model for the kinetics of catalytic pyrolysis of tars main products, i.e. gases, lighter tars and solid carbon or char; 2) the validation of the proposed model by the experimental catalytic pyrolysis of different tars; and, 3) The determination of the kinetic and catalytic deactivation parameters of the model. It may be noted that flow rate used in this project is inferred from this literature.

P. Morf et al, 2001 studied the change of mass and composition of biomass tar due to secondary reactions in an experimental set-up consisting of wood pyrolyser, a catalytic tubular reactor for heterogeneous reactions of tar and finally gas analyzer for product measurement and characterization. Spruce woods chips of 10-40 mm dia were sent to pyrolyser at a rate of 1.6 kg h^{-1}. The wood pyrolysis gas obtained at a mean temperature of 350°C was sent to the reactor containing tar approx. 300g nm^{-3}. The residence time in the reactor was 0.2 s after a steady state was attained. The reactor was operated in a temperature range of 500-1000°C. The author classified tar according to Milne T. A. et al, 1998 and fed external oxidizer. The reactions occurring in the reactor was analyzed and found the product gas to contain mostly of CO_2, CH_4, CO, H_2O & H_2. The results reflected that CO is the major product. The overall product distribution remains stable within the temperature range of 450-600 °C. Then the product concentration increased linearly with temperature especially for CH_4 and CO.

Rath et al, 2001 conducted an experimental study to investigate the vapor phase cracking of tar obtained from pyrolysis of spruce wood (0.5-1.0 mm) using a thermogravimetric analyzer (TGA) and in coupling of the TGA with a consecutive tubular reactor. The products from the reactor were analyzed using GC-MS analyzer. In all cases the TGA was heated from 105 °C to 1050 °C at a rate of 5 K min^{-1} and the reactor consisted of

three different heating zones namely 600 °C, 700 °C, 900 °C in order to achieve different residence times for the volatiles. The motto this study was to analyze three different types of tars that were produced from gasification of spruce wood under different thermal conditions and the way these tars catalytically cracked. The tubular reactor was fed with 3.62 mg/min of wood volatiles. There were in total nine (9) experimental runs with variations in residence time. The kinetic model proposed by him was used in the CFD analysis done in this project. The table 3.1 below shows his findings.

Table 03-1: Kinetic parameters for cracking of three different tars

Parameter	Tar 1	Tar 2	Tar 3
K_0	8.20e+07 s^{-1}	1.01e+14 s^{-1}	3.02e+21(g mg^{-1} s^{-1})
E (KJ/mol)	117.0	197.5	320.2
n	1	1	2

Source: Rath et al, 2001

3.2 CATALYST REVIEW

Dolomite is a calcium magnesium ore with general chemical formula CaMg (CO3)2, and is generally used as raw material in the manufacture of magnesium. In recent years, it has been discovered that calcined dolomite is also a highly efficient catalyst for removing tar from the product gases of gasifier.

Taralas et al, 2003 investigated the cracking of tar obtained from pyrolysis of exhausted olive husks (kernels) using calcined dolomite as catalyst. The pyrolysis was carried out in a screw reactor at 975 K at a bio-fuel feed rate of 0.101 kg/h. the volatiles produced were introduced into the catalytic reactor (20mm dia and 400mm long) using N_2 as carrier gas with flow rate of 0.5-0.1 L/h. The catalyst particles were less than 1mm in dia. The basic motto of this study was to study feasibility of the dolomite as a catalyst and determining the difference it makes in product concentration obtained from thermal cracking as well as catalytic cracking. The results obtained from his study shows considerable increase in product concentration at lower temperatures, i.e, and 1175K for thermal cracking versus 1075K for catalytic cracking. It was also observed that thermal cracking required a considerable residence time about 20seconds more as compared to catalytic cracking to obtain the same exit gas concentration from the catalytic reactor.

Kumar et al, 2009 did a study of existing processes for biomass gasification and its subsequent processing for effective commercial application. In relation to gasification products clean-up and effective carbon conversion they analyzed tar cracking using addition reactor such as fixed bed reactors consecutive to the gasifier for different sets of catalysts such as dolomite, olivine, Ni and hot sand. After 20 hours of test they concluded that dolomites and olivine proved as a better catalyst then Ni and hot sand w.r.t to various operating parameters such as temperature, flow rate, bed height, residence time and carbon conversion. Although olivine and dolomite faired equally but olivine was beaten when it came to bed capacity (tar processing capability for same amount of catalyst loading) and dolomite fails when it comes to attrition.

Tasaka et al, 2006 analyzed steam reforming of tar produced from cellulose gasification using Co/MgO as catalyst. The reactor was 22mm in dia and 300mm long. The catalyst particles were 0.5-0.3mm in dia. The tests were conducted for 120 min at a feed rate of 15gm/min at a temperature of 623 K and three sets of catalyst loading namely 12% Co/MgO, 24% Co/MgO and 36% Co/MgO. They finally concluded that at 36% Co/MgO the concentration of CO and H_2 remained for whole 2hrs.

Lopamudra Devi, 2005 in her analysis for catalyst selection for tar cracking studies three catalysts Ni, dolomite and untreated olivine. Although dolomite and Ni-based steam reforming catalysts have been proven to be active in terms of tar reduction, dolomite is relatively soft and very easily eroded, whereas Ni-based catalysts are easily deactivated. Olivine has advantages over dolomite in terms of its attrition resistance. The experiments were conducted at the facility of ECN, (Petten, Netherlands). A slip stream of the biomass gasification gas from the lab-scale atmospheric bubbling fluidized bed gasifier was passed through a secondary fixed the stainless steel secondary reactor has a 3 cm internal diameter and is 50 cm long. The experiments were performed in a temperature range of 800-900°C and temperature across the catalyst was taken to be constant during each experiment. The catalysts were mixed with sand (0.17 mass fraction of catalyst) and the mixture was placed on top of a bed of coarse sand. The reactor was fed with 1kg/h with a residence time of 20s for each catalyst (200-300μm). Experiments were also carried out using sand only as the catalyst. The figure3.1 below shows the results obtained from her experiments for 900°C. It can be clearly seen that dolomite is an excellent catalyst for tar cracking.

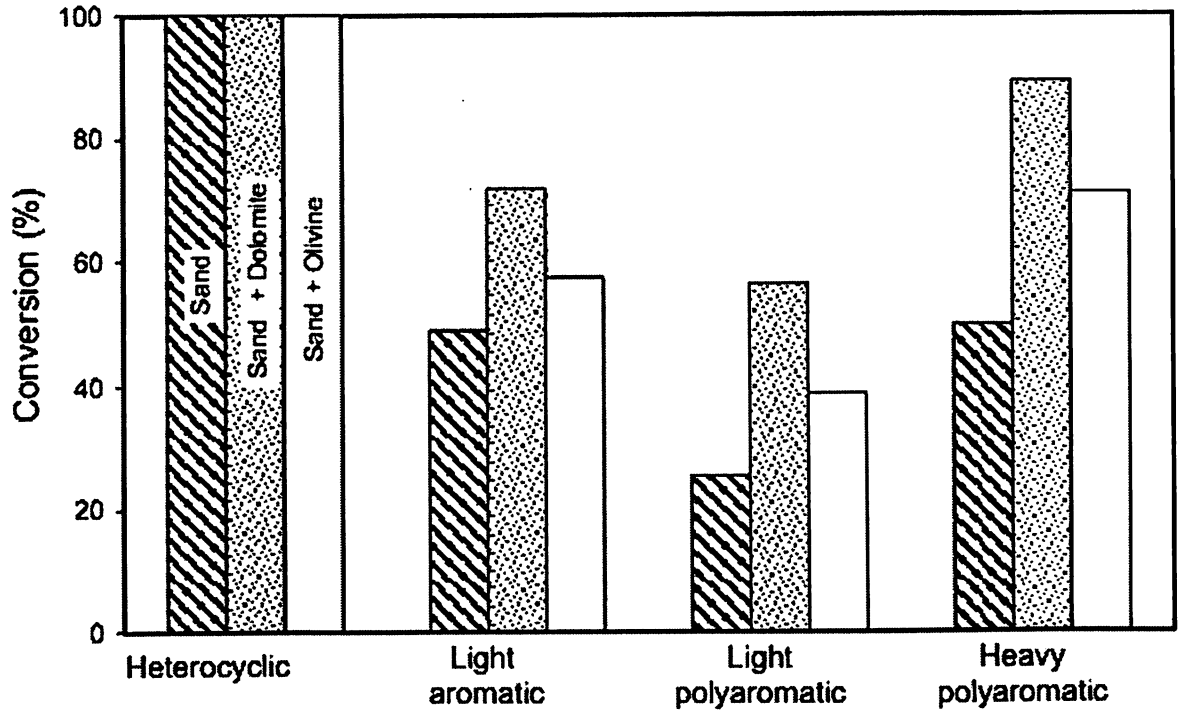

Figure 03-1: Conversion of tars with different additives TR = 9000C; Gas flow: 1.2 l min-1; τ'=0.26 s; τ = 0.066kg h m-3

Source: Lopamudra Devi; University of Eindhoven, Netherlands; 2005.

Zhang et al; 2004 investigated tar catalytic destruction in a tar conversion system consisting of a guard bed and catalytic reactor. Three Ni-based catalysts (ICI46-1, Z409 and RZ409) were proven to be effective in eliminating heavy tars (499% destruction efficiency). Hydrogen yield was also improved by 6–11 vol% (dry basis). The experimental results also demonstrated that increasing temperature boosted hydrogen yield and reduced light hydrocarbons (CH_4 and C_2H_4) formation, which suggested that tar decomposition was controlled by chemical kinetics.

Dou et al; 2003 compared five catalysts on tar removal from fuel gases in a fixed-bed reactor. The Y-zeolite and NiMo catalysts were found to be the most effective; such that 100% tar removal can be achieved at 550 °C. It was also observed that process variables like temperature and space velocity had very significant effect on tar removal. The visual observation demonstrated that only very small amount of coke appeared at the surface of catalyst even with 168 h operation.

Although the dolomite can effectively remove tar in some cases, there are still many problems during biomass gasification. Zhang Xiodong; 2003 reviewed the shortcomings of dolomite as the following: The conversion rate of tar catalyzed by dolomite was difficult to reach or exceed 90–95%; Although dolomite could reduce the tar in syngas and change the distribution of tar compositions, it was difficult to convert the heavy tars by dolomite; The dolomite would be inactive since the particle was easily broken during gasification; The melting point of dolomite was low and the catalyst would be inactive resulting from the melting of dolomite.

In the table below are the results of experiment conducted to analyze and compare the catalytic cracking of gasifier tars using different catalysts. The study was conducted using a 20cm long reactor and 5cm in diameter. 1.03 kg of catalysts of each type was used in this study. Temperature stated is the averaged value along the length of the reactor.

Table 03-2: Catalytic Cracking Of Gasifier Tars Using Different Catalysts

Run Conditions				Tar Concentration		
Temp. °C[a]	Flow Rate kg/h	Residence Time(t), s	Space Vel g/g-h	Before(C1) mg/Nm^3	After(C2) mg/Nm^3	Rate-k L/s[b]
Catalyst: Dolomite[c]						
600	0.73	0.34	0.33	9574	3597	2.84
750	0.73	0.29	0.29	3169	1294	3.05
820	0.73	0.28	0.27	18082	2674	6.95
960	0.73	0.24	0.24	8346	1113	8.26
750	0.20	1.07	1.04	3169	200	2.58
750	0.40	0.54	0.52	7537	2408	2.13
Catalyst: Si-Al Catalyst[d]						
432	0.51	1.54	2.02	18082	4654	0.88
432	0.51	1.54	2.02	22070	1313	1.83
552	0.56	1.20	1.57	5929	333	2.40
415	0.48	1.68	2.19	4863	695	1.16
343	0.49	1.84	2.40	4654	847	0.93
287	0.51	1.94	2.54	5605	780	1.02
Catalyst: Crystalline Silica S-155[e]						
416	0.59	0.91	1.68	8280	790	2.58
406	0.39	1.40	2.57	15237	2303	1.35
469	0.34	1.47	2.70	15189	3359	1.03
505	0.48	0.99	1.83	11725	3131	1.33
613	0.47	0.89	1.64	25305	3930	2.10
812	0.42	0.81	1.50	9184	1075	2.64

Catalyst selection has always been major concern in process industry. It is been found that for the same process we actually have lot of options in selecting the catalyst. In the case of tar cracking dolomite, olivine, Ni-based catalysts, Co/Mo based catalysts and Si-based catalysts are available, but literature shows that dolomite is most apt catalysts for high surface area and active sites concentration per unit surface area, easily available and cheap. Also, it

can catalyze tar at lesser temperatures than olivine which is the next best catalyst. The only drawback of dolomite is that it has high attrition rate. This can be controlled to a certain extent by using calcined dolomite. Calcinations of dolomite also increase its surface adsorptivity.

2.3 MODEL COMPOUND REVIEW

In a lab scale experiment by Nikola Sundac; 2003 related to biomass gasification and tar cracking. He analyzed dolomite and olivine catalysts but it was only preparation phase. Now instead of using real tar the author considered using model compounds like Naphthalene and Xylene. The author presented the following arguments to support the use of model compounds:

1) These compounds show similar cracking activity as real tar.
2) Ease of formulation of a kinetic model,
3) Simplicity to design, and
4) These compound constitute 4.5% in real tar composition.

Milne T.A. et al; 1998 investigated biomass gasification and their conversion using three model compounds Naphthalene, toluene and cyclo-hexane. The author justified the use of these compounds by comparing the reaction kinetics they show when compared real tar cracking. Although there was not an exact match in output obtained from cracking of real tar versus models compounds but they faired equivalently. On the basis of this research toluene was considered as model compound in the study done in this project.

Coll et al; 2001 also studied the model compounds like benzene; toluene, naphthalene, anthracene, and pyrene. All of these were cracked using two commercial nickel catalysts: UCG90-C and ICI46-1 at 700–800 °C. The order of these model tars reactivity was: benzene > toluene > anthracene > pyrene > naphthalene. Toluene conversion rate ranged from 40% to 80% with the ICI46-1 catalyst, and 20% to 60% for the UCI G90-C catalyst.

Simell et al; 1999 compared a commercially available metal based catalyst (NiMo/γ–Al_2O_3) with non-metallic mineral catalysts during the catalytic pyrolysis of toluene. The non-metallic mineral catalysts included Norwegian dolomitic magnesium oxide [MgO], Swedish

low surface quicklime [CaO], and calcined dolomite [$CaMg(O)_2$]. Among these catalysts, the catalytic effect followed the sequence: $CaO > CaMg(O)_2 > MgO > NiMo/\gamma-Al_2O_3$.

Gil et al; 1999 also investigated the impact of temperature on the composition of tar samples obtained from steam cracking of wood at 700–900°C. He listed the compositions and concentration of tar at 700, 800 and 900°C, respectively, as shown in Table 02-3. It can be seen that phenol, cresols and toluene were predominant at 700 1C, while naphthalene and indene were the major components at 900 °C.

Table 03-3: Effect of temperature on distribution of major organic tar compounds (g/kg dry wood)

Analyte	700 (°C)	800 (°C)	900 (°C)
Phenol	1.069	0.941	0.753
o-Cresol	0.929	0.737	0.300
m-Cresol	1.140	0.917	0.503
p-Cresol	0.739	0.545	0.276
2,5-Xylenol	0.340	0.303	0.137
3,4-Xylenol	0.260	0.184	0.077
2,6-Xylenol	0.260	n.d	0.174
o-Ethylphenol	0.353	0.381	0.240
Toluene	1.125	0.274	0.538
o-Xylene	0.580	0.356	0.653
Indene	0.649	0.628	1.425
Naphthalene	0.345	0.494	1.722
2-Methylnaphthalene	0.242	0.277	0.456
1-Methylnaphthalene	0.164	0.187	0.289
Biphenyl	0.044	0.053	0.125
Acenaphthylene	0.208	0.285	n.d.
Fluorene	0.119	0.149	0.276
Phenanthrene	0.065	0.100	0.368
Anthracene	0.017	0.042	0.107
Pyrene	0.049	0.038	0.140
Pyridine	0.168	n.d.	n.d.
2-Picoline	0.041	n.d.	n.d.
3-Picoline	0.027	n.d.	n.d.

Source: Gill J et al; Biomass Bio-energy; 1999.

CHAPTER 04. CFD IN PACKED BED MODELLING

4.1 CFD (COMPUTATIONAL FLUID DYNAMICS)

CFD is one of the branches of fluid mechanics that uses numerical methods and algorithms to solve and analyze problems that involve fluid flows. Computers are used to perform the millions of calculations required to simulate the interaction of fluids and gases with the complex surfaces used in engineering. However, even with simplified equations and high speed supercomputers, only approximate solutions can be achieved in many cases. More accurate codes that can accurately and quickly simulate even complex scenarios such as supersonic or turbulent flows are an ongoing area of research.

4.1.1 Applications of CFD

CFD useful in a wide variety of industrial and non-industrial applications. Currently, it is been seen an advanced engineering tool to provide data, which suits to solving a lot of real time situations seen in this physical world. Applications of CFD are numerous and wide spread, some which are as follows:

i. In chemical industry, CFD is very useful in analyzing the flow conditions in a CSTR, Fluidized bed reactor, Fixed bed reactor, Heat Exchangers, combustion systems and material and polymer handling equipments.

ii. Designing of aerodynamically stable ground vehicles, spacecrafts, jets and passenger crafts, missiles CFD is considered as very effectives and successful.

iii. CFD has found its application bio-medical engineering to analyze the flow in arteries and veins.

iv. In structures it is found that CFD is good tool to analyze the affects of wind and water on tall structures.

v. In steel industry, due to opacity of steel CFD has been very successful in determining the flow conditions of liquid molten steel in the furnace vessels.

vi. CFD is has provided with reliable results when analyzing turbo-machinery equipments like diffusers, compressors and turbines.

4.1.2. Discretization Methods in CFD

There are three discretization methods in CFD:

1. Finite difference method (FDM)
2. Finite volume method (FVM)

3. Finite element method (FEM)

4.1.2.1. Finite difference method (FDM): A finite difference method (FDM) discretization is based upon the differential form of the PDE to be solved. Each derivative is replaced with an approximate difference formula (that can generally be derived from a Taylor series expansion). The computational domain is usually divided into hexahedral cells (the grid), and the solution will be obtained at each nodal point. The FDM is easiest to understand when the physical grid is Cartesian, but through the use of curvilinear transforms the method can be extended to domains that are not easily represented by brick-shaped elements. The discretization results in a system of equation of the variable at nodal points, and once a solution is found, then we have a discrete representation of the solution.

4.1.2.2. Finite volume method (FVM): A finite volume method (FVM) discretization is based upon an integral form of the PDE to be solved (e.g. conservation of mass, momentum, or energy). The PDE is written in a form which can be solved for a given finite volume (or cell). The computational domain is discretized into finite volumes and then for every volume the 12 governing equations are solved. The resulting system of equations usually involves fluxes of the conserved variable, and thus the calculation of fluxes is very important in FVM. The basic advantage of this method over FDM is it does not require the use of structured grids, and the effort to convert the given mesh in to structured numerical grid internally is completely avoided. As with FDM, the resulting approximate solution is a discrete, but the variables are typically placed at cell centers rather than at nodal points. This is not always true, as there are also face-centered finite volume methods. In any case, the values of field variables at non-storage locations (e.g. vertices) are obtained using interpolation.

4.1.2.3. Finite element method (FEM): A finite element method (FEM) discretization is based upon a piecewise representation of the solution in terms of specified basis functions. The computational domain is divided up into smaller domains (finite elements) and the solution in each element is constructed from the basis functions. The actual equations that are solved are typically obtained by restating the conservation equation in weak form: the field variables are written in terms of the basis functions, the equation is multiplied by appropriate test functions, and then integrated over an element. Since the FEM solution is in terms of specific basis functions, a great deal more is known about the solution than for either FDM or

FVM. This can be a double-edged sword, as the choice of basis functions is very important and boundary conditions may be more difficult to formulate. Again, a system of equations is obtained (usually for nodal values) that must be solved to obtain a solution.

Comparison of the three methods is difficult, primarily due to the many variations of all three methods. FVM and FDM provide discrete solutions, while FEM provides a continuous (up to a point) solution. FVM and FDM are generally considered easier to program than FEM, but opinions vary on this point. FVM are generally expected to provide better conservation properties, but opinions vary on this point also.

4.1.3. How does a CFD code work?

CFD codes are structured around the numerical algorithms that can be tackle fluid problems. In order to provide easy access to their solving power all commercial CFD packages include sophisticated user interfaces input problem parameters and to examine the results. Hence all codes contain three main elements:

1. Pre-processing.
2. Solver
3. Post-processing.

4.1.3.1. Pre-Processing:

This is the first step in building and analyzing a flow model. Preprocessor consist of input of a flow problem by means of an operator –friendly interface and subsequent transformation of this input into form of suitable for the use by the solver. The user activities at the Pre-processing stage involve:

- Definition of the geometry of the region: The computational domain.
- Grid generation the subdivision of the domain into a number of smaller, non-overlapping sub domains (or control volumes or elements Selection of physical or chemical phenomena that need to be modeled).
- Definition of fluid properties
- Specification of appropriate boundary conditions at cells, which coincide with or touch the boundary. The solution of a flow problem (velocity, pressure, temperature

etc.) is defined at nodes inside each cell. The accuracy of CFD solutions is governed by number of cells in the grid. In general, the larger numbers of cells better the solution accuracy. Both the accuracy of the solution & its cost in terms of necessary computer hardware & calculation time are dependent on the fineness of the grid. Efforts are underway to develop CFD codes with a (self) adaptive meshing capability. Ultimately such programs will automatically refine the grid in areas of rapid variation.

GAMBIT (CFD PREPROCESSOR): GAMBIT v2.4.6 is a state-of-the-art preprocessor for engineering analysis. With advanced geometry and meshing tools in a powerful, flexible, tightly-integrated, and easy-to use interface, GAMBIT can dramatically reduce preprocessing times for many applications. Complex models can be built directly within GAMBIT's solid geometry modeler, or imported from any major CAD/CAE system. Using a virtual geometry overlay and advanced cleanup tools, imported geometries are quickly converted into suitable flow domains. A comprehensive set of highly-automated and size function driven meshing tools ensures that the best mesh can be generated, whether structured, multiblock, unstructured, or hybrid.

4.1.3.2. Solver:

The CFD solver does the flow calculations and produces the results. FLUENT, FloWizard, FIDAP, CFX and POLYFLOW are some of the types of solvers. FLUENT is used in most industries. FloWizard is the first general-purpose rapid flow modeling tool for design and process engineers built by Fluent. POLYFLOW (and FIDAP) are also used in a wide range of fields, with emphasis on the materials processing industries. FLUENT and CFX two solvers were developed independently by ANSYS and have a number of things in common, but they also have some significant differences. Both are control-volume based for high accuracy and rely heavily on a pressure-based solution technique for broad applicability. They differ mainly in the way they integrate the fluid flow equations and in their equation solution strategies. The CFX solver uses finite elements (cell vertex numeric's), similar to those used in mechanical analysis, to discretize the domain. In contrast, the FLUENT solver uses finite volumes (cell centered numerics). CFX software focuses on one approach to solve the governing equations of motion (coupled algebraic multigrid), while the FLUENT product offers several solution approaches (density-, segregated- and coupled-pressure-based methods)

The **FLUENT CFD** code has extensive interactivity, so we can make changes to the analysis at any time during the process. This saves time and enables to refine designs more efficiently. Graphical user interface (GUI) is intuitive, which helps to shorten the learning curve and make the modeling process faster. In addition, FLUENT's adaptive and dynamic mesh capability is unique and works with a wide range of physical models. This capability makes it possible and simple to model complex moving objects in relation to flow. This solver provides the broadest range of rigorous physical models that have been validated against industrial scale applications, so we can accurately simulate real-world conditions, including multiphase flows, reacting flows, rotating equipment, moving and deforming objects, turbulence, radiation, acoustics and dynamic meshing. The FLUENT solver has repeatedly proven to be fast and reliable for a wide range of CFD applications. The speed to solution is faster because suite of software enables us to stay within one interface from geometry building through the solution process, to post-processing and final output.

The numerical solution of Navier–Stokes equations in CFD codes usually implies a discretization method: it means that derivatives in partial differential equations are approximated by algebraic expressions which can be alternatively obtained by means of the finite-difference or the finite-element method. Otherwise, in a way that is completely different from the previous one, the discretization equations can be derived from the integral form of the conservation equations: this approach, known as the finite volume method, is implemented in FLUENT (FLUENT v6.3 User's guide, 2006), because of its adaptability to a wide variety of grid structures. The result is a set of algebraic equations through which mass, momentum, and energy transport are predicted at discrete points in the domain. In the freeboard model that is being described, the segregated solver has been chosen so the governing equations are solved sequentially. Because the governing equations are non-linear and coupled, several iterations of the solution loop must be performed before a converged solution is obtained and each of the iteration is carried out as follows:

- Fluid properties are updated in relation to the current solution; if the calculation is at the first iteration, the fluid properties are updated consistent with the initialized solution.
- The three momentum equations are solved consecutively using the current value for pressure so as to update the velocity field.
- Since the velocities obtained in the previous step may not satisfy the continuity equation, one more equation for the pressure correction is derived from the continuity

equation and the linearized momentum equations: once solved, it gives the correct pressure so that continuity is satisfied. The pressure–velocity coupling is made by the SIMPLE algorithm, as in FLUENT default options.

- Other equations for scalar quantities such as turbulence, chemical species and radiation are solved using the previously updated value of the other variables; when inter-phase coupling is to be considered, the source terms in the appropriate continuous phase equations have to be updated with a discrete phase trajectory calculation.
- Finally, the convergence of the equations set is checked and all the procedure is repeated until convergence criteria are met.

The conservation equations are linearized according to the implicit scheme with respect to the dependent variable: the result is a system of linear equations (with one equation for each cell in the domain) that can be solved simultaneously. Briefly, the segregated implicit method calculates every single variable field considering all the cells at the same time. The code stores discrete values of each scalar quantity at the cell centre; the face values must be interpolated from the cell centre values. For all the scalar quantities, the interpolation is carried out by the second order upwind scheme with the purpose of achieving high order accuracy. The only exception is represented by pressure interpolation, for which the standard method has been chosen.

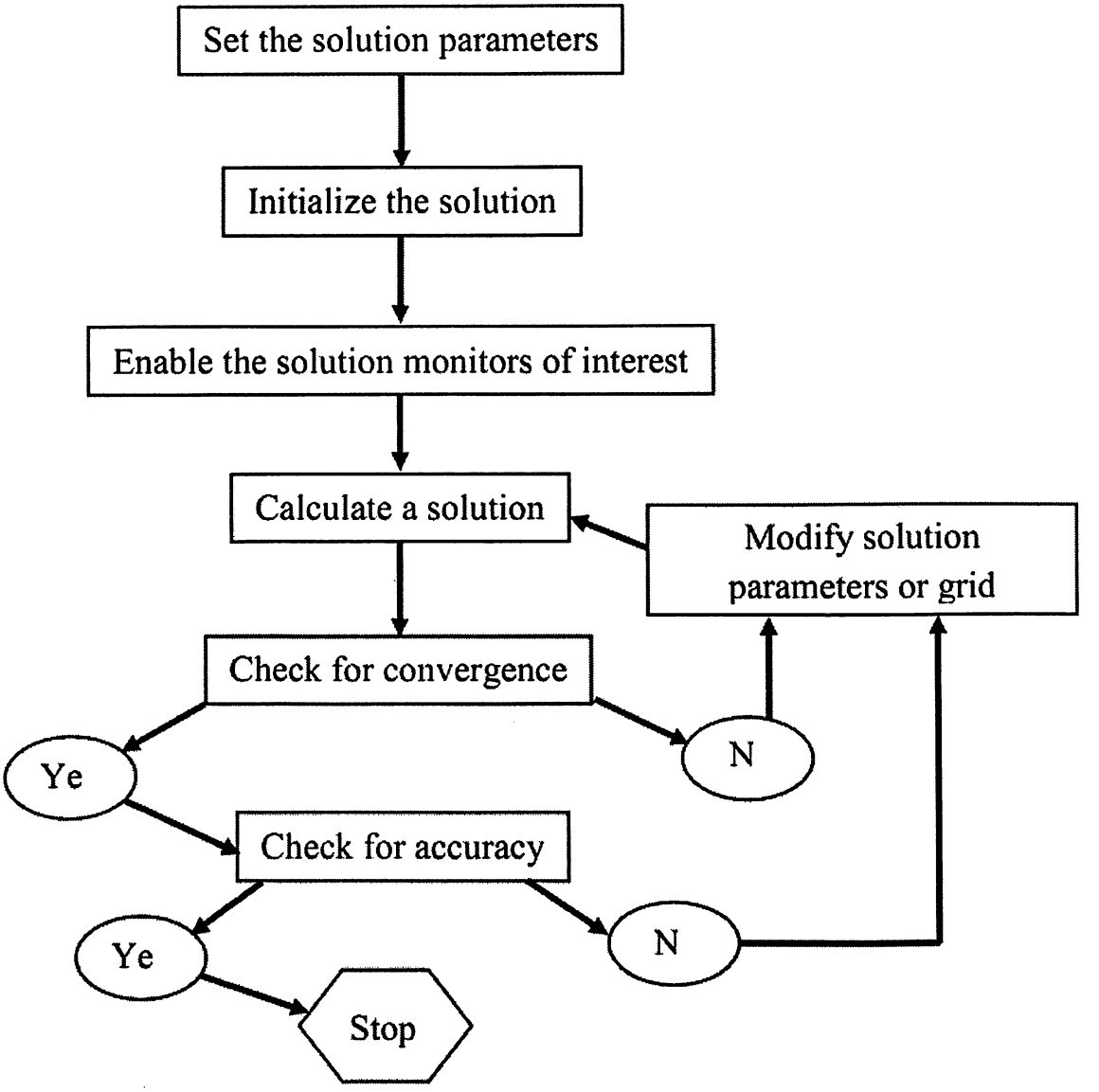

Figure 04-1: Algorithm of numerical approach used by simulation softwares.

Source: Amit Kumar; CFD Modeling of Gas-Liquid-Solid Fluidized Bed; NIT Rourkela; 2009

4.1.3.3 Post-Processing:

This is the final step in CFD analysis, and it involves the organization and interpretation of the predicted flow data and the production of CFD images and animations. Fluent's software includes full post processing capabilities. FLUENT exports CFD's data to third-party post-processors and visualization tools such as Ensight, Fieldview and TechPlot as well as to VRML formats. In addition, FLUENT CFD solutions are easily coupled with structural codes such as ABAQUS, MSC and ANSYS, as well as to other engineering process simulation tools. Thus FLUENT is general-purpose computational fluid dynamics (CFD)

software ideally suited for incompressible and mildly compressible flows. Utilizing a pressure-based segregated finite-volume method solver, FLUENT contains physical models for a wide range of applications including turbulent flows, heat transfer, reacting flows, chemical mixing, combustion, and multiphase flows. FLUENT provides physical models on unstructured meshes, bringing you the benefits of easier problem setup and greater accuracy using solution-adaptation of the mesh. FLUENT is a computational fluid dynamics (CFD) software package to simulate fluid flow problems. It uses the finite-volume method to solve the governing equations for a fluid. It provides the capability to use different physical models such as incompressible or compressible, inviscid or viscous, laminar or turbulent, etc. Geometry and grid generation is done using GAMBIT which is the preprocessor bundled with FLUENT. Owing to increased popularity of engineering work stations, many of which has outstanding graphics capabilities, the leading CFD are now equipped with versatile data visualization tools. These include

- Domain geometry & Grid display.
- Vector plots.
- Line & shaded contour plots.
- 2D & 3D surface plots.
- Particle tracking.
- View manipulation (translation, rotation, scaling etc.)

4.1.4. Advantages of CFD:

Over the past few decades, CFD has been used to improve process design by allowing engineers to simulate the performance of alternative configurations, eliminating guesswork that would normally be used to establish equipment geometry and process conditions. The use of CFD enables engineers to obtain solutions for problems with complex geometry and boundary conditions. A CFD analysis yields values for pressure, fluid velocity, temperature, and species or phase concentration on a computational grid throughout the solution domain. Advantages of CFD can be summarized as:

i. It provides the flexibility to change design parameters without the expense of hardware changes. It therefore costs less than laboratory or field experiments, allowing engineers to try more alternative designs than would be feasible otherwise.

ii. It has a faster turnaround time than experiments.

iii. It guides the engineer to the root of problems, and is therefore well suited for trouble-shooting.

iv. It provides comprehensive information about a flow field, especially in regions where measurements are either difficult or impossible to obtain.

v. CFD solutions are reliable can very much depict the real flow conditions. The numerical methods embedded in FLUENT solver is improving day-by-day. The results too obtained are consistent with experimental results.

vi. CFD allows an engineer to analyze and examine data at numerous locations in the model. In the experimental models data can be extracted at specific locations only.

vii. CFD can simulate a lot of real time flow and heat transfer processes, e.g., hypersonic flow and processes occurring at high temperatures and pressures etc. CFD can be used for simulation of almost all theoretical processes.

4.1.5 Limitations of CFD:

In spite of large advantages of CFD, it has some limitations which are as follows (Bakker, 2002):

Physical models – CFD solutions rely upon physical models of real world processes (e.g. turbulence, compressibility, chemistry, multiphase flow, etc.).The CFD solutions can only be as accurate as the physical models are.

Numerical errors – Solving equations on a computer invariably introduces numerical errors. Round-off error is due to finite word size available on the computer. Round-off errors can be always found in CFD solutions but they may be very small in most cases. Second most common error found in CFD solution is truncation error, due to approximations in numerical models.

Boundary conditions – The CFD solution will only be as good as the initial/boundary conditions provided to the numerical model.

CHAPTER 05. CFD SIMULATION OF PACKED BED REACTOR FOR TAR CRACKING

5.1 COMPUTATIONAL FLOW MODEL

All of CFD is based on the fundamental governing equations of fluid dynamics, i.e, the continuity, momentum and energy conservation equations. These are mathematical statements of three fundamental physical principles upon which whole of fluid dynamics is based. They are:

- Mass is conserved.
- Newton's second law.
- Energy is conserved.

A solid body is rather easy to say and define but on the other hand fluid is a squishy substance that is hard to grab hold of. If a sold body is in translational motion, the velocity of each part of the body was assumed to be same but if a fluid was in motion, the velocity may be different at each location in the fluid. It's a question how a moving fluid can be visualized so as to apply in it the fundamental physical principles. For a continuum fluid, one of the four models described below is to be constructed so as to apply it in fundamental physical principles (Anderson. J; 1995):

i. Model of finite control volume fixed in space.
ii. Model of finite control volume moving with fluid flow.
iii. Model of infinitesimally small fluid elements fixed in space.
iv. Model of infinitesimally small fluid element moving with fluid flow.

The governing equations can be obtained in various different forms. For most application theory the particular form of the equations makes little difference but however, for a given algorithm in CFD, the use of equations in one form may lead to success, whereas the use of alternate forms may lead to different numerical results as in incorrect or unstable results. Therefore, in the world of CFD, the various forms of equations are of vital role in application. The governing equations which come from finite control volume are in integral form where as those originates from model of an infinitesimally small fluid element are in differential form. Fig 5.1 shows the generation of basic governing form used in CFD from fundamental physical principles.

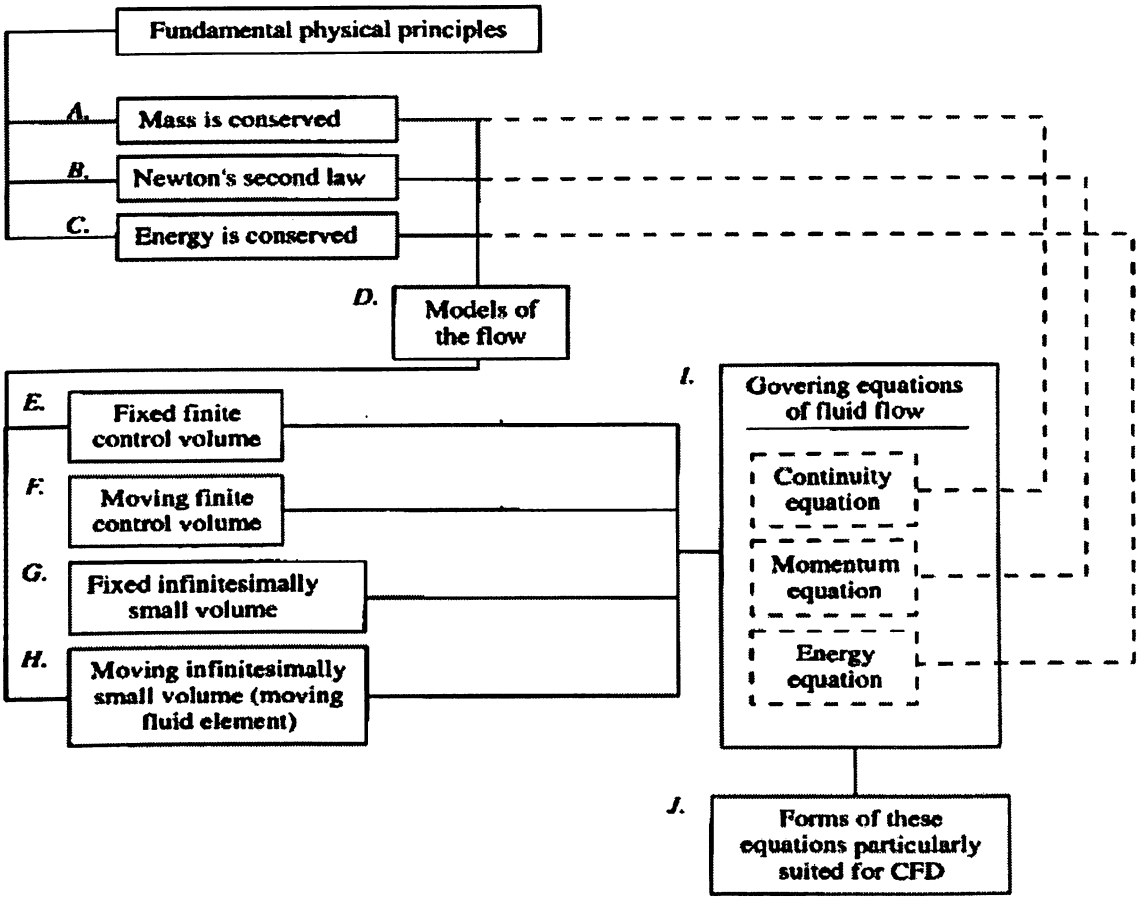

Figure 05-1: Basic governing forms used in CFD from fundamental physical principles.

Source: Anderson. J; 1995.

4.1.1 Governing Equations

In the present work model of finite volume fixed in space is considered which is differential and conservation form. In the 2D model a single homogenous phase of catalyst and reacting fluid (gas) mixture was assumed while in the 3D model two phases were assumed solid catalyst particles and reacting fluid (gas phase). In the both the case motion of each phase was governed by respective mass and momentum conservation equations.

Continuity:

$$\frac{d}{dt}(\rho\varepsilon_k) + \nabla.(\rho\bar{u}) = 0$$

Equation 05-1: Continuity equation

Where,

ρ is the density of gas.

ε_k is volume fraction of solids.

ū denotes superficial velocity of the gas.

Momentum:

$$\rho\left[\frac{1}{\varepsilon_k}\frac{d}{dt}u_x + \frac{u_x}{{\varepsilon_k}^2}.\frac{d}{dx}u_x\right] = \rho g_x - \frac{dP}{dx} - \left(\frac{\mu}{k} + \frac{\rho.C}{K^{0.5}}u_x\right).u_x + \frac{\mu}{\varepsilon_k}\frac{d^2u_x}{dx^2}$$

Equation 05-2: Momentum equation

If we assume that the system is at steady state with no appreciable body forces, insignificant viscous dissipation and taking the axial velocity diffusion to be negligible then the momentum equation reduces to the Ergun equation:

$$\frac{dP}{dx} = 150\frac{(1-\varepsilon)^2}{{\varepsilon_k}^3}\frac{\mu u_x}{{d_p}^2} + 1.75\frac{1-\varepsilon_k}{{\varepsilon_k}^3}\frac{\rho {u_x}^2}{d_p}$$

Equation 05-3 : Ergun Equation

Where,

P is the pressure.

μ is the effective viscosity.

Energy:

$$\left[\rho C_p\varepsilon + \rho_s C_{p,s}(1-\varepsilon_k)\right].\frac{dT}{dt} + \rho C_p u_x.\frac{dT}{dx} = \left[k\varepsilon_k + k_s(1-\varepsilon_k).\frac{d^2T}{dx^2}\right] + \left[\varepsilon_k q + (1-\varepsilon_k)\,q_s\right] + u_x\left[-\frac{dP}{dx} + \frac{\mu}{\varepsilon_k}\frac{d^2u_x}{dx^2} + \rho q\right]$$

Equation 05-4 : Energy Equation

Where,

C_p, $C_{p,s}$ are specific heat capacity of fluid and solids respectively.

k, k_s are thermal conductivity of fluid and solids respectively.

q, q_s are heat for fluid and solid phases respectively.

5.1.2 Turbulence Modeling

It is a very unfortunate fact that no single turbulence model is universally accepted as being superior for all classes of problems. The choice of turbulent model will depend on considerations such as the physics encompassed in the flow, the established practice for a specific class of problem, the level of accuracy required, the available computational

resources, and the amount of time available for simulation. In present simulation (κ-ε) model has been taken for turbulence modeling.

The standard (κ-ε) model is a semi-empirical model based on model transport equations for the turbulent kinetic energy (κ) and its dissipation rate (ε). The model transport equation for turbulent kinetic energy is derived from the exact equation, while the model transport equation for dissipation rate is extracted from Fluent v6.3 User's Guide, 2006. The equations are as follows:

$$\frac{\partial}{\partial t}(\rho\kappa) + \frac{\partial}{\partial x_i}(\rho\kappa v_i) = \frac{\partial}{\partial x_j}\left[\left(\mu + \frac{\mu_t}{\sigma_k}\right)\frac{\partial \kappa}{\partial x_i}\right] + G_k + G_b - \rho\varepsilon - Y_m + S_\kappa$$

Equation 05-5: Model transport equation for turbulence.

And

$$\frac{\partial}{\partial t}(\rho\varepsilon) + \frac{\partial}{\partial x_i}(\rho\varepsilon v_i) = \frac{\partial}{\partial x_j}\left[\left(\mu + \frac{\mu_t}{\sigma_\varepsilon}\right)\frac{\partial \varepsilon}{\partial x_i}\right] + C_{l\varepsilon}\frac{\varepsilon}{\kappa}(G_k + C_{3\varepsilon}G_b) - C_{2\varepsilon}\rho\frac{\varepsilon^2}{\kappa} + S_\varepsilon$$

Equation 05-6: Model transport equation for turbulent energy dissipation.

Source: Anderson.J; 1995

In the equations above (equation 4.5 & 4.6), G_κ represents the generation of turbulent kinetic energy due to mean velocity gradients, G_b is the generation of turbulent kinetic energy due to buoyancy, Y_M represents the contribution of fluctuation dilatation in compressible turbulence to the overall dissipation rate, $C_{1\varepsilon}$, $C_{2\varepsilon}$ and $C_{3\varepsilon}$ are constants. σ_κ and σ_ε are the turbulent Prandtl numbers for turbulent kinetic energy and dissipation rate respectively. S_κ and S_ε are user defined source terms with C_μ being constant.

The turbulent viscosity (μ_t), is calculated using κ and ε as follows:

$$\mu_t = \rho C_\mu \frac{\kappa^2}{\varepsilon}$$

Equation 05-7: Turbulent viscosity

Source: Anderson.J; 1995

Where, C_μ is constant.

5.1.3 Discretization

To obtain an approximate numerical solution, we have to use a discretization method which approximates the differential equations by a system of algebraic equations, which can then be further solved. The approximations are applied to small domains of space of time so that the numerical solutions provide results at discrete locations in space in time. It concerns

to the process of transferring models and equations into the discrete counterparts. This process is usually carried out as a first steps toward making them suitable for numerical evaluation and implementation on digital computers. For a given, differential equation there are many possible ways to derive the discretized equations such as finite difference, finite element and finite volume to achieve a stable numerical result as explained by fig 5.2.

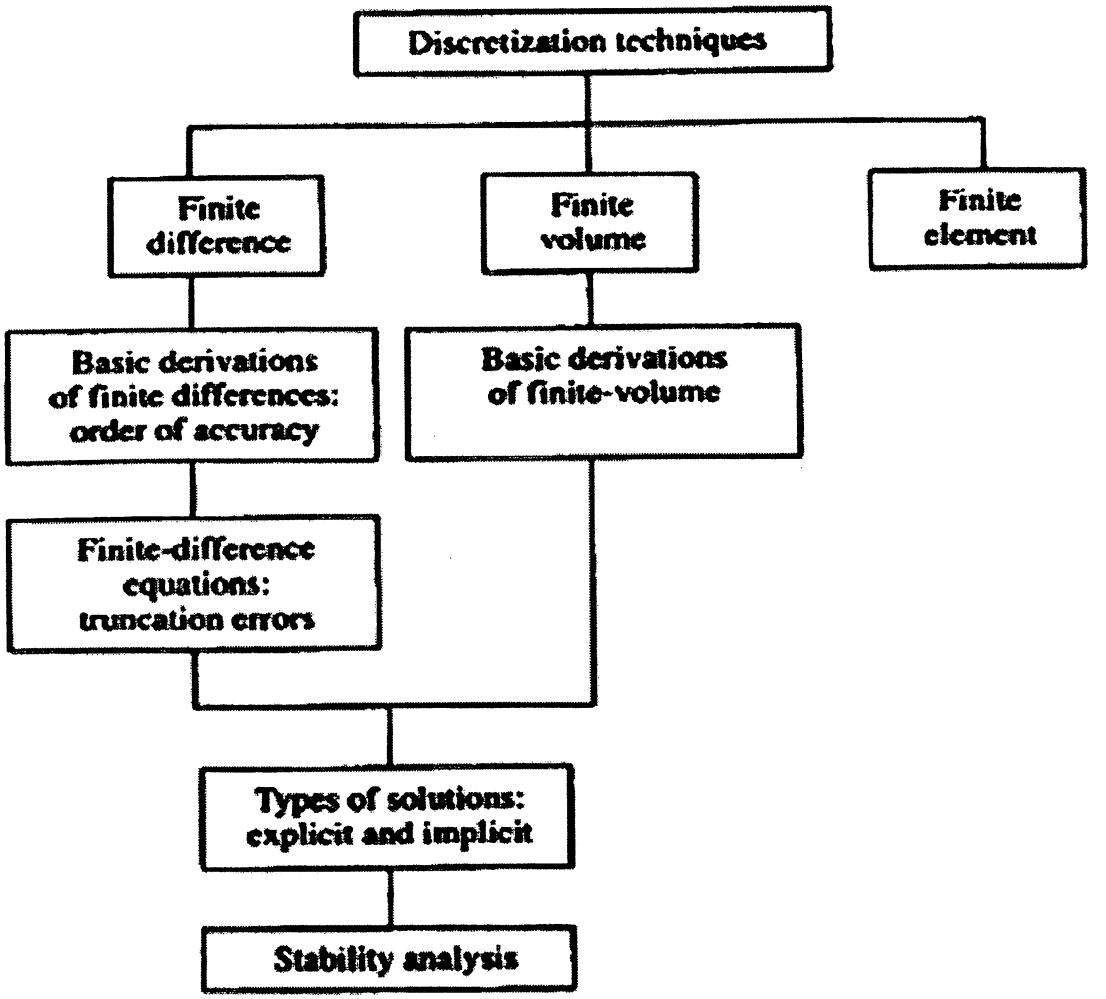

Figure 05-2: Discretization Techniques (Anderson, 1995)

Finite volume methods ensure integral conservation of mass and momentum over any group of control volumes. The effectivity of the numerical solution depends on the type and quality of the discretization method used. Each type of method yields quite similar results if the grid used is very fine; however, some problems require some specific set of discretization method (Ferziger, 2002). In the present work discretization based on finite volume method is used.

Fluent uses Finite Volume Analysis (FVM) of discretization to convert governing equation to algebraic equation to solve them numerically in an effective manner. FVM recasts

the PDE's (Partial Differential Equations) of the Navier's – Stoke Equation in the conservative form and discretized this equation. The solution domain is divided into finite number of contiguous control volumes (CV), where conservation equations are applied. At the centroid of each CV, there lies a computational node at which the values of the variables are calculated. Interpolation is used to express the variable values at the CV surface in terms of nodal (CV centre) values. Surface and volume integrals are approximated using suitable quadrature formulae. The integration approach yields a method that is inherently conservative (i.e., quantities such as density remain physically meaningful). This is demonstrated by the following equation written in integral form for any arbitrary control volume, V as:

$$\frac{\partial}{\partial t}\iiint Q\, dV + \iint F\, dA = 0$$

Equation 05-8: Integral form of a differential equation for any elemental control volume 'dV'

Where,

Q is the vector of conserved variables.

F is the vector of fluxes.

V is the cell volume.

A is the cell surface area.

The FVM approach is the simplest to understand and easy to program, also it can accommodate any kind of grid and as such, it can be used for complex grid analysis too. The grid defines only the control volume boundaries and need not to be related to coordinate systems. There are three levels by which a system can be solved by FV Analysis, i.e. approximation, interpolation and differentiation. So it is the disadvantage of the FVA that systems higher than second (2^{nd}) order cannot be very effectively solved by FV method for 3D systems.

5.1.4 Computation of Energy Flows

In packed bed reactors the energy in the gas feed stream is evenly distributed in the mean flow of the gas and liquid (if any produced) and very tiny solid particles (attrition of solid particles). Also, a part of the input energy is dissipated in the turbulence created in the bed and some is lost due to friction between the gas and solid phases and the walls of the reactor. Apart, from these energy dissipation factors energy is lost to surroundings, collision among gas and solid particles and solid fluctuations. Although model in this study is a single phase system with solid particles as obstacles in fluid flow these modes of energy dissipation

cannot be quantified. Hence, these terms are neglected in the energy calculation. In general, the difference in energy between the input and output stream should account for the energy loss due to dissipation in the bed. Thus, energy lost in this system by a very simple rule, i.e.

$$Energy\ difference = E_1 - E_{out} - E_T - E_e - E_{Bls} - E_{Blg}$$

Equation 05-9: Energy calculation.

Where,

E_1 is entering the packed bed reactor.

E_{out} is energy in the exit stream from packed bed.

E_T is energy gained by the solid particles.

E_e is energy dissipated by gas phase dissipation.

E_{blg} is energy dissipated due to interaction between gas and solid catalyst particles.

CHAPTER 06. NUMERICAL METHODOLOGY

In the present work of tar cracking in packed bed reactor using dolomite as catalysts. The bed of catalysts remains static during the whole analysis and model compound toluene is introduced in to reactor. In the 2d model a PFR was considered with single homogeneous phase of solid and gas whereas two distinct phases dolomite (solid) and toluene vapor was taken in consideration. The model equations described in Chapter 04 are solved using commercial CFD software package Fluent v6.3.26. Fig 5.1 shows the general procedure for simulating using Fluent software.

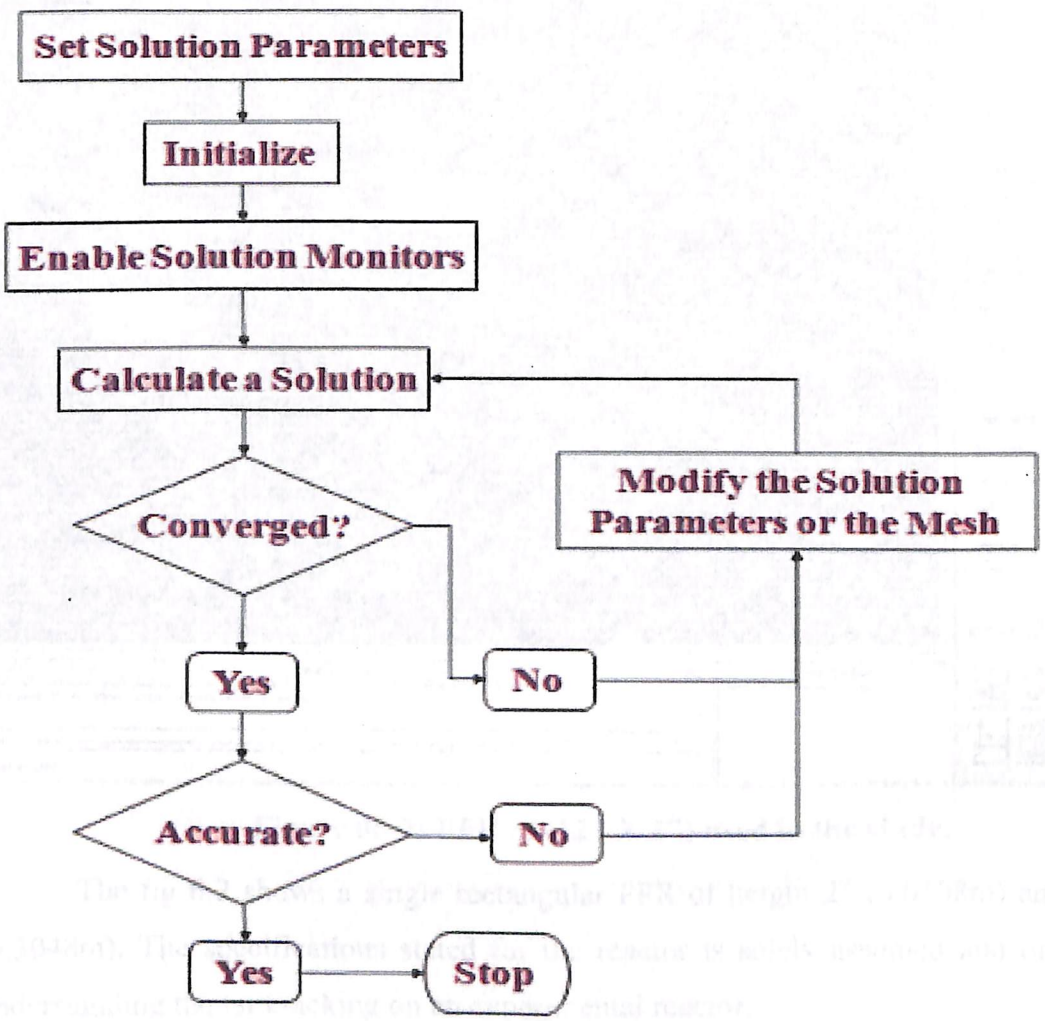

Figure 06-1: Algorithm for simulation occurring in Fluent software (Anderson, 1995)

6.1 GEOMETRY CREATION

The first phase in CFD simulation of a packed bed reactor in Fluent is preprocessing, which is done by using GAMBIT tool. The creation of the geometry and meshing is done in GAMBIT. Below analysis can be done in Fluent, it requires the domain in which flow takes

place to evaluate the solution. The flow domain as well as the grid generation into the specific domain have been created in GAMBIT and are shown below:

6.1.1 The 2D model

6.1.1.1 Geometry creation

As stated earlier the 2D model consists of a single homogeneous phase solution domain. Fig 6.2 below shows the rectangular PFR used in the study.

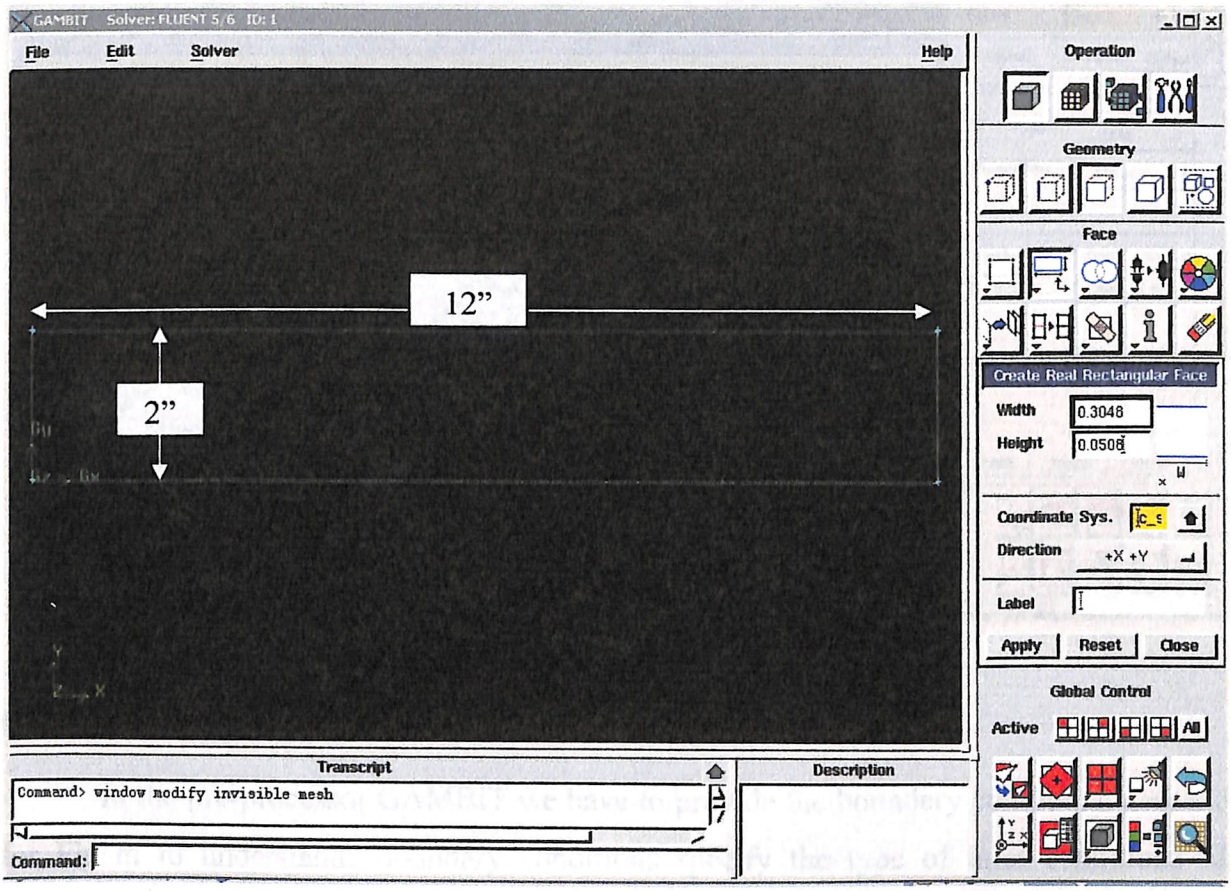

Figure 06-2: PFR of (12" X 2") used in the study.

The fig 6.2 shows a single rectangular PFR of height 2” (0.0508m) and weight 12” (0.3048m). The specifications stated for the reactor is solely assumed and on the basis of understanding the tar cracking on an experimental reactor.

6.1.1.2 Meshing

In fig 6.3 we mesh the rectangular PFR using quad scheme with pave type meshing. A mesh count of 300 was applied. The mesh count selected is fine enough to show fine and even meshing all along the flow region. Meshing is a very part of CFD, upon meshing a body we create a grid all along the body. As stated earlier, finite volume analysis will be used to determine the flow condidtions so meshing creates the nodal points along which the

implicit/explicit finite volume analysis will be used using the initial boundary conditions as reference values.

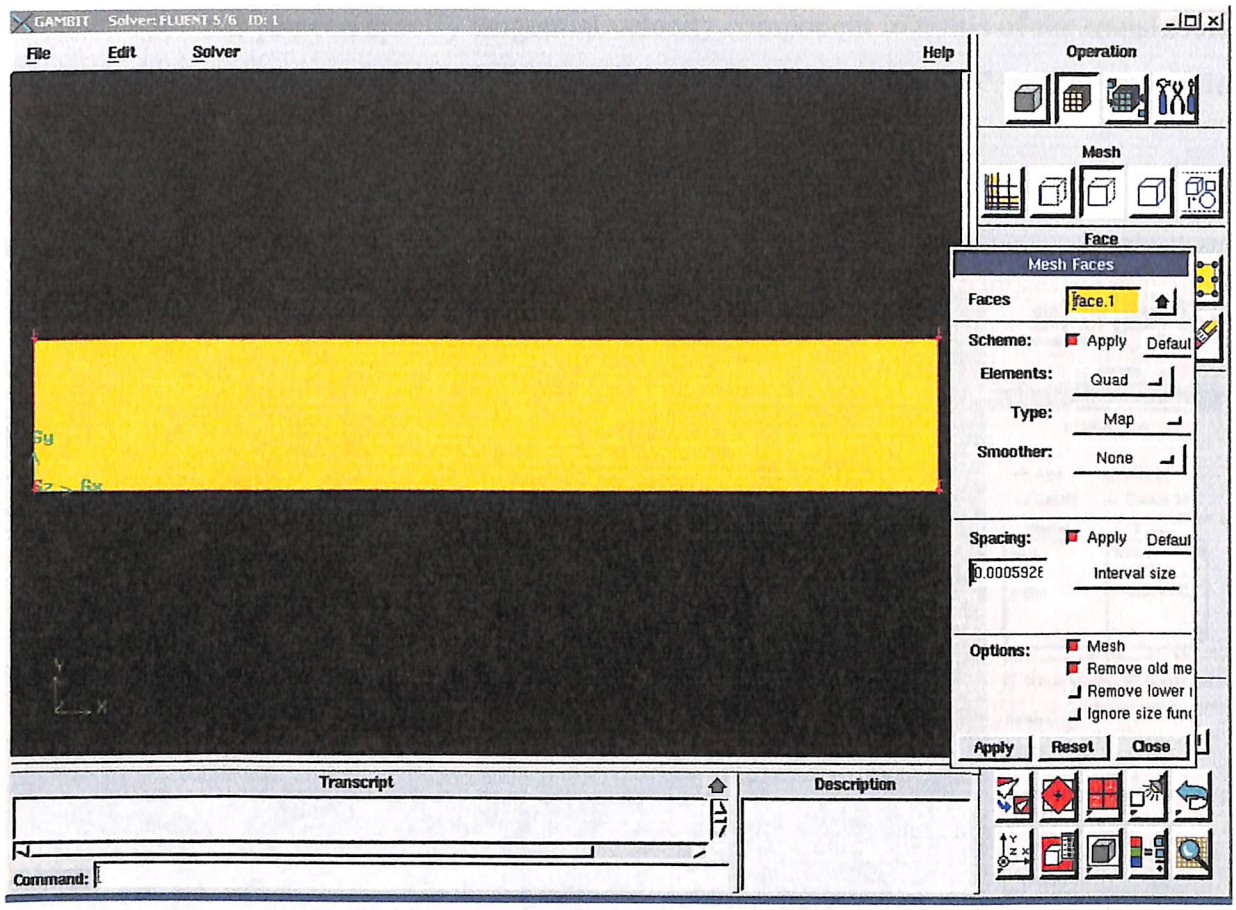

Figure 06-3: Meshing scheme and meshed body

6.1.1.3 Boundary conditions

In the pre-processor GAMBIT we have to provide the boundary conditions necessary for Fluent to understand. Boundary conditions specify the type of inlet conditions like velocity inlet, pressure outlet, mass flow inlet etc.

In fig 6.4 below there are three types of boundary conditions:

- Mass flow inlet – In chemical engg. mass flow inlet conditions is the best way to specify as we can specify individual species mass fraction also along with amount of mass of fluid that is to be processed.
- Pressure outlet – Pressure outlet boundary conditions are used to define the static pressure at flow outlets(and also other scalar variables, in case of back flow).The use of a pressure outlet boundary condition instead of an outflow condition often results in a better rate of convergence when backflow occurs during iteration.

- Wall – Wall boundary conditions are used to bound fluid and solid regions. In viscous flows, the no-slip boundary condition is enforced at walls by default, but you can specify tangential velocity component in terms of the translational or rotational motion of the wall boundary, or model a ”slip" wall by specifying shear

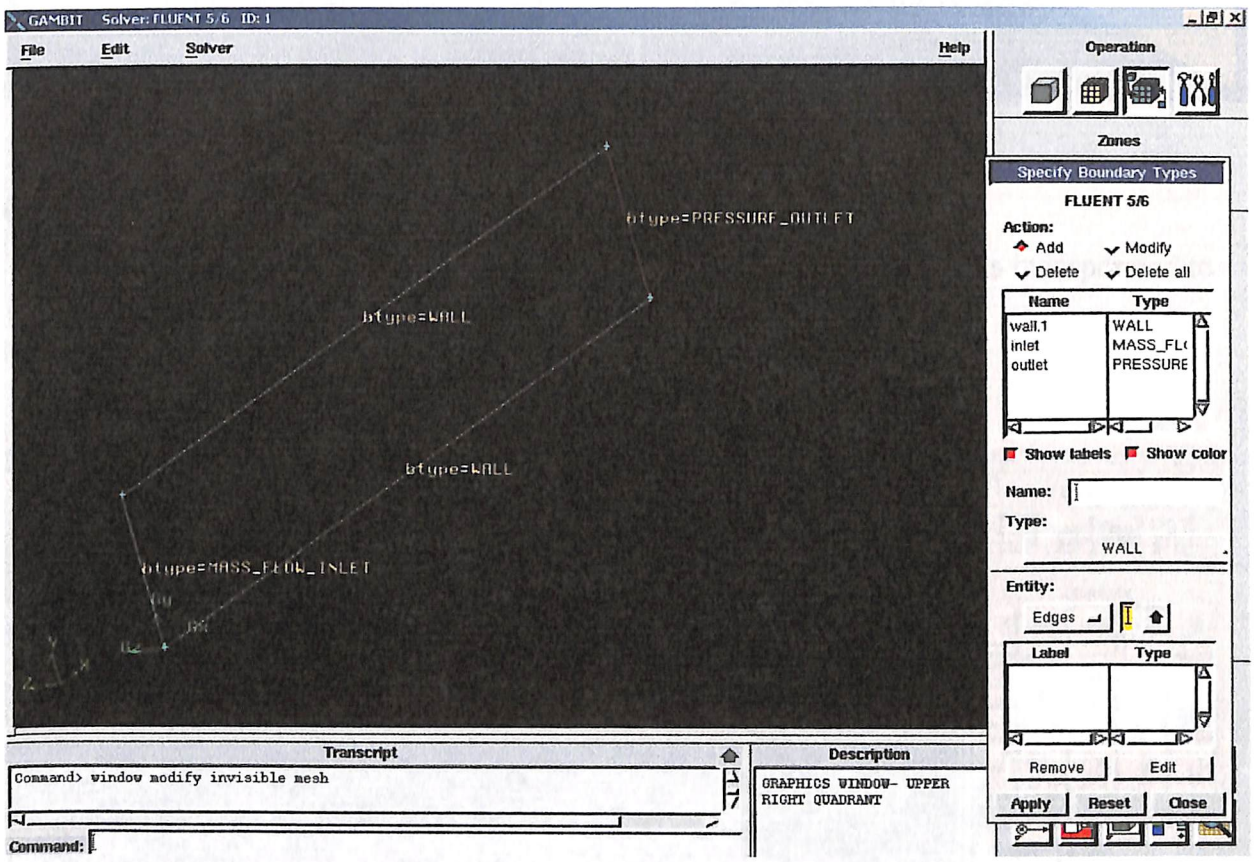

Figure 06-4: Initial boundary conditions

After we have stated the boundary conditions save the file and export the meshed file in .msh format and save it in desired folder. As this geometry is 2D we check the “export 2D (X-Y) mesh”, refer *“Figure 06-5: Mesh file export”*

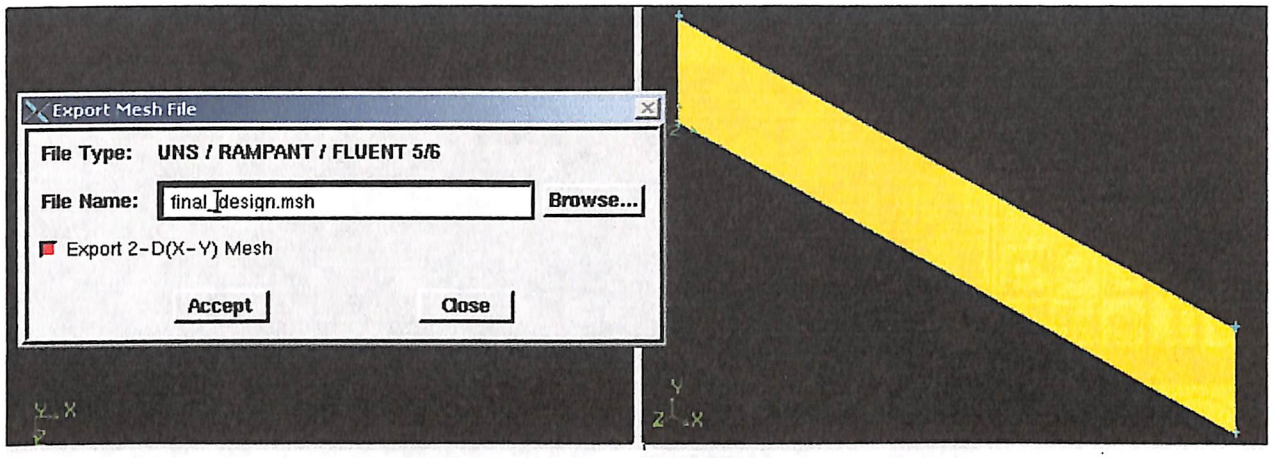

Figure 06-5: Mesh file export

6.1.2 The 3D Model

Unlike the 2D model in the 3D model there are lot of changes which is incorporated to

6.1.2.1 Geometry creation

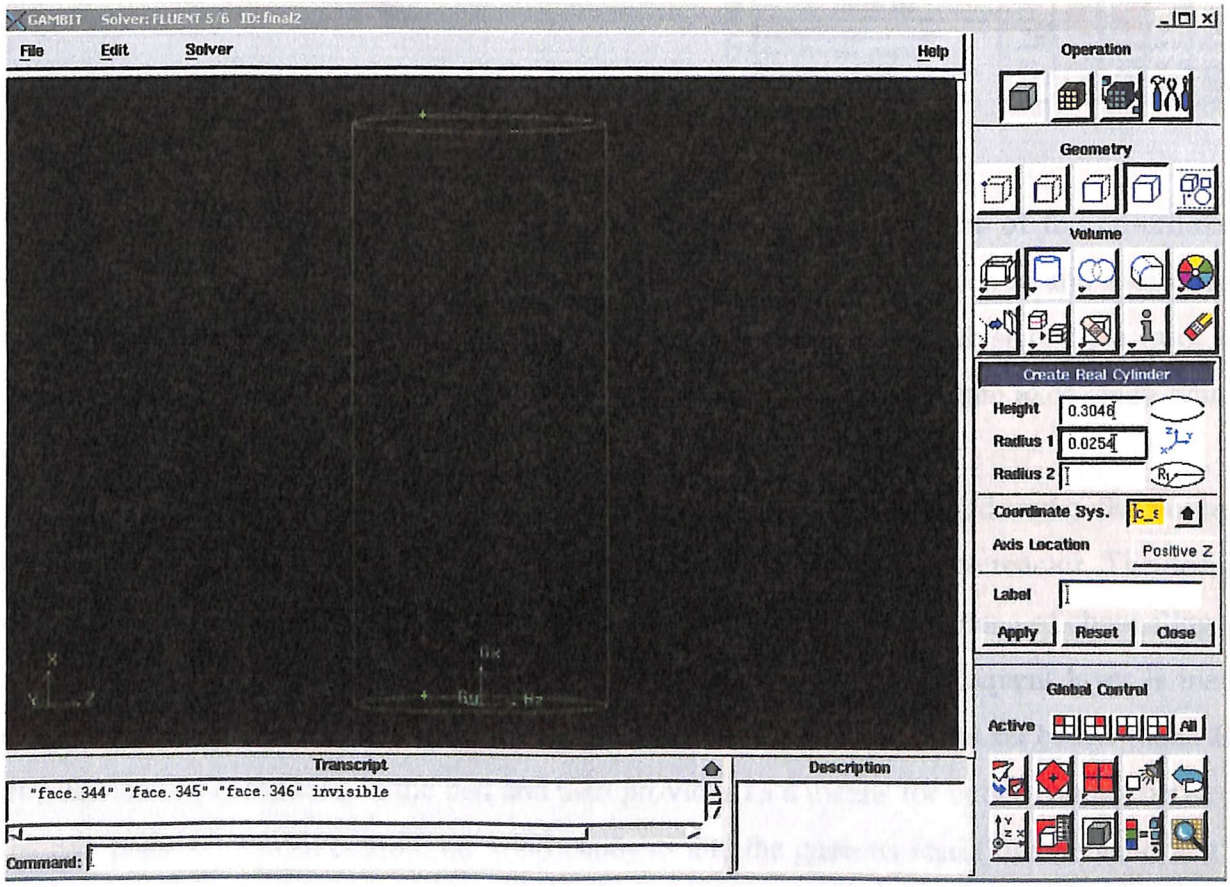

Figure 06-6: Cylindrical packed bed reactor (1"radius and 12"length).

The next step is creation of the spherical catalyst particle of 0.5" diameter which is shown in fig 6.6.

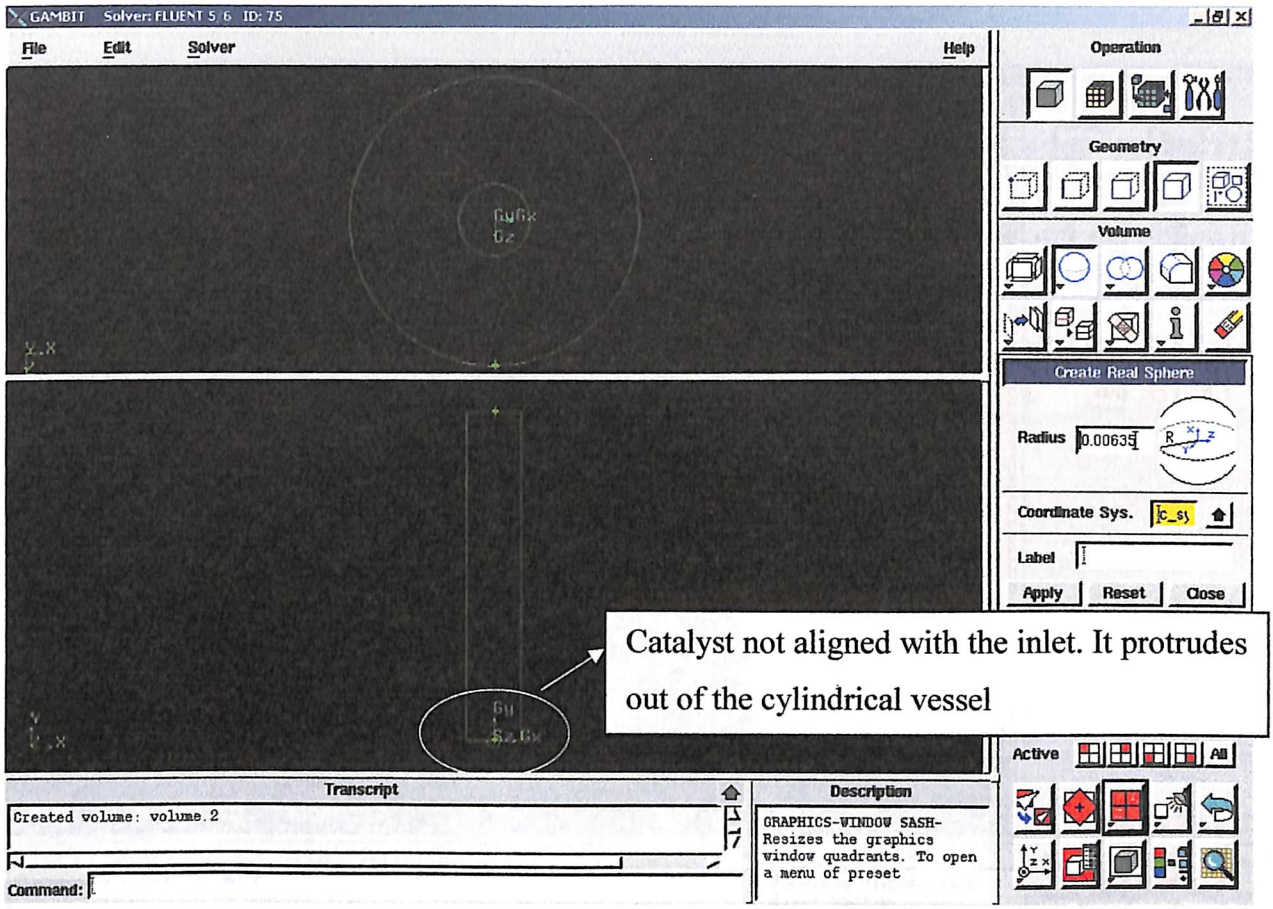

Figure 06-7: Creation of a single catalyst particle.

It can be seen fig 6.7 that first particle is created at the centre of the co-ordinate system. After that by move volume command we move it in the y-direction and x-direction and bring it in alignment which is demonstrated by fig 6.8. The catalyst particle must be aligned in all the axes and should occupy space in all the three coordinate axes along which the span of whole cylindrical vessel exists.

In the subsequent figures we perform copy operations embedded under the volume creation command and form the bed. The bed height is taken same as the reactor. The design of the bed is done in structured form with effort to minimize the phenomena of channeling as much as possible. Initially the first layer of bed is made then the subsequent layer is made such that each particle in layer-2 (group-2) lies between the two particles set below them. By this channeling is reduced in the bed and also provides as a means for better contact between the two phases in consideration, i.e. solid catalysts and the gaseous feed (toluene vapor). It is considered that a random arrangement of bed is better but in designing a randomly arranged bed in GAMBIT we have to imagine a random bed or randomness which is quite impossible.

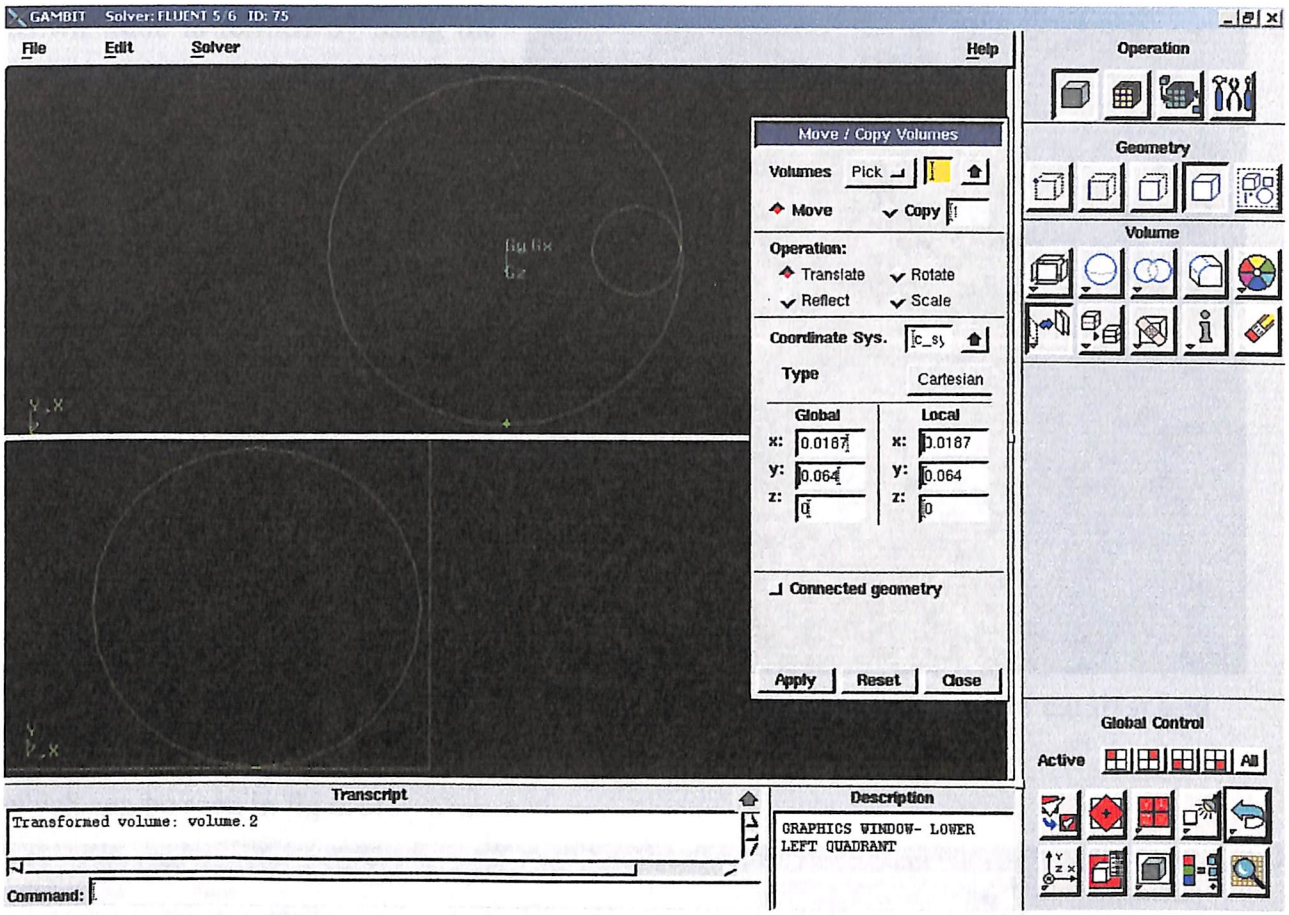

Figure 06-8: Alignment of the catalyst particle

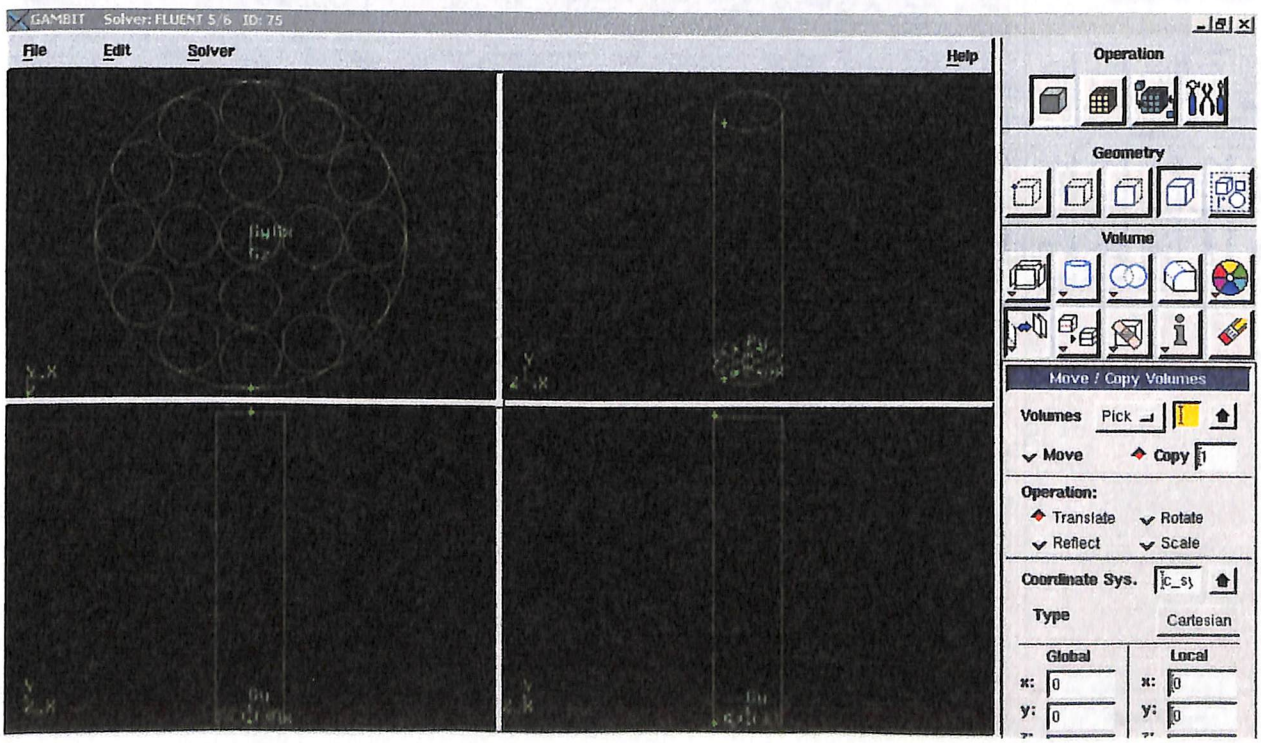

Figure 06-9: The first layer of catalyst bed formed using copy command button

The second layer of catalysts shown aside is formed by using the first layer. We rotate each catalysts particle lying on the extremities of the cylindrical vessel by 75^0 around the Y-axis. Now, particles adjacent to the former are rotated along Y-axis at 45^0. The centrally lying particle is common on all the layers. Initially when the second layer was constructed as by the procedure stated above, the whole layer is selected and moved along the Y-axis, i.e., rose along the Y-axis by 0.015m, which can be seen in fig 6.11.

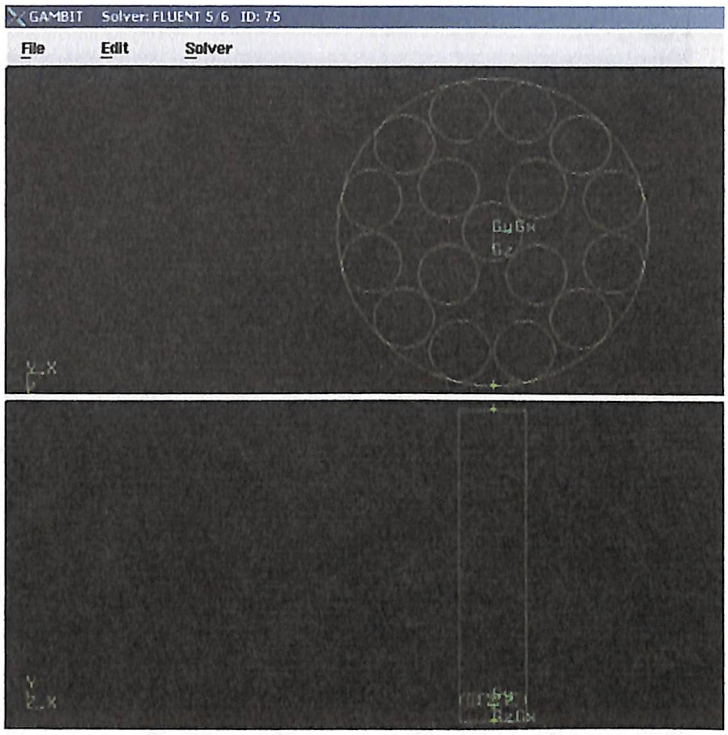

Figure 06-10: The second layer of catalyst bed

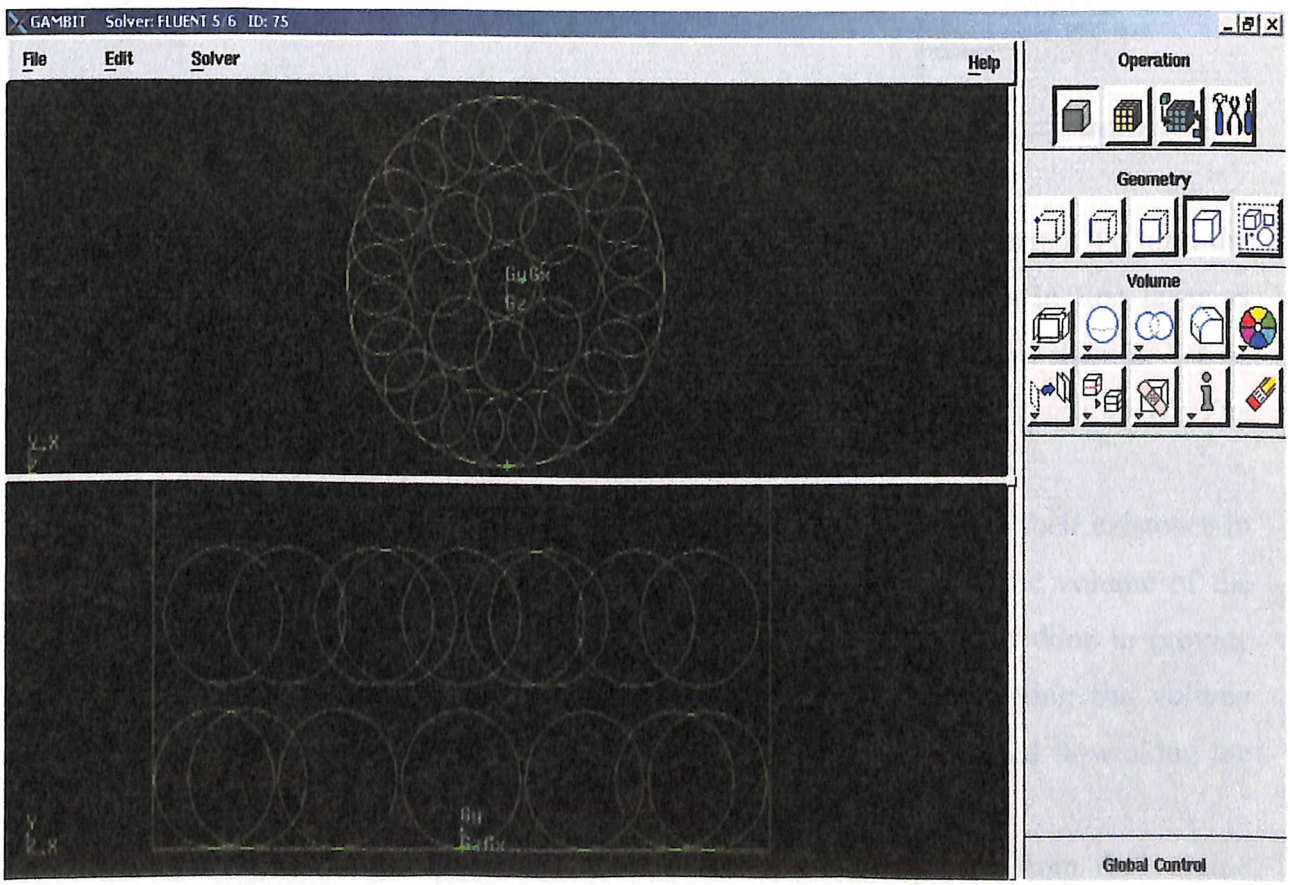

Figure 06-11: The two layers of catalysts bed, after the copy and move operations.

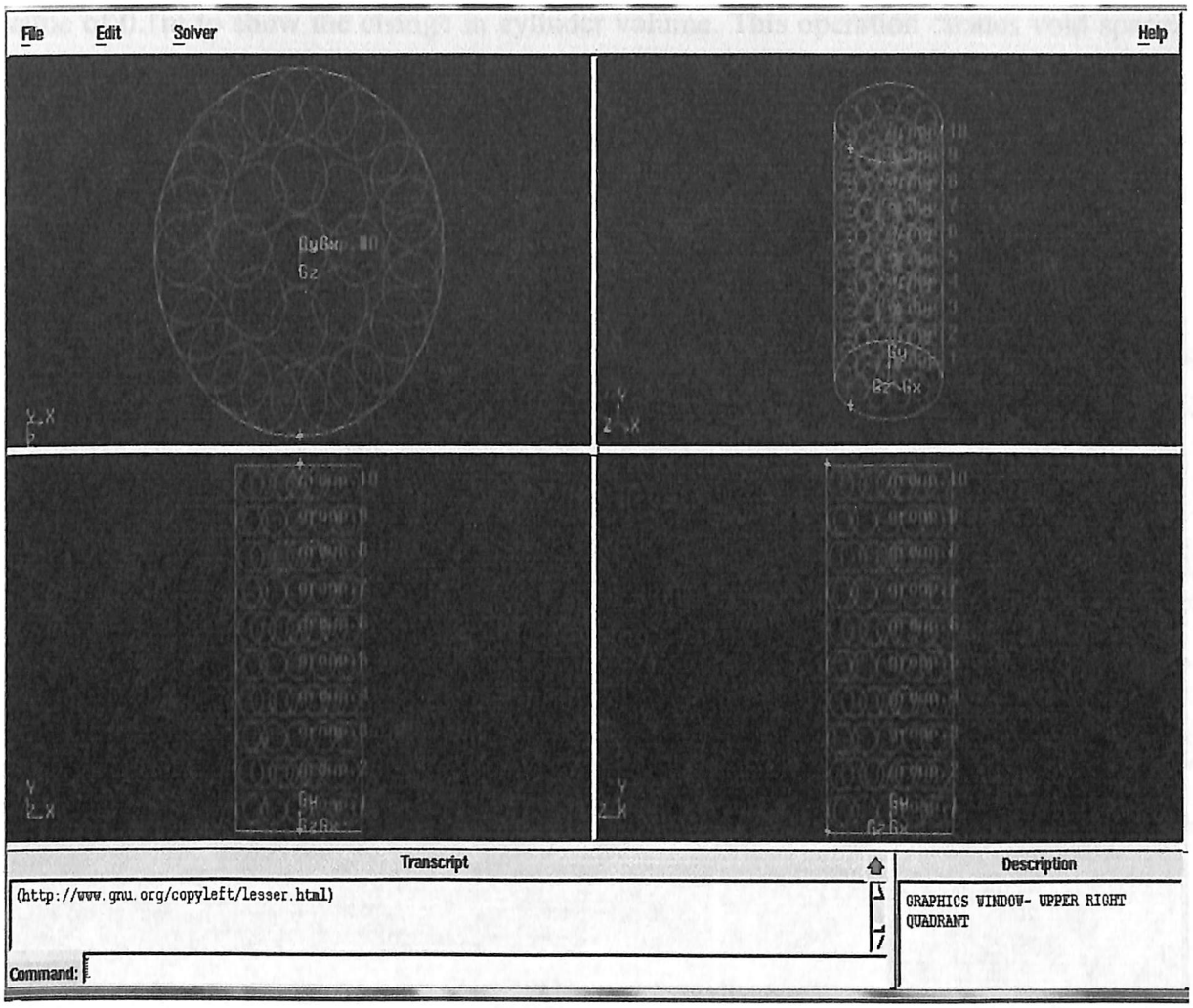

Figure 06-12: The complete bed of catalysts.

In fig 6.12 the whole bed of catalysts is formed by using copy command. To form the whole bed we initially form groups, i.e. we group the spherical particles in first layer as group-1 and the second layer as group-2. Then we select each group and copy them in Y-axis at 0.03m (2 x 0.015m, value at which the second layer is moved, refer *"Figure 06-10: The second layer of catalysts bed").*

Now, these catalysts particles are solids but for fluent to understand their existence in the flow domain we subtract the volume occupied by the spheres from the volume of the cylinder and retain the volume of spheres. This operation in GAMBIT is done to provide individuality to the spheres. If Fluent analysis is done without subtracting the volume occupied by spheres from cylinder volume then we will observe unhindered flow along the flow regime.

In fig 6.13 below we subtract the volume occupied the spheres from the volume occupied by the cylinders and after that we move the groups of catalysts along X-axis by a

value of 0.1m to show the change in cylinder volume. This operation creates void spaces in the cylinder volume which makes Fluent to understand that there is no flow through these voids or volume occupied by catalysts. We retain the volume of spheres because flows through these are based on porous media concept the parameters for which are to be dictated in Fluent solver.

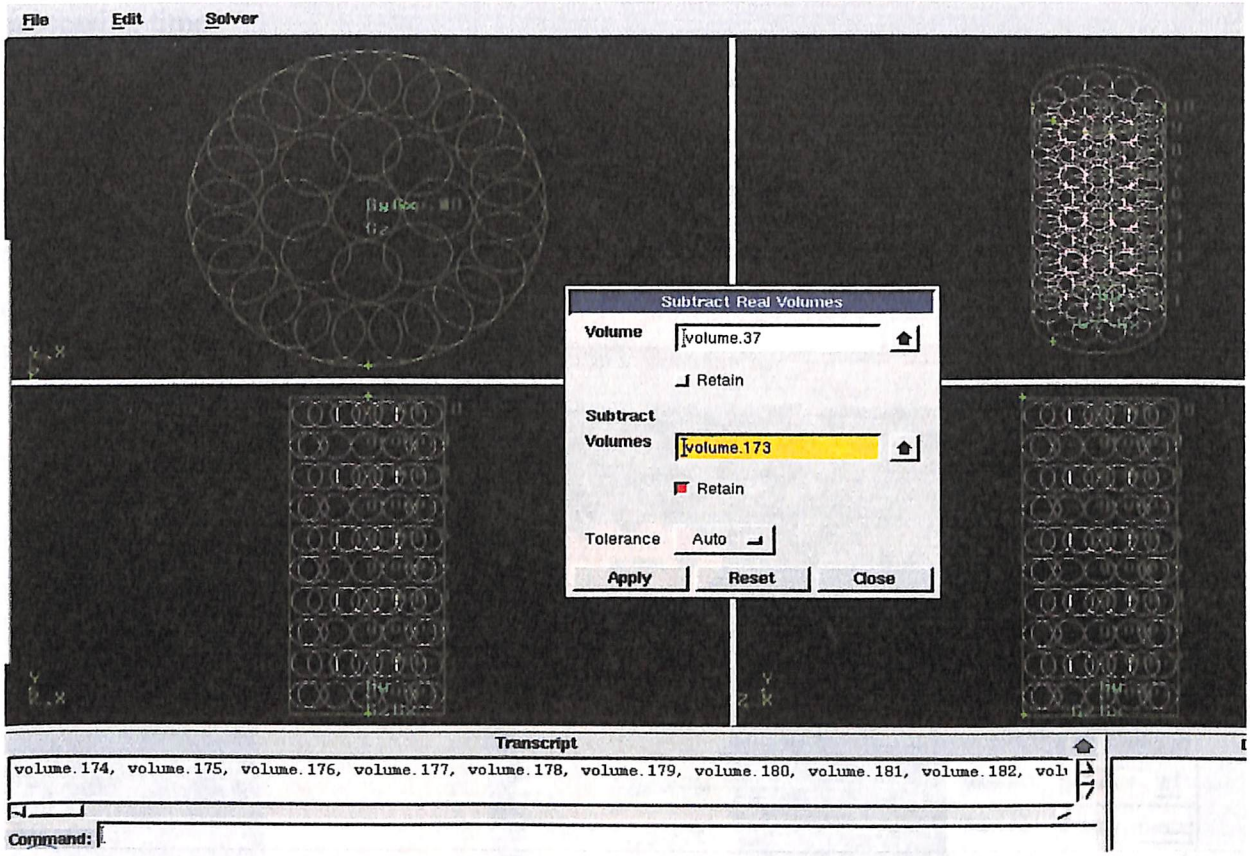

Figure 06-13: Subtraction of volumes

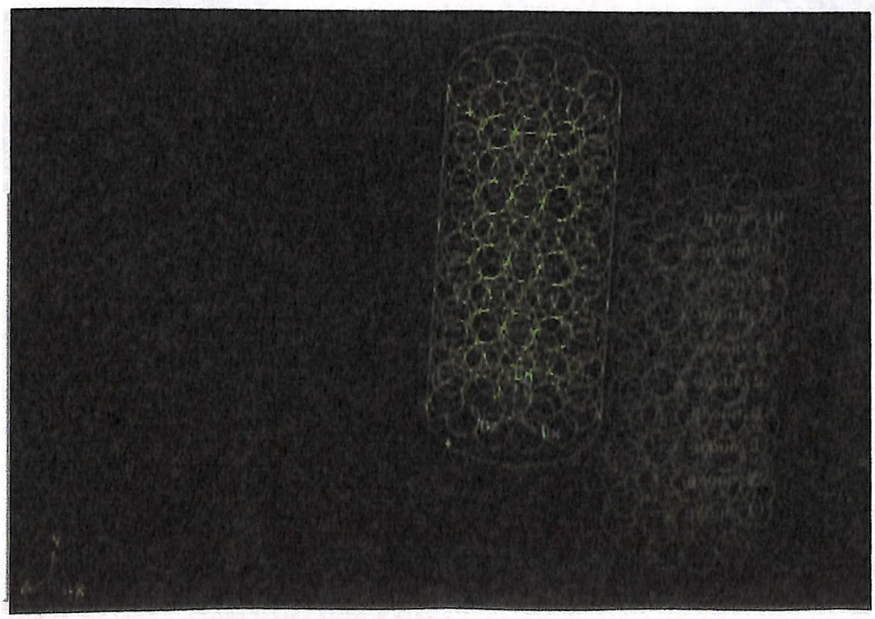

Figure 06-14: Change in flow domain due to subtraction operation.

6.1.2.2 Meshing

Meshing is a very important operation in CFD analysis. As stated in "*4.1.3. How does a CFD code work?"* that finite volume analysis needs that the region of analysis to be divided into several grids. Meshing operation is done so as to divide the flow domain into grids. The finer the meshing operation better are the simulation results, but at the expense of more processing time.

In fig 6.15 we initially perform mesh operations on the face, i.e. we first mesh the circular faces of the spherical catalysts with an interval size of 0.001 using quad scheme with pave type. The reason for using quad-pave combination is because it's the only meshing scheme applicable for surfaces without edges. We similarly also mesh the three faces of the cylindrical vessel.

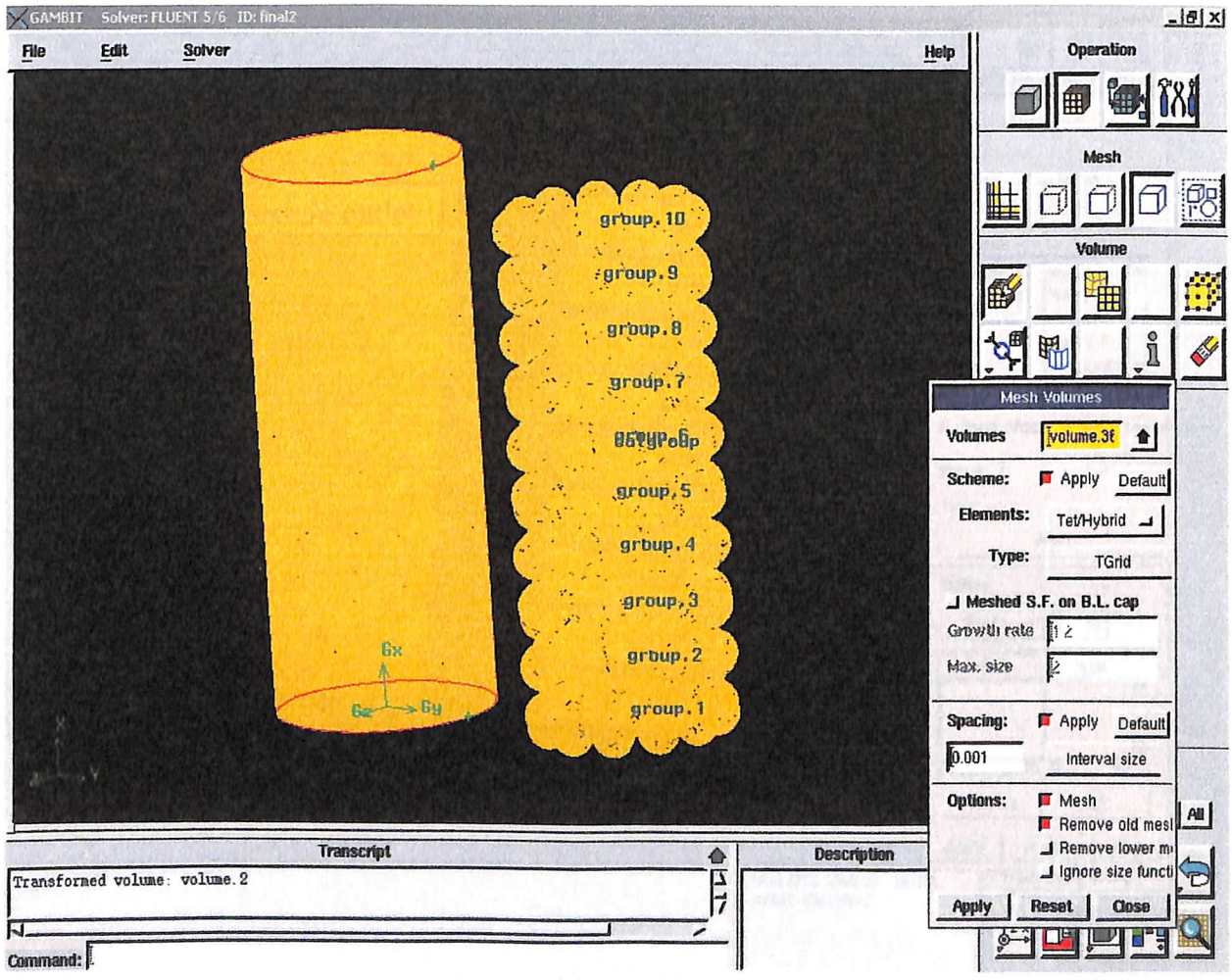

Figure 06-15: Meshing of the packed reactor

On completion of face mesh, we perform volume meshing. We mesh the cylindrical and the spherical catalysts particles using the "Tet/Hybrid volume meshing elements option" and " TGrid volume meshing type".

The Elements parameter defines the shape(s) of the elements that are used to mesh the volume. The Type parameter defines the meshing algorithm and, therefore, the overall pattern of mesh elements in the volume. The Smoother specification determines the type of smoothing algorithm (if any) used to smooth a mapped mesh during the meshing operation.

Thus, " Tet/Hybrid volume meshing elements option" specifies that the mesh is composed primarily of tetrahedral elements but may include hexahedral, pyramidal, and wedge elements where ever appropriate and "TGrid volume meshing type" specifies that the mesh is composed primarily of tetrahedral mesh elements but may include hexahedral, pyramidal, and wedge elements where appropriate.

6.1.2.3 Boundary conditions

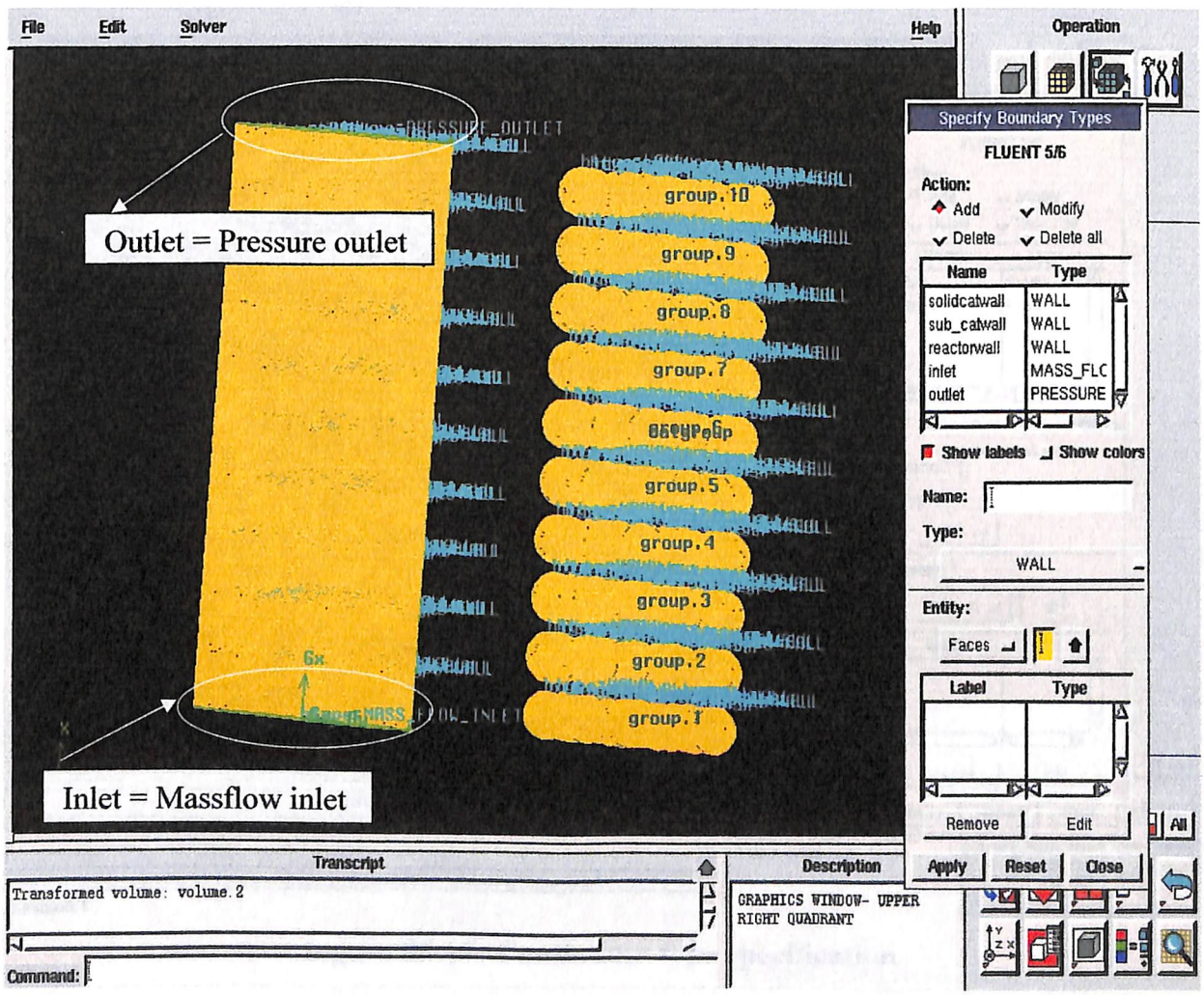

Figure 06-16: Boundary condition specifications

Each computational solver is associated with a unique set of allowable boundary types. In this study, the boundary types stated are:

Table 06-1: Boundary conditions specifications.

Name	Boundary Type
Inlet	Mass flow inlet
Outlet	Pressure outlet
Spherical catalysts, subtracted spherical, cylindrical vessel walls.	Wall

6.1.2.4 Continuum type specification

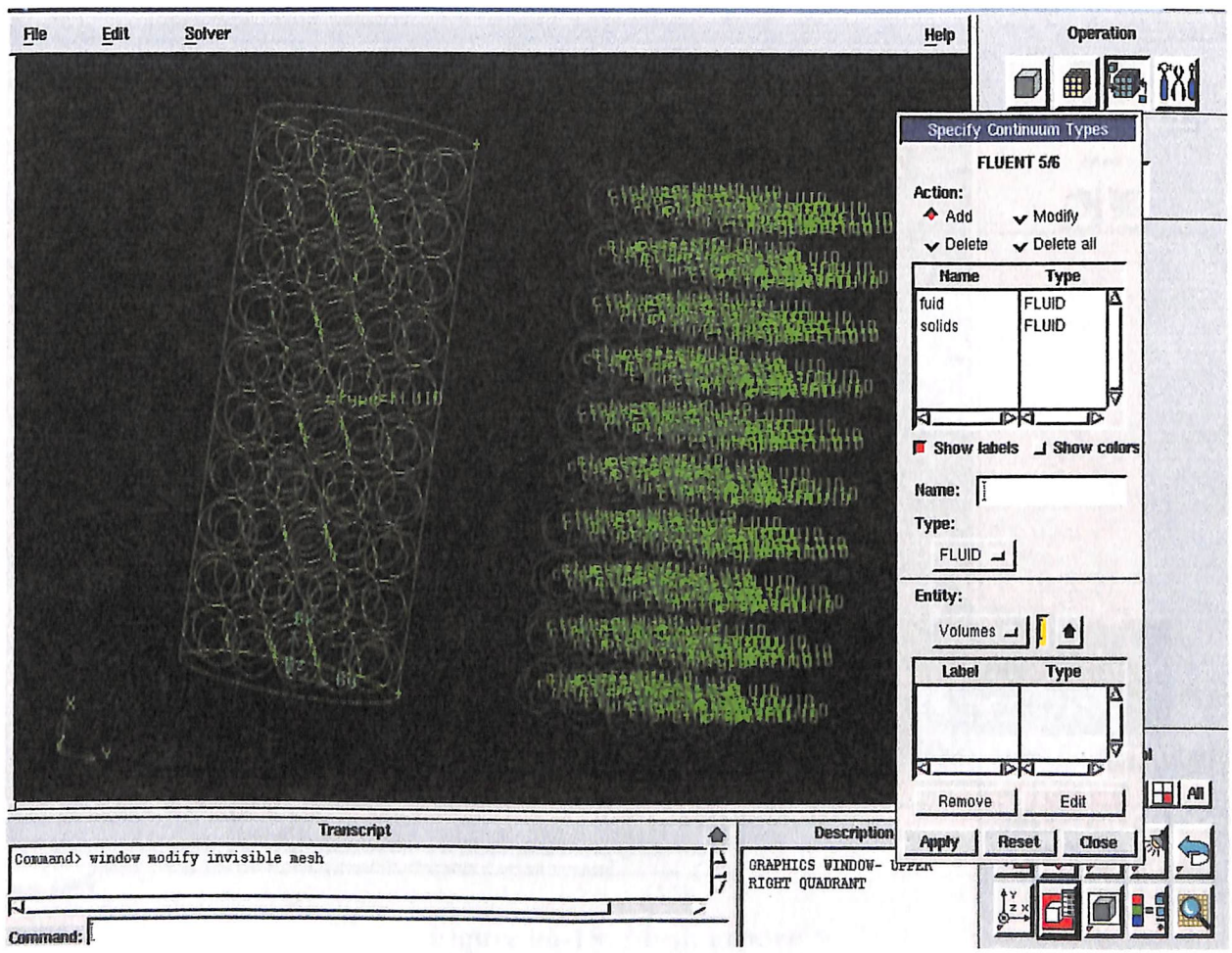

Figure 06-17: Continuum type specification

The Specify "Continuum Types operation" creates, modifies, or deletes continuum-type specifications that define the physical characteristics of the model in any region defined by a set of topological entities. The physical characteristics, in turn, determine which transport equations apply to the problem.

Now, both the volume of the cylinder as well as the solid catalysts is defined as fluid. The reason for defining the solid catalysts as fluid is because the fluid flow through the catalysts is based on porous media concept and to define porous flow through them in Fluent we have to define the solid catalysts as fluid, only then can we express the parameters for the porous solids, i.e. porosity (ε) is 0.4 and surface-to-volume ratio (A_s/V), where A_s defines the surface area.

Also defining the solid catalysts as fluid continuum allows embedding the tar cracking reaction in these catalysts by allowing wall reactions as defined in "*7.2.2.2 Species transport and reaction.*"

6.1.2.5 Mesh Export

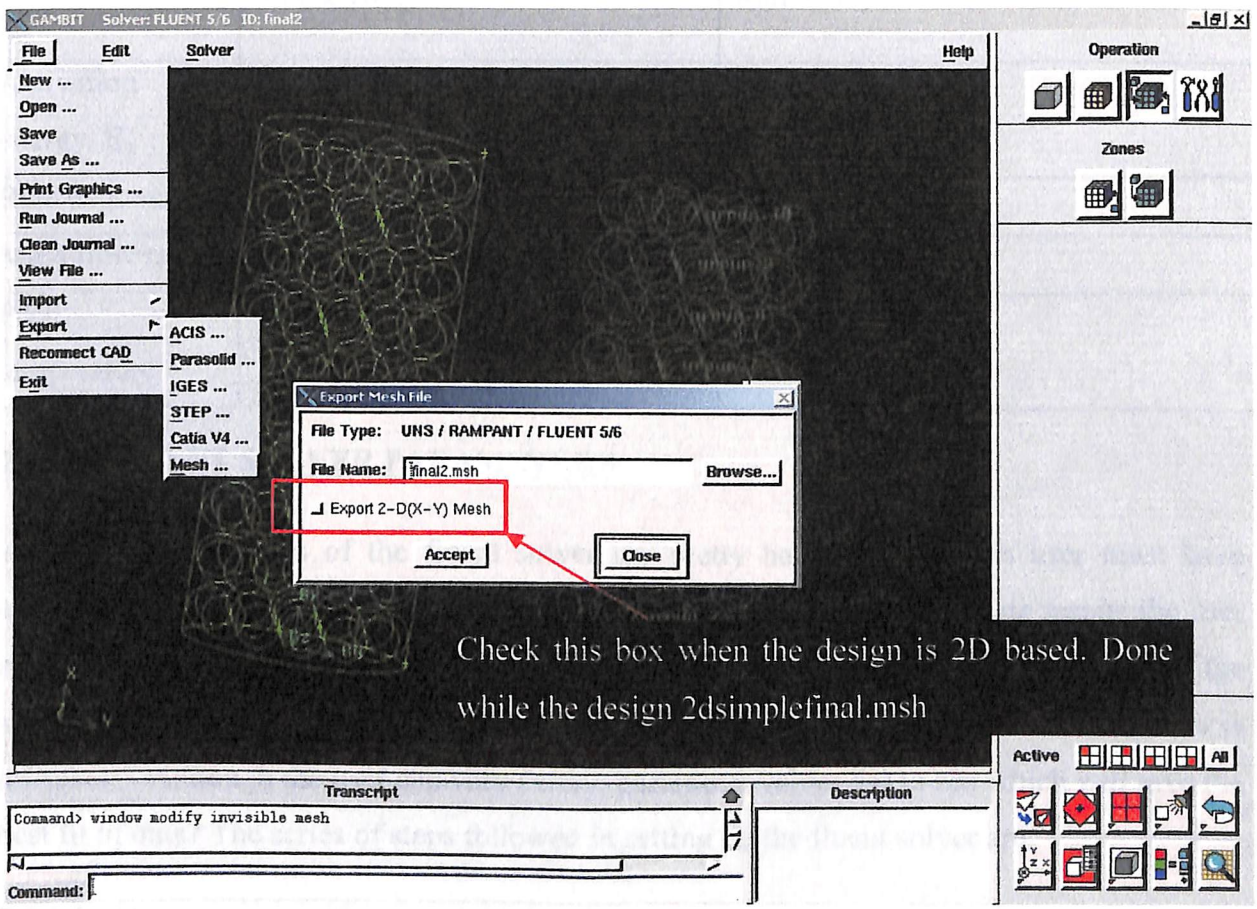

Figure 06-18: Mesh export

After the specification of the boundary conditions and the continuum types, we save it as "final2.dbs". The .dbs files are readable by the Gambit software, for fluent to read the design made in Gambit we export in .msh format. We do this by –

FILE → EXPORT → MESH

CHAPTER 07. FLUENT SOLVER PARAMETERS

7.1 SOLVER PARAMETERS

Table 07-1: Reaction parameters for fluent

Parameter	Value	Reference
Model compound	Toluene (C_6H_5-CH_3)	Coll et al; 2001. Milne T.A. et al; 1998 . Nikola Sundac; 2003
Reaction	$2C_6H_5$-CH_3 + $8.5O_2$ = 6CO + $5CO_2$ + $3CH_4$ + H_2 + H_2O	Self
Rate exponent, k_0	8.20×10^7 s^{-1}	Rath et al, 2001
Activation energy, E_a	117.0 J/kmol	Rath et al, 2001
Rate exponent, n	1	Rath et al, 2001
Mass flow rate	0.003 kg s^{-1}	Faundez et al, 2001
Feed temperature	973.15 K	Rath et al, 2001

7.2 FLUENT SOLVER PARAMETERS

The parameters of the fluent solver are pretty basic, but for this user must have appropriate knowledge of the process parameters. For fluent to give accurate results the user must have complete knowledge of the process, i.e. how are the trends going to look like if the solution of fluent is "converged". As it is said, "The software will make mistake if the user is mistaken." Although the user can vary certain parameter values for to see which will give the best fit of data? The series of steps followed in setting up the fluent solver are:

7.2.1 Grid

Applicable to both 2D and 3D model.

1. The first step is to read the .msh file. In this case it is "2dsimple.msh"

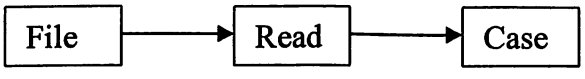

2. Check the grid.

FLUENT will perform various checks on the mesh and will report the progress in the console window. Pay particular attention to the reported minimum volume. Make sure this is a positive number.

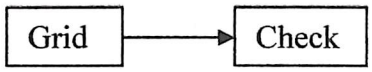

3. Display the grid.

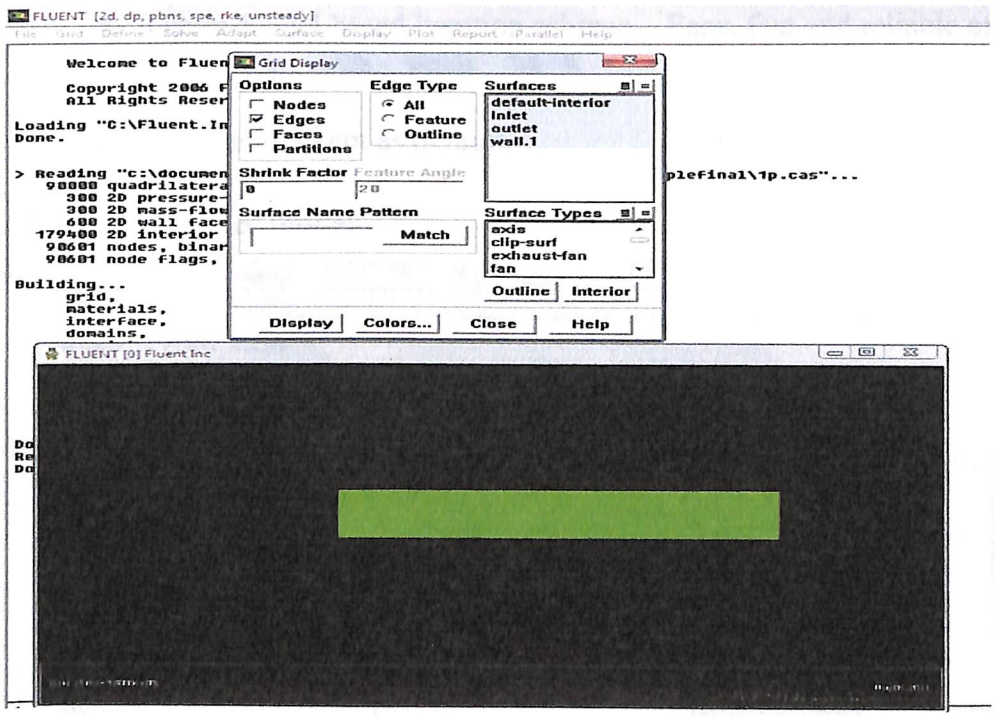

Figure 07-1: Grid display

7.2.2 Solver selection

7.2.2.1 Models

Applicable to both 2D and 3D model.

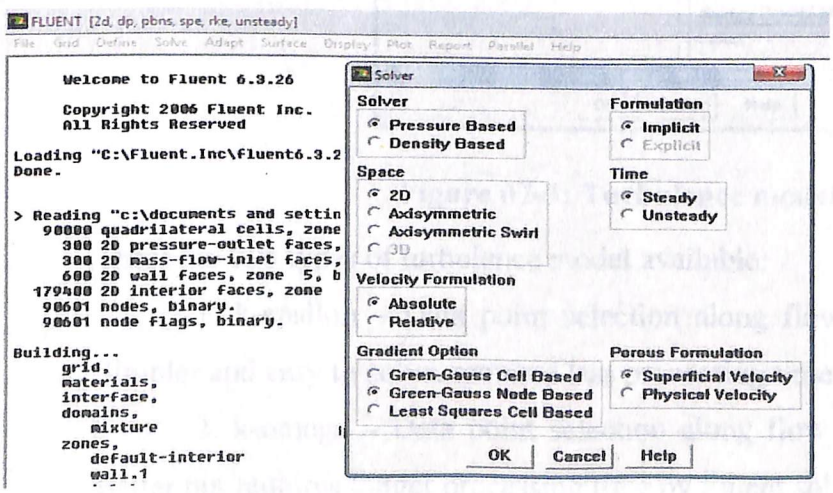

Figure 07-2: Solver conditions

Fig 7.2 states the solver conditions.

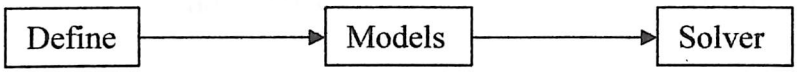

1. Pressure based solver – To maintain simplicity and ideal gas consideration.
2. Implicit formulation – Easy, fast and reliable and works well with 2D models.
3. Steady state analysis.
4. Gauss-Siedel based iteration scheme – Easy, fast and reliable and works well with 2D models.
5. Rest factors kept as default.

7.2.2.1 Turbulence model

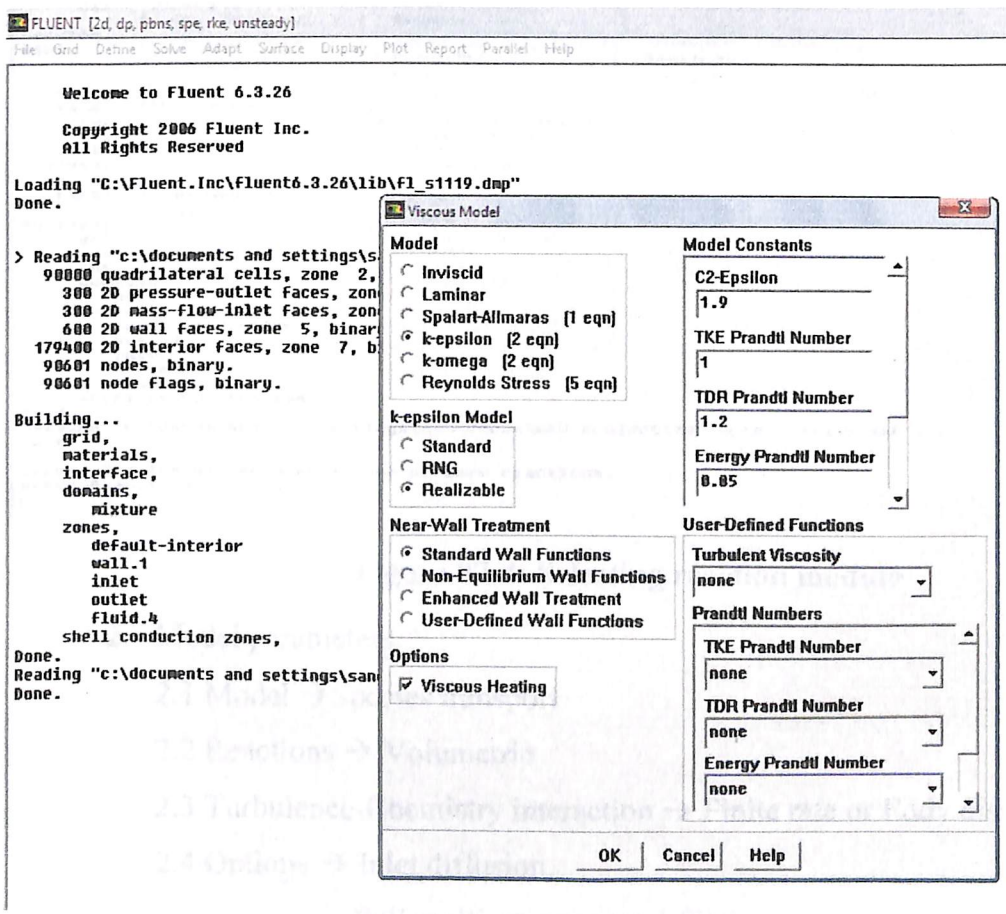

Figure 07-3: Turbulence model

There are two types of turbulence model available:

1. k-epsilon – Data point selection along flow domain at regular intervals. Simpler and easy to solve, requires less processing time.

2. k-omega – Data point selection along flow domain at irregular intervals. Better but requires longer processing time by Fluent solver.

In the present study the parameter for turbulence modeling and the values remain same for both 2D and 3D model. Also, the values of the parameters are taken as default.

7.2.2.2 Species transport and reaction.

This model is quite untouched in CFD studies, and reason being the complexicity and accurate data sets required for getting appropriate results out of the fluent solver. The parameter values remain same for both 3D and 2D model.

1. Define → Models → Species → Transport and reaction

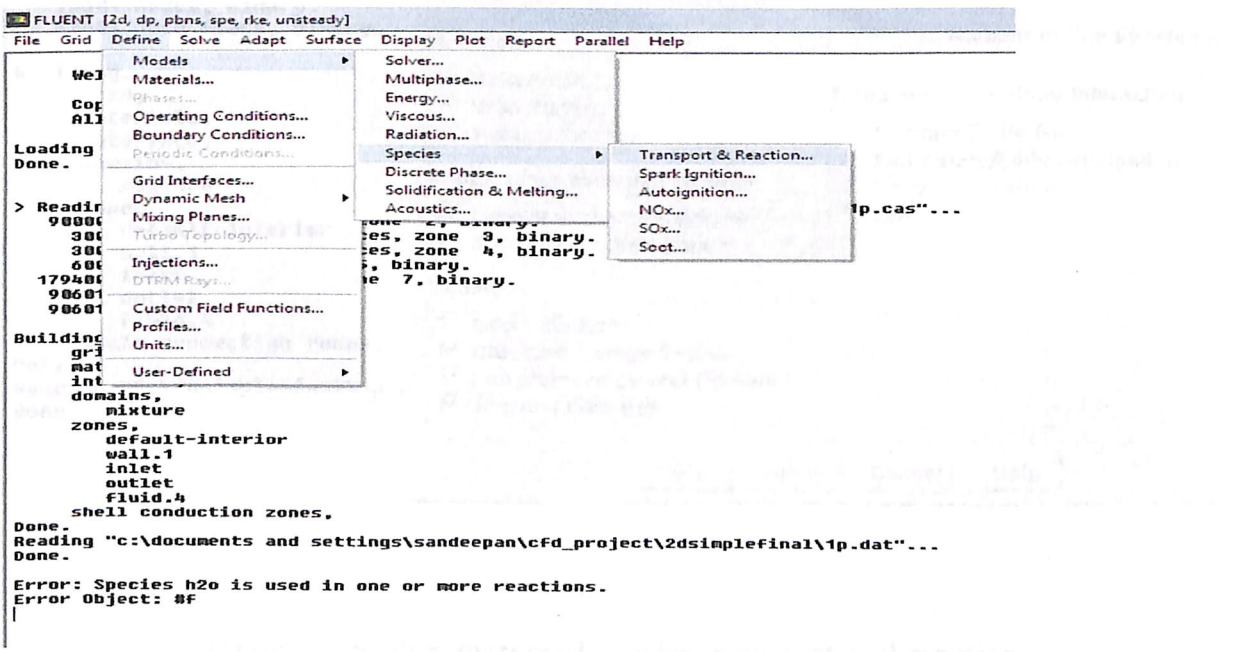

Figure 07-4: Selecting reaction module

2. Model parameters

   2.1 Model →Species transport

   2.2 Reactions → Volumetric

   2.3 Turbulence-Chemistry interaction → Finite rate or Eddy dissipation

   2.4 Options → Inlet diffusion,

   Full multi-component diffusion,

   Thermal diffusion.

   2.5 Click "Apply"

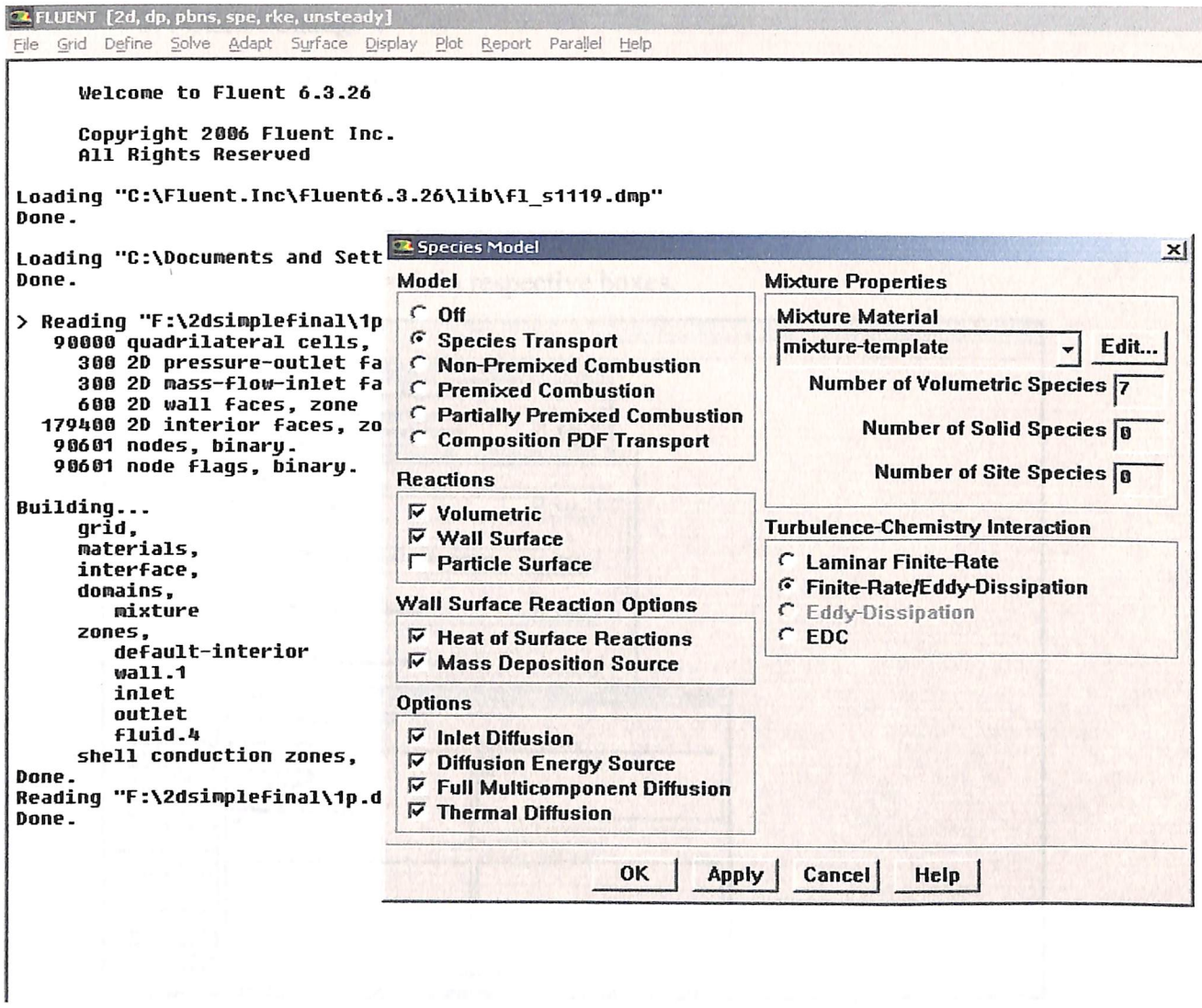

Figure 07-5: Parameters of species transport and reaction.

3. Species

   3.1 Click "Edit" beside mixture template.

   3.2 This opens a new tab "Properties of mixture-template". Click "Edit" beside Mixture species.

   3.3 On this we see two partitions, fig 6.1.1.3

   Available materials → Shows the species (Chemical compounds) available. This list is generated from the materials we have selected from the materials tab.

   Selected species → Shows the chemical compounds already available under the mixture template, generally H_2O, O_2 and N_2.

   In this study, C_7H_8, CO_2, CO, CH_4, H_2, H_2O will be listed under "Available materials"; check them and select "Add" while select N_2 and select "Remove".

3.4 Click "Change".

4. Reaction – This is the most important segment In Fluent while analyzing hydrodynamics with Chemical reaction.

4.1 Insert no. of reactions = 1.

No. of reactants = 2.

No. of Products = 5, in respective boxes.

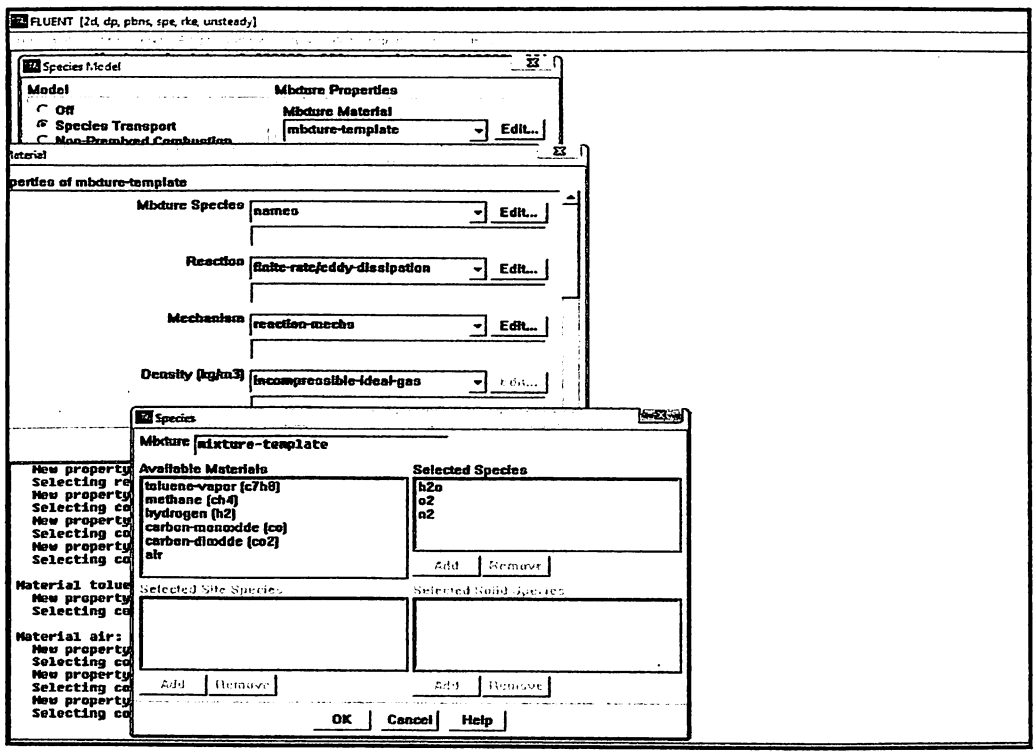

Figure 07-6: Selection of reacting species.

4.2 4.2.1 Scroll in under reactants tab to select the desired reactants (C_7H_8 and O_2) and the same for products (CO_2, CO, CH_4, H_2, H_2O).

4.2.2 Then simultaneously enter the respective stoichiometric co-efficient and rate exponent if any. In this study, reaction in consideration is –

First order so n =1

Reaction is irreversible so n = 0 for the products.

E_a, activation energy = 117 J/ kmol.

K_0, Pre-exponential factor = 8.20×10^7 sec^{-1}.

Reaction:

$2C_6H_5\text{-}CH_3 + 8.5O_2 = 6CO + 5CO_2 + 3CH_4 + H_2 + H_2O$

The tar cracking reaction is composed of several reactions in parallel and series along with side reactions. But, the reaction in consideration in this study is a

linear first order reaction and is the total overall reaction. Any side reactions or parallel reactions are not considered to maintain the simplicity of the project.

There is a single reaction mechanism and no other reactions take place along the flow domain. Several runs were made with various data sets for E_a and k_0 to analyze the flow domain so to observe that correct trends are developed in the region of interest.

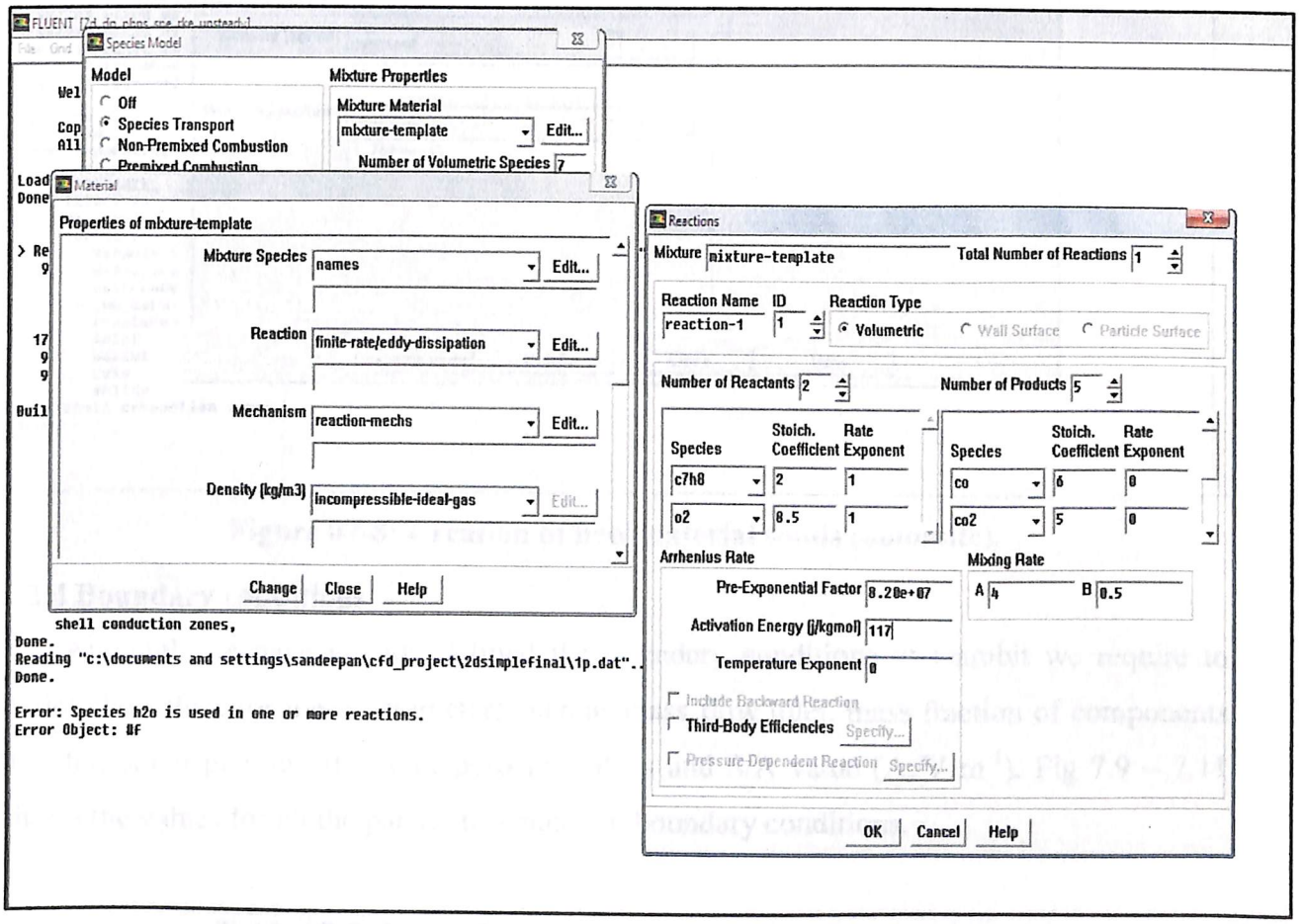

Figure 07-7: Reaction details

7.2.3 Materials

Applicable to only 3D model. Under this section, the highlight is to create a new fluid entity called solids using the parameters of the dolomite from fluent database, fig 6.8 shows how the density of the material " solids" which is basically a fluid has density and viscosity equal to actual solid catalysts dolomite, i.e. density (ρ) = 2872 kg/m^3 and viscosity (μ) = 1.7894e-05 kg/m-s.

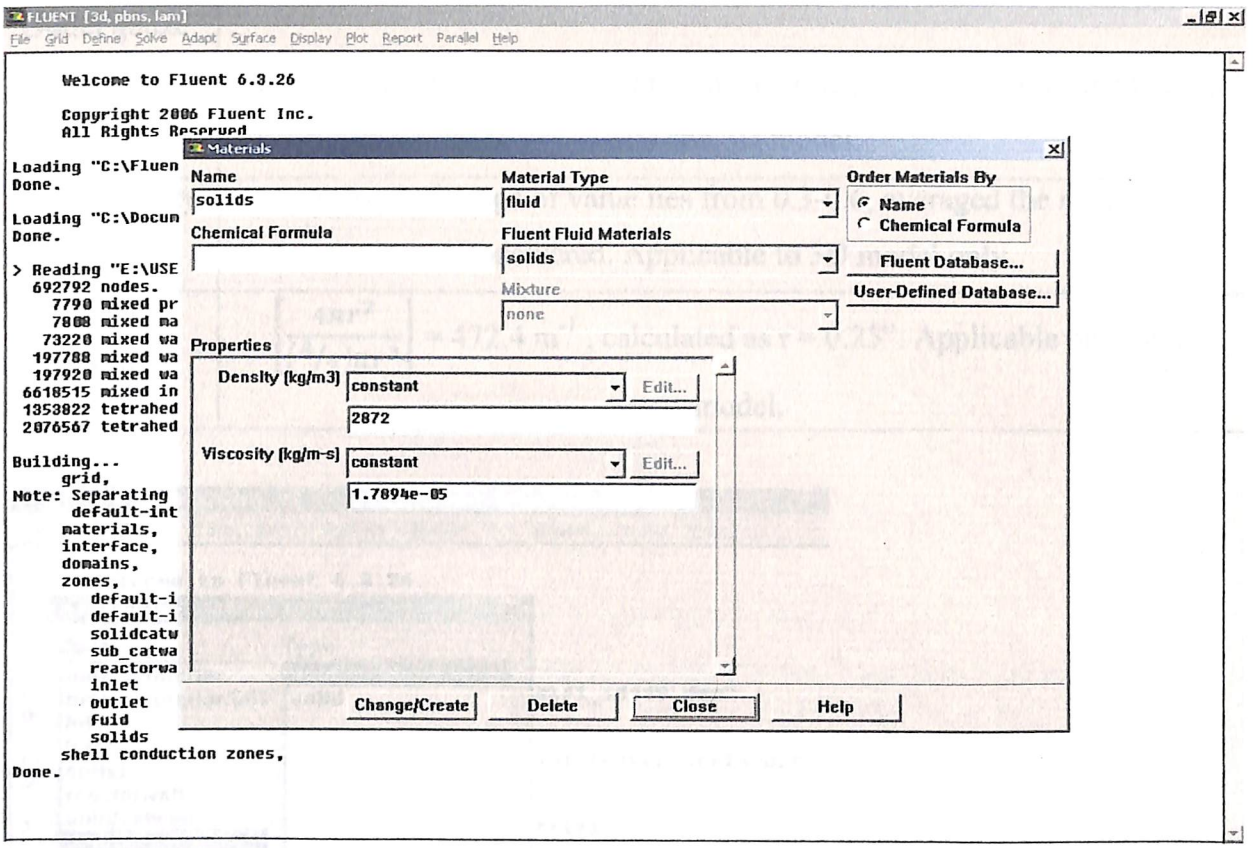

Figure 07-8: Creation of new material solids (dolomite).

7.2.4 Boundary conditions

Although we have already defined the boundary conditions in Gambit we require to define the values for these parameters such as mass flow inlet, mass fraction of components in inlet, outlet pressure if any or porosity values and S/A value (A_s/V m^{-1}). Fig 7.9 – 7.11 shows the values for all the parameters stated in boundary conditions.

Table 07-2: Fluent boundary condition parameter values.

Parameter	Value
Mass flow inlet (kg/s)	0.138e-04 (5mg/min) [Faundez et al, 2001].Applicable to both 2D and 3D model.
Feed temperature	973.15K [Rath et al,2001].Applicable to both 2D and 3D model.
Mass fraction	C_7H_8 = 0.4 ; O_2 = 0.6 [assumed and stated fit by analyzing other combinations of mass fractions based on product concentration and feed component concentration at outlet]. Applicable to both 2D and 3D model.

Outlet gauze pressure	0, i.e. outlet pressure is equal to atmospheric pressure. Applicable to both 2D and 3D model.
Solid porosity (ε)	0.4 [typical range of value lies from 0.3-0.6, averaged the range and considered. Applicable to 3D model only.
S/V ratio (A_s/V m^{-1})	$\left[\frac{4\pi r^2}{(4/3)\pi r^3}\right]$ = 472.4 m^{-1} , calculated as r = 0.25". Applicable only to 3D model.

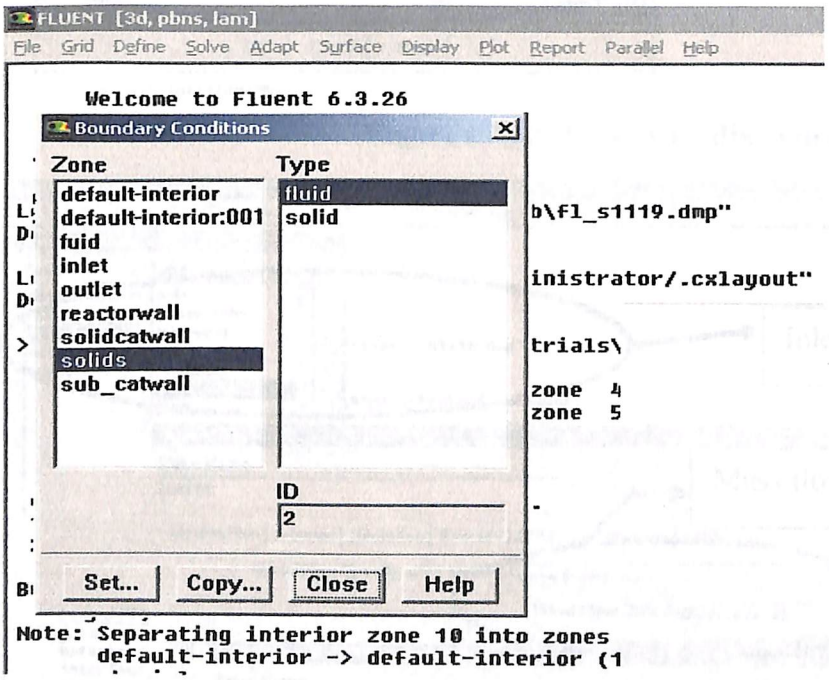

Figure 07-9: Solids with continuum type as fluid.

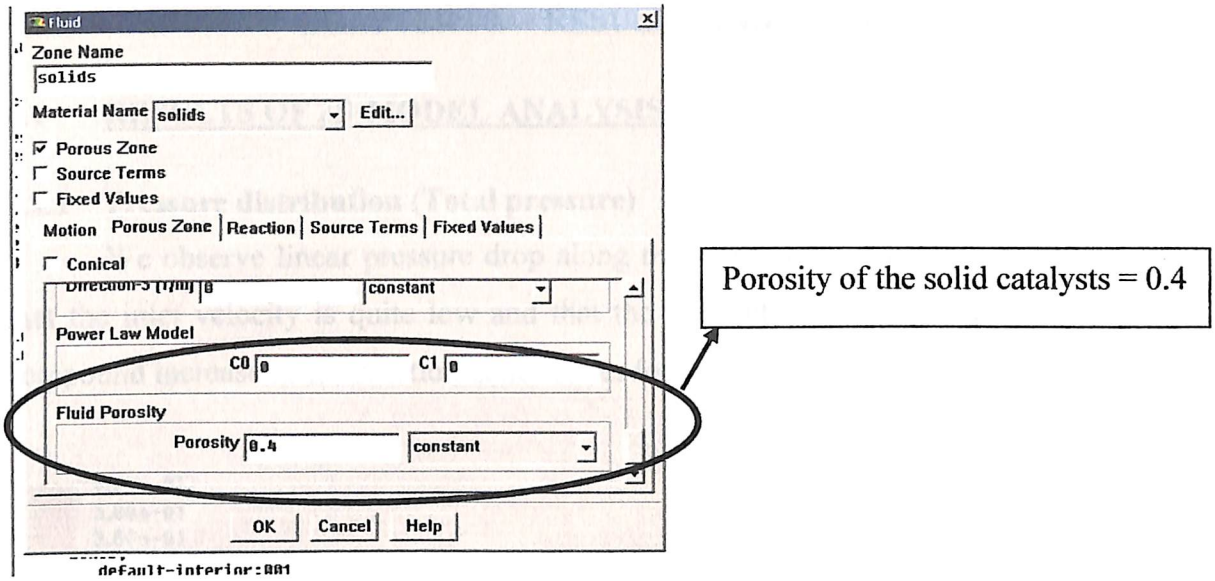

Figure 07-10: Porous media concept

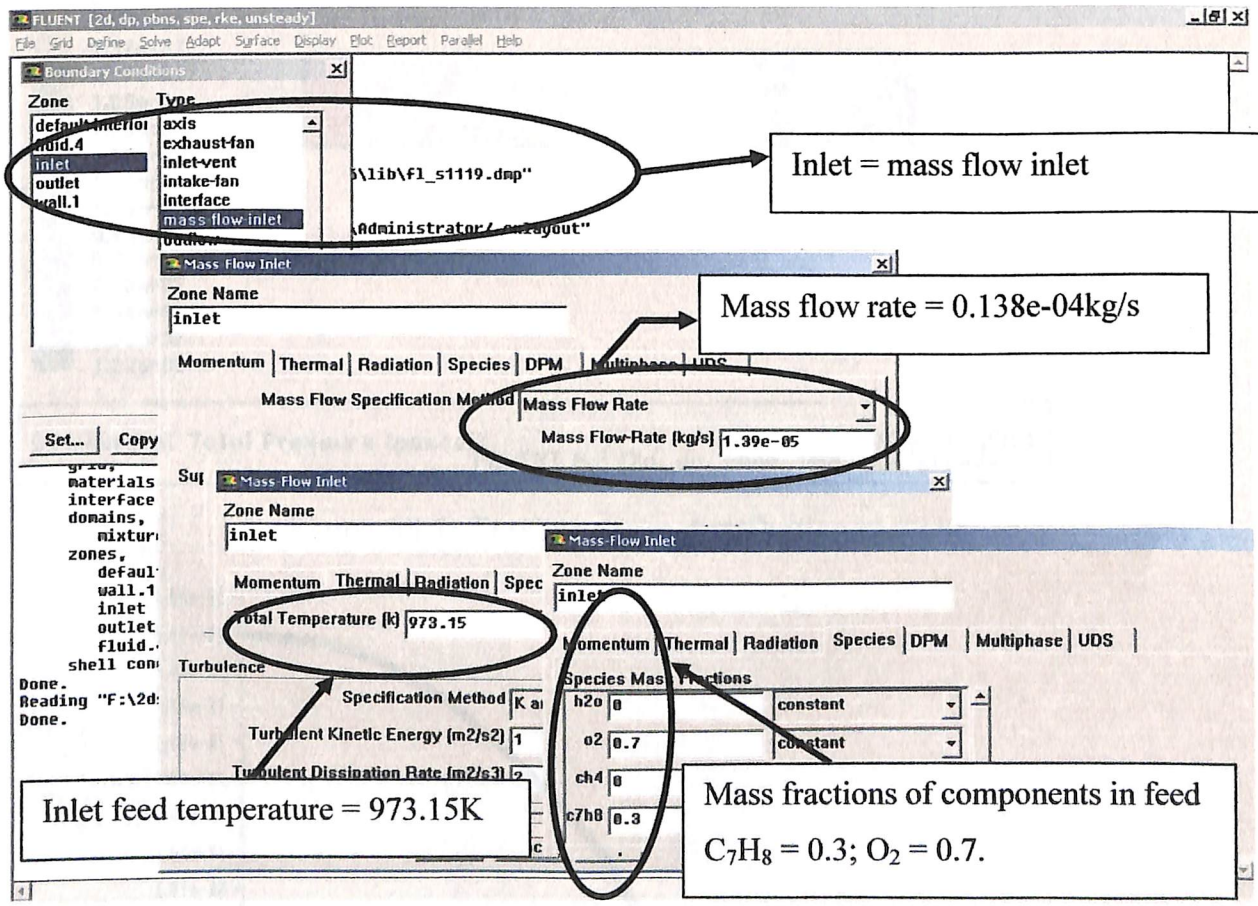

Figure 07-11: Inlet conditions

CHAPTER 08. RESULTS AND DISCUSSIONS

8.1 RESULTS OF 2D MODEL ANALYSIS

8.1.1 Pressure distribution (Total pressure)

We observe linear pressure drop along the length of the reactor, because of the fact that the inlet velocity is quite low and that the concentration of heavier molecular weight compound increase as the reaction zone moves forward.

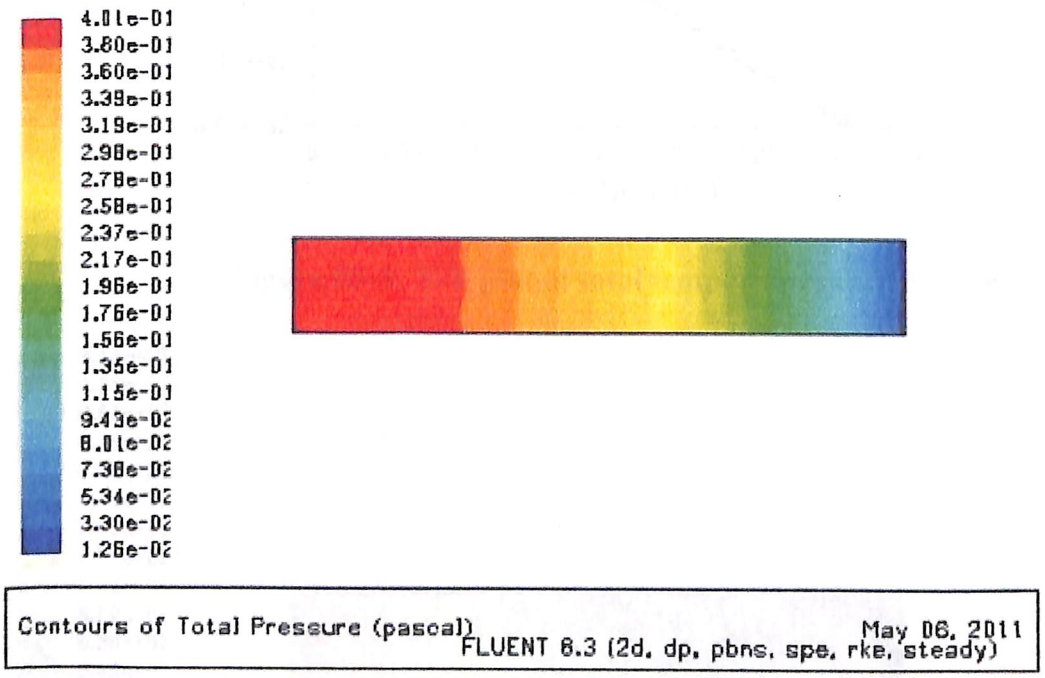

Figure 08-1: Total pressure distribution contour

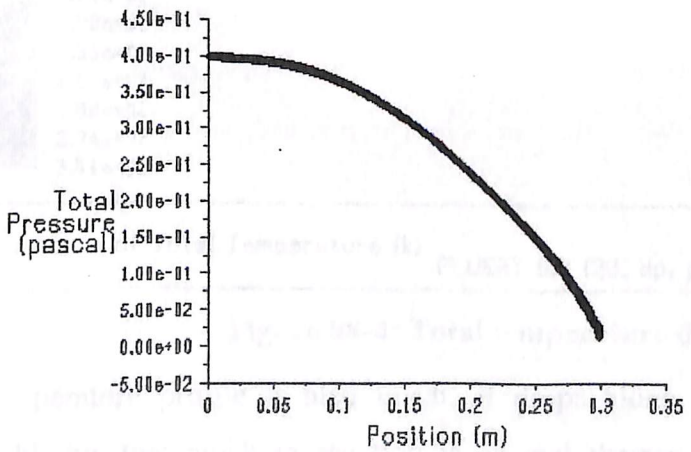

Figure 08-2: X-Y plot of total pressure distribution

8.1.2 Total temperature distribution

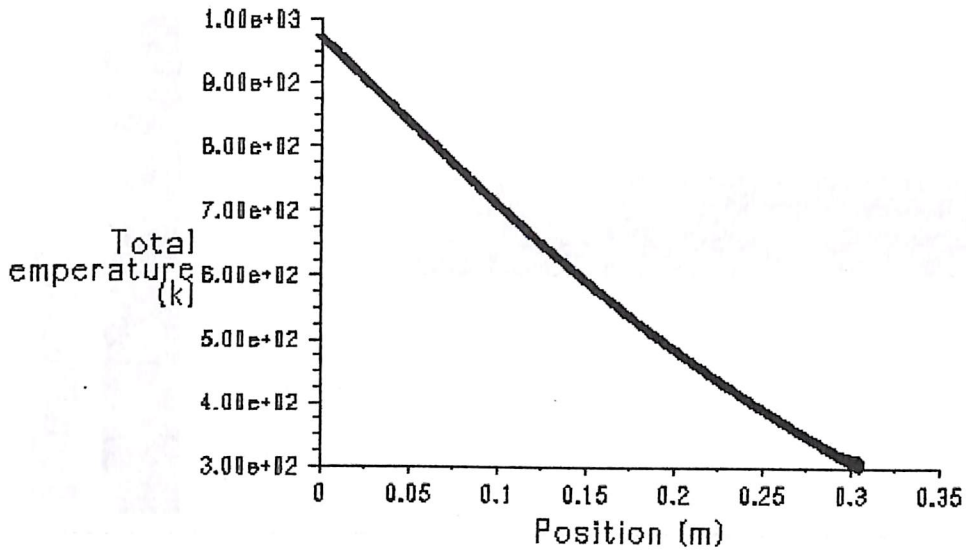

Figure 08-3: X-Y plot of total temperature distribution

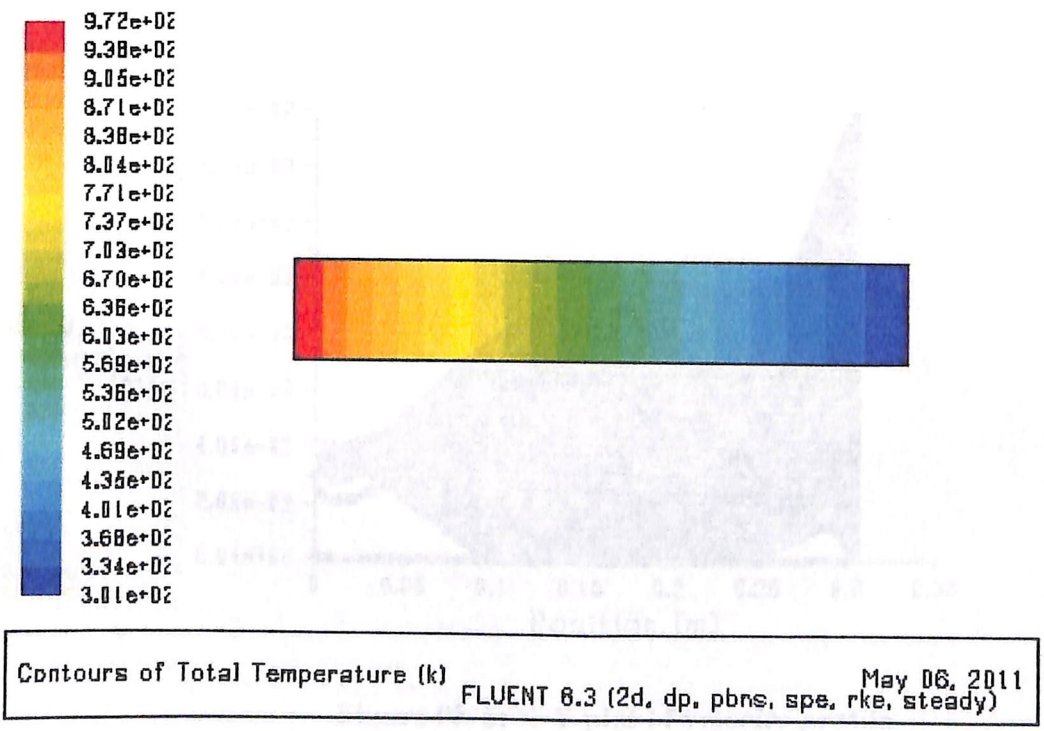

Figure 08-4: Total temperature distribution contour

Temperature profile is also linear. It drops along the length of the reactor which also highlights that cracking reaction is an endothermic reaction. The inlet temperature is at 973.15K and at the outlet temperature as seen from fig 087-3 and fig 08-4 is around 300K which is around room temperature, 27^0C.

8.1.3 Velocity profile

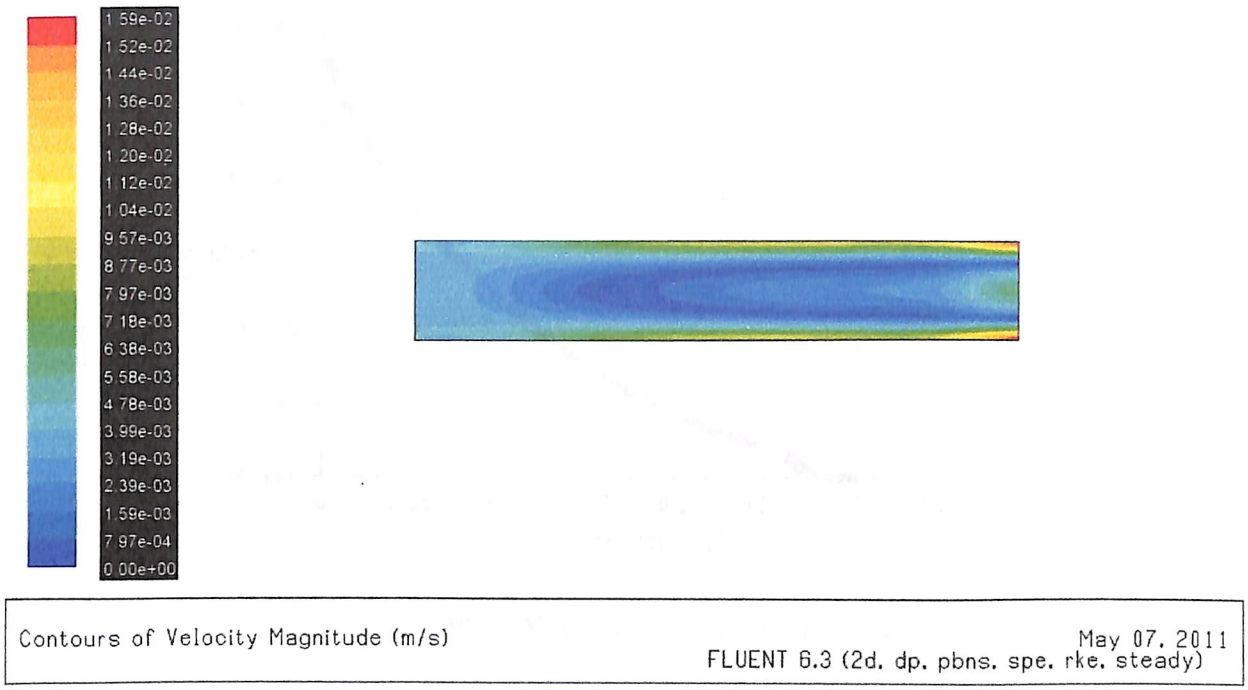

Figure 08-5: Velocity Profile contours

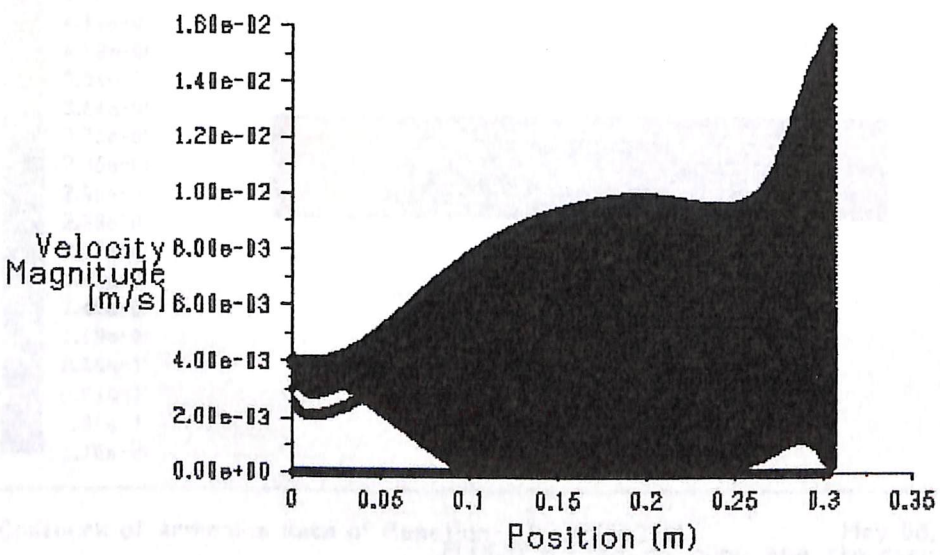

Figure 08-6: X-Y plot of velocity profile.

Non-linear velocity profile observed along the flow zone, and complete stagnant zones seen in the flow domain. This can be explained by the fact that more mass concentration at the centre area, i.e. both of products as well as reactants at same time. Velocity near the reactor walls has higher range of values due turbulence or vortices at around the central zone. Average velocity throughout is around 5 m/s.

8.1.4 Rate of reaction

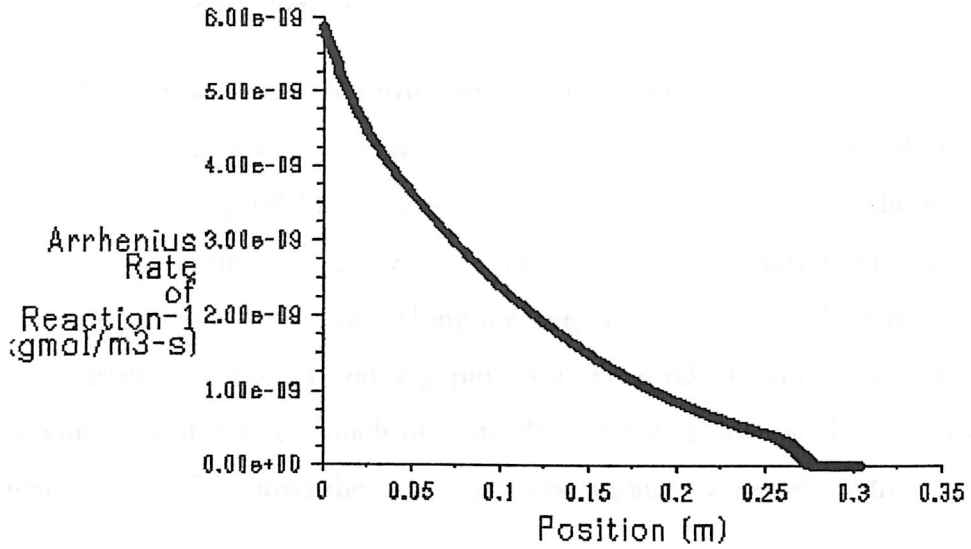

Figure 08-7: X-Y plot of rate of reaction.

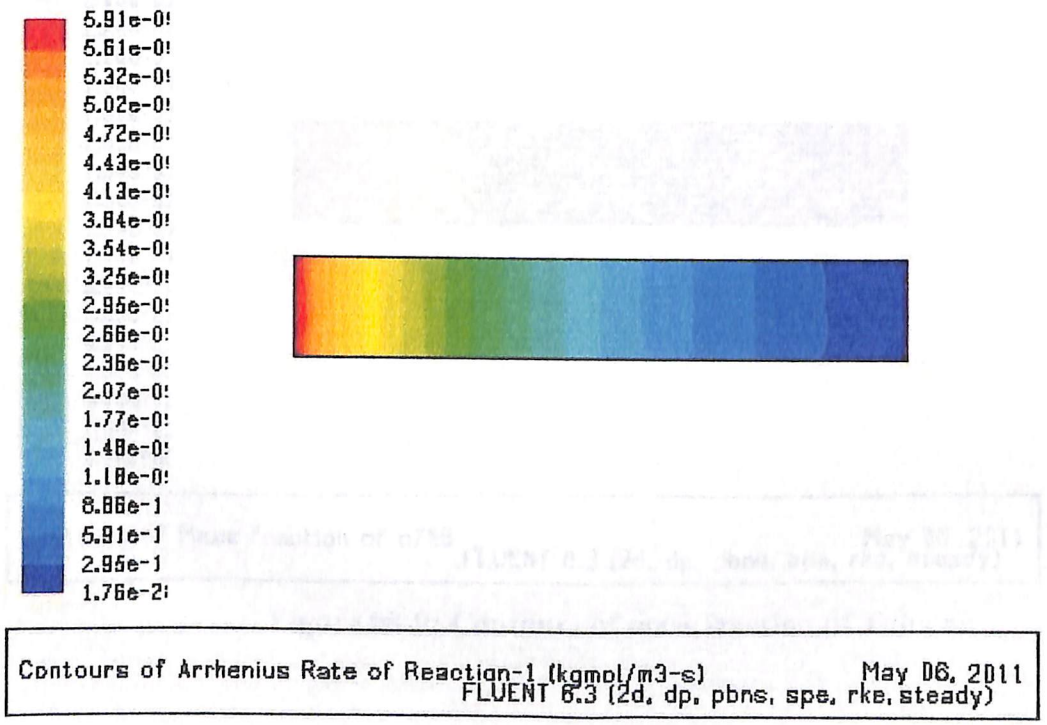

Figure 08-8: Rate of reaction contour.

The rate of reaction also shows a linear profile. At regions near the entrance there is high conversion due to the high temperature of the feed which gives necessary energy for the reaction to occur. As the flow moves forward there is subsequent consumption of the reactants and formation of products. As there is only a single reaction and no other side reaction or parallel or simultaneous reaction involving the products so the rate of reaction

decreases near the end of the reactor. The maximum rate of reaction located at the entrance is around is approx 6.00e-09 kg m^{-3} s^{-1}.

8.1.5 Mass fraction distribution in the flow domain.

It can be clearly seen that the mass fraction distribution also follows a linear pattern. Fig from 08-9 till fig 08-12 relate to mass fraction distribution for the reactants. The x-y plots show it much clearly that profile followed is linear in nature and there is a steady drop in concentration of the reactant along the length of the reactor. Figs 08-13 till fig 08-22 are the mass fraction contours and x-y plots for the products along the flow domain. In case of products we don't see much of a steady rise but an averaged value along the length of the reactor, table 7.1 shows the maximum concentration value of products at output.

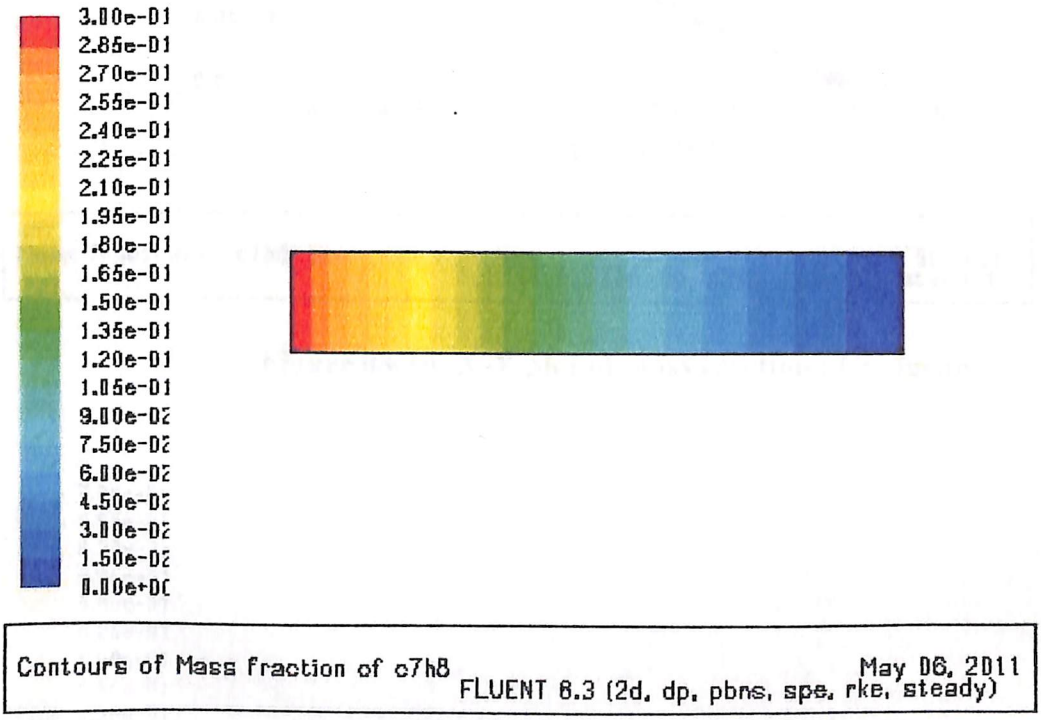

Figure 08-9: Contours of mass fraction of Toluene

Table 08-1: Approx mass fractions of various components at outlet

Compound name	Mass fraction at outlet (approx)
Toluene, oxygen	Complete consumption in reaction
Methane	0.05
Carbon monoxide	0.03
Hydrogen	0.0025

Carbon dioxide	0.92
Water	0.004

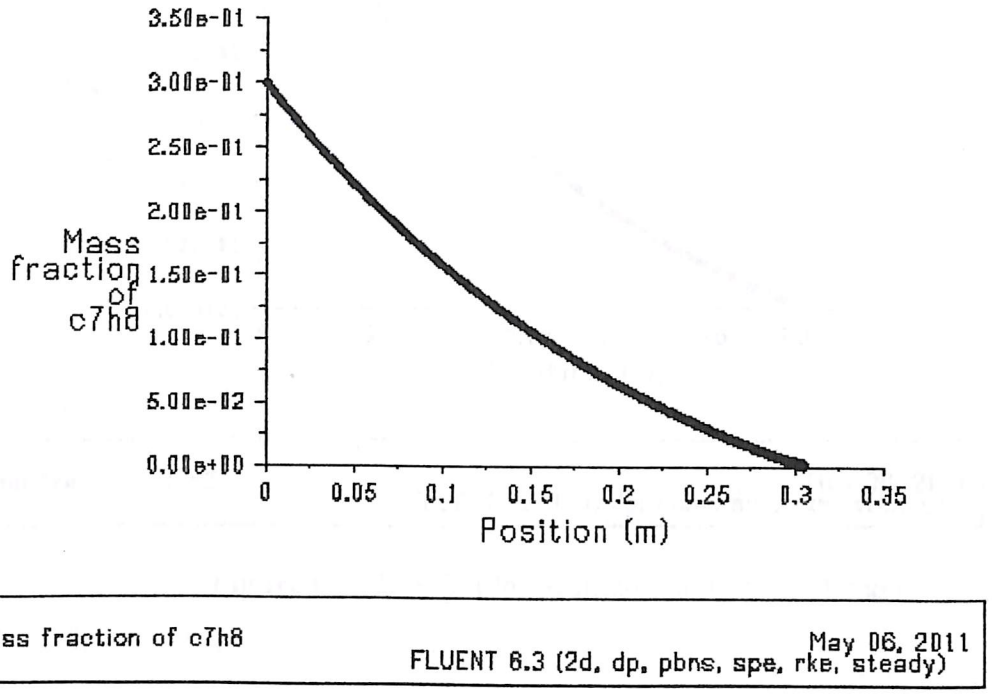

Figure 08-10: X-Y plot of mass fraction of Toluene

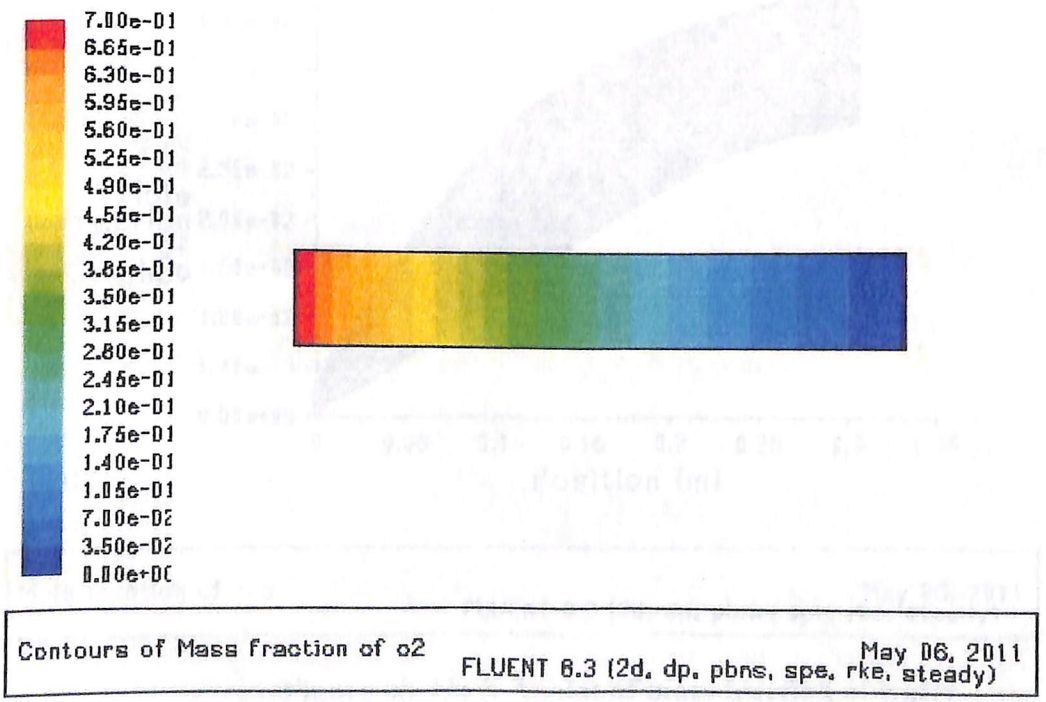

Figure 08-11: Contours of mass fraction of Oxygen

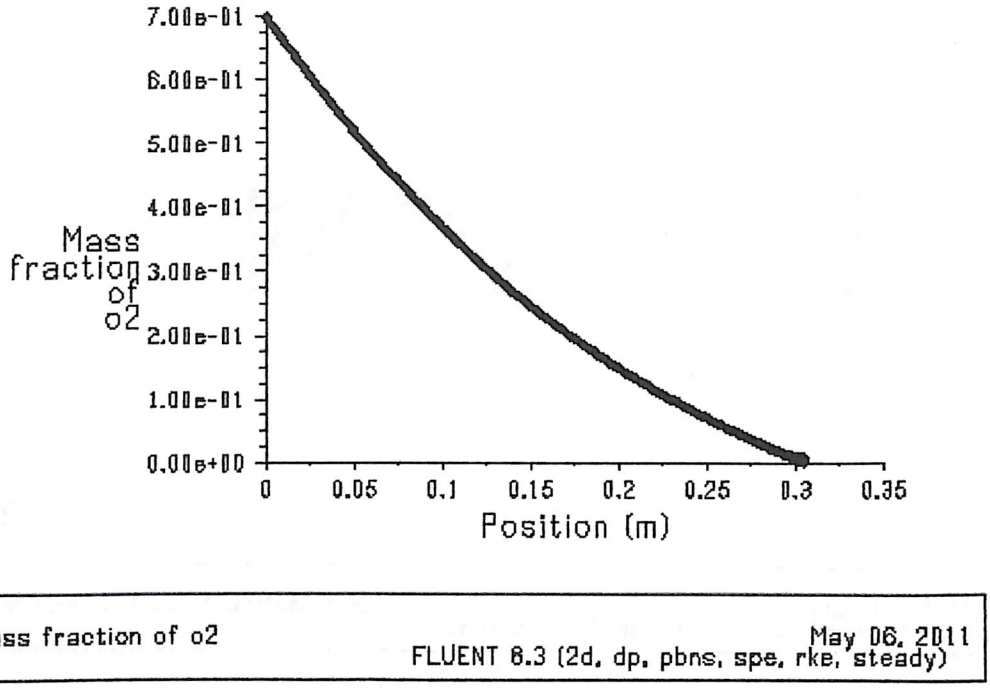

Figure 08-12: X-Y plot of mass fraction of Oxygen.

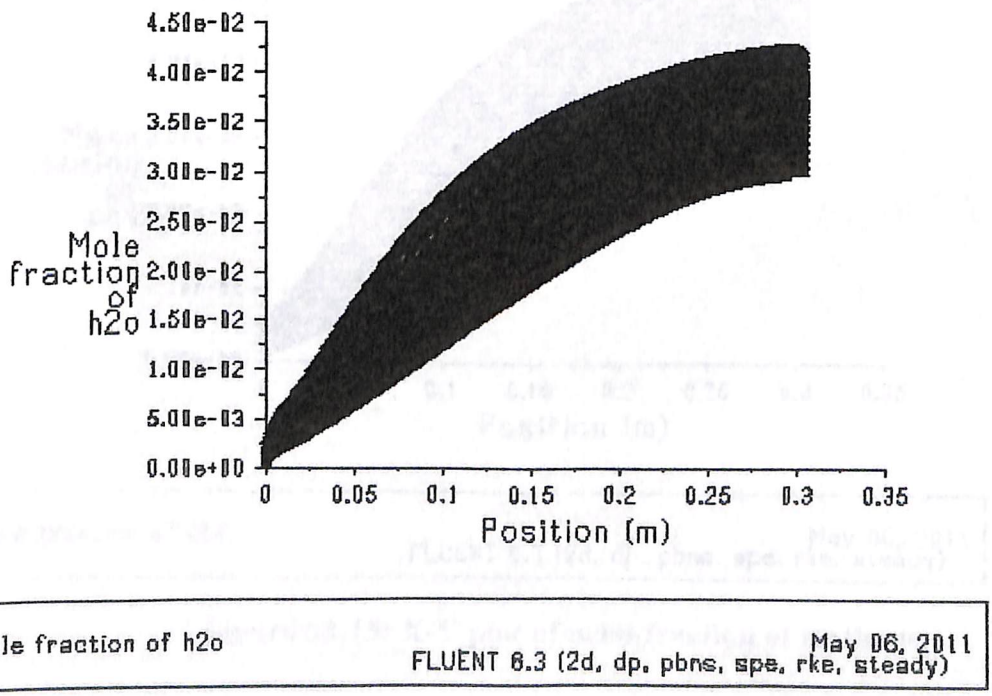

Figure 08-13: X-Y plot of mass fraction of water

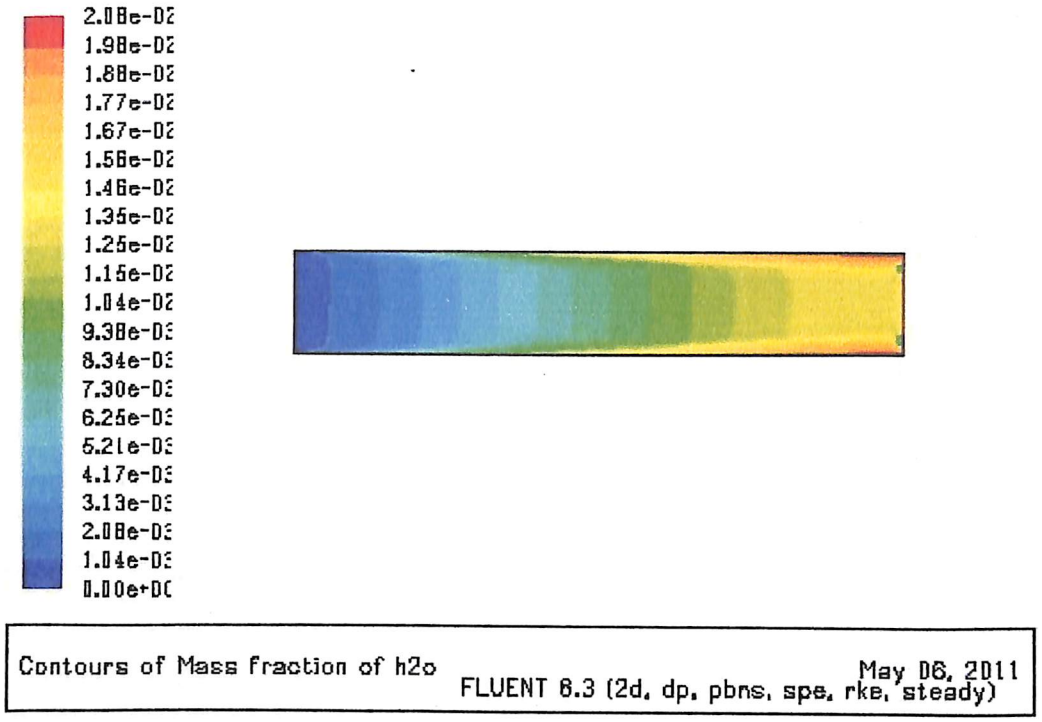

Figure 08-14: Contours of mass fraction of water

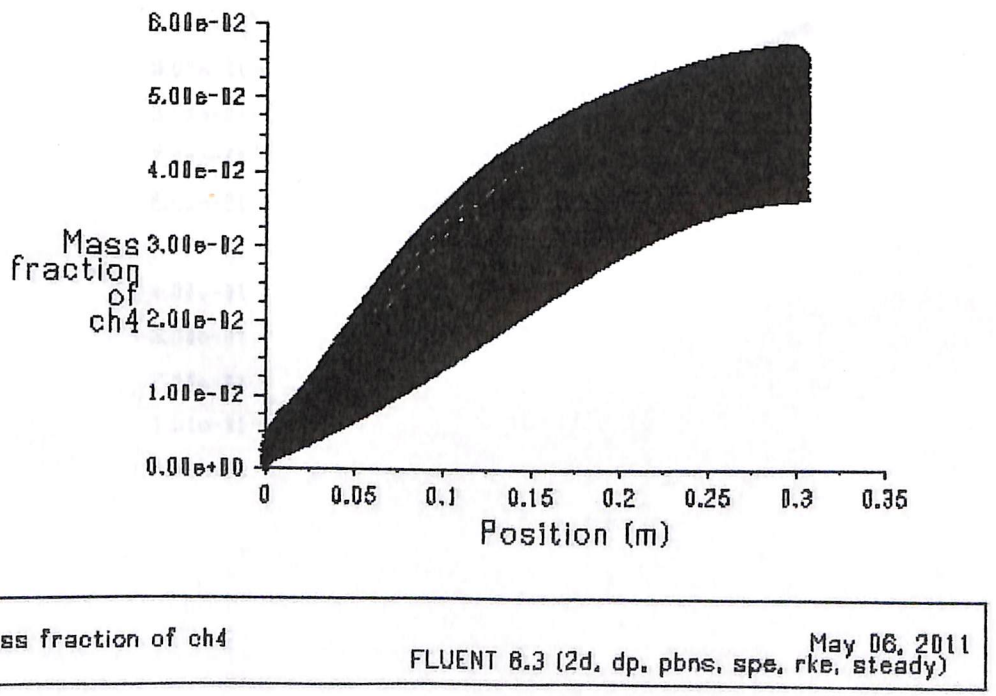

Figure 08-15: X-Y plot of mass fraction of methane.

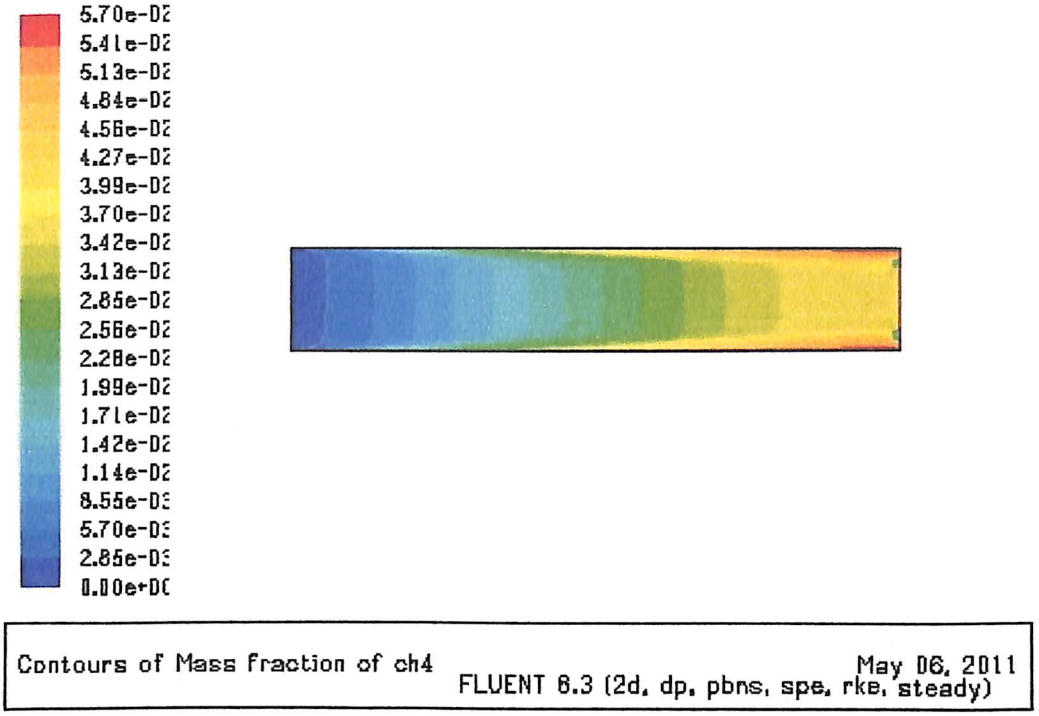

Figure 08-16: Contours of mass fraction of methane

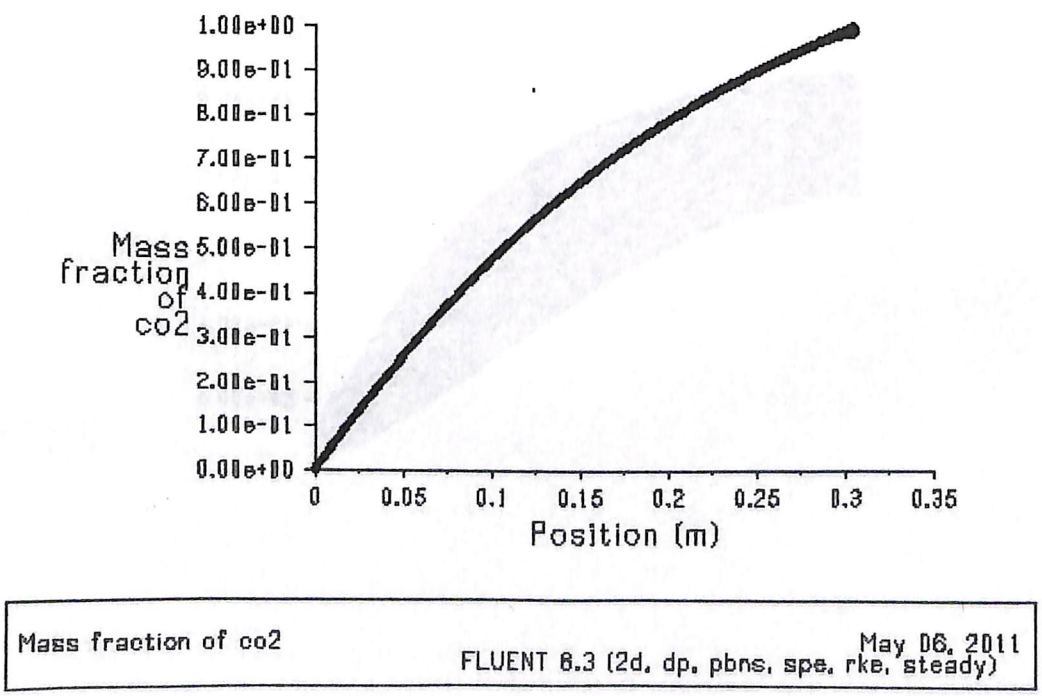

Figure 08-17: X-Y plot of mass fraction of carbon dioxide

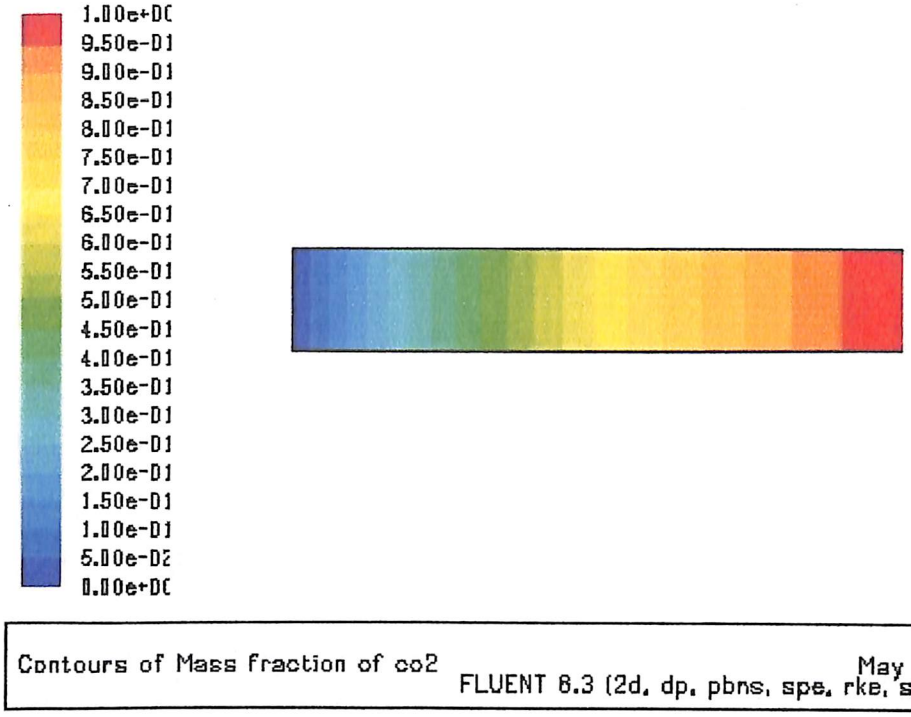

Figure 08-18: Contours of mass fraction of carbon dioxide.

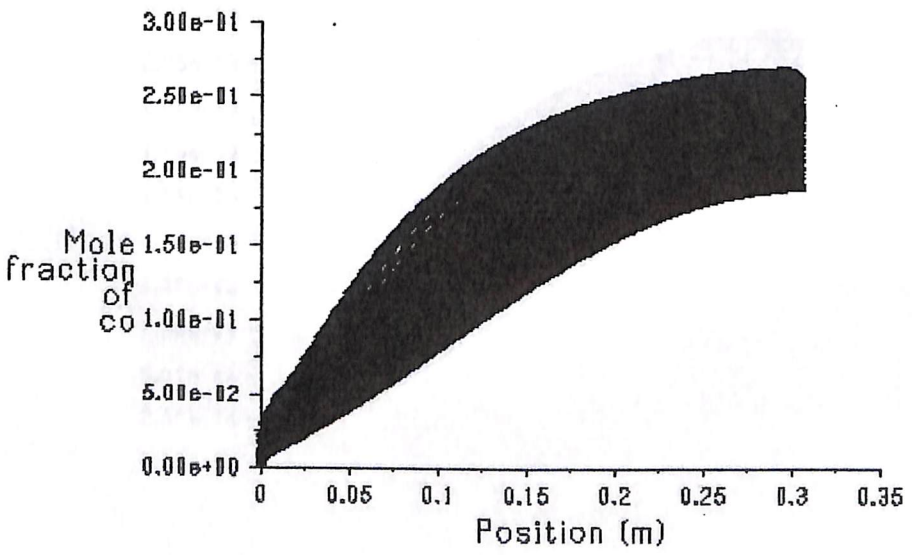

Figure 08-19: X-Y plot of mass fraction of carbon monoxide.

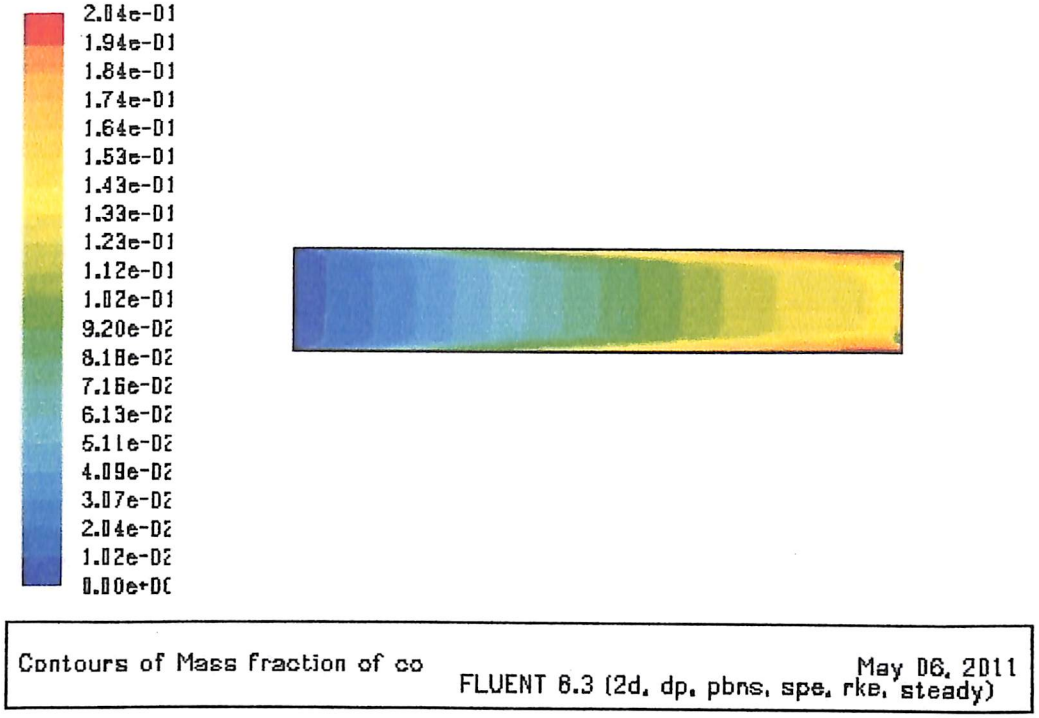

Figure 08-20: Contours of mass fraction of carbon monoxide

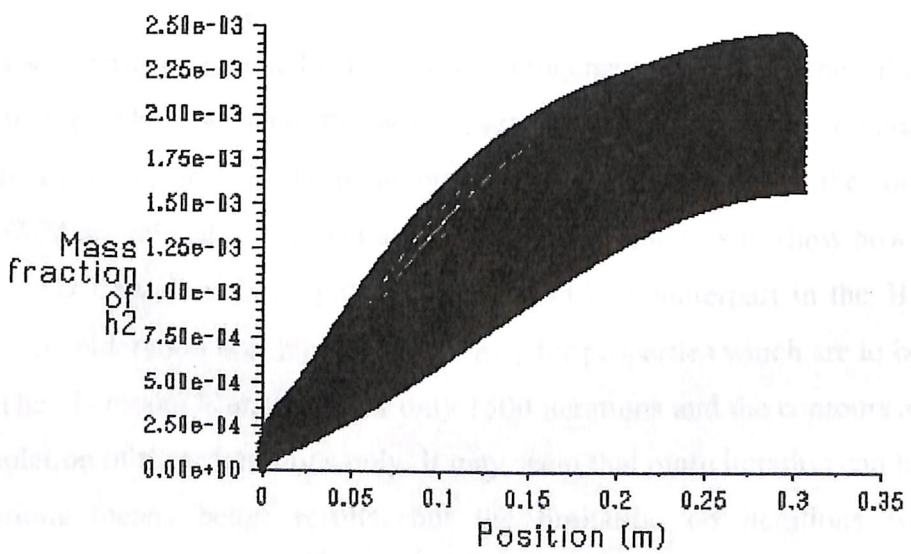

Figure 08-21: X-Y plot of mass fraction of Hydrogen.

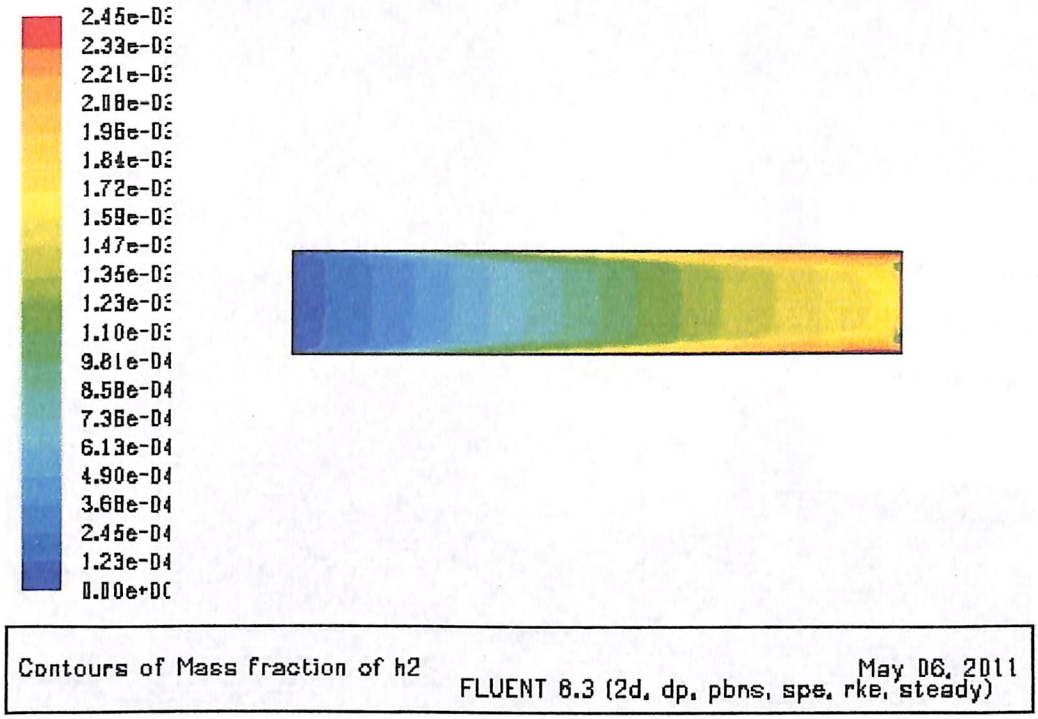

Figure 08-22: Contours of mass fraction of hydrogen

8.2 RESULTS OF 3D MODEL ANALYSIS

The 3D model as stated is based on heterogeneous phase and the solid and gaseous phases are distinct. The analysis of the system was based on same chemical parameters as for the 2D model only change is in the parameters while defining them for the solid phase. Figs 07-23 till 07-31 are related to the 3D model. The primary focus is to show how the reaction kinetics in the 3D flow domain is quite different from its counterpart in the 3D model. The region under consideration is exhibits non-linearity for properties which are to be analyzed.

The 3D model is analyzed for only 1500 iterations and the contours are analyzed after the completion of these iterations only. It may seem that more iteration can be performed as more iterations means better results, but the limitation on iterations was imposed as 3D computations require a lot of processing time and there were many hit-and-trials to get an agreeable standard of results which do not contemplate the real trends. The results seem to be quite in agreement with what we say can be fairly reasonable from the point of a chemical engineer.

Product concentrations may not be agreement which is due to fact that the fluent solver was not allowed to perform iterations till convergence of solution.

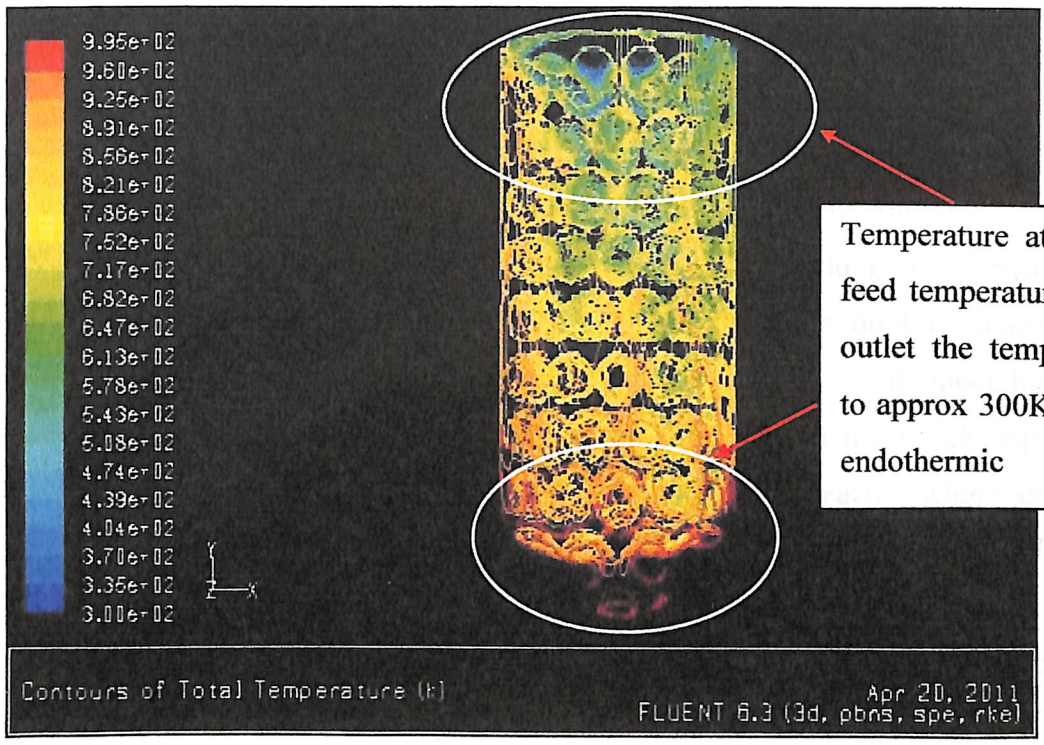

Temperature at inlet is equal to feed temperature of 973K and at outlet the temperature decreases to approx 300K as the reaction is endothermic

Figure 08-23: Contours of total temperature distribution

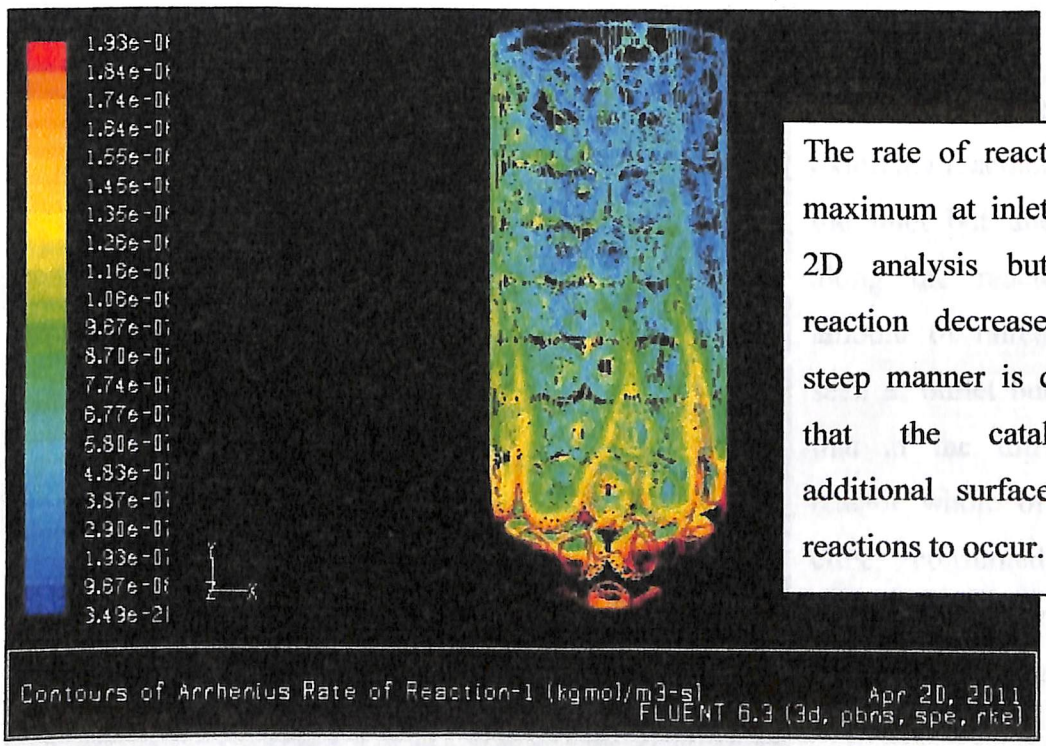

The rate of reaction as seen is maximum at inlet similar to the 2D analysis but the rate of reaction decreases in a much steep manner is due to the fact that the catalysts provide additional surface area for the reactions to occur.

Figure 08-24: Contours of rate of reaction in the flow domain.

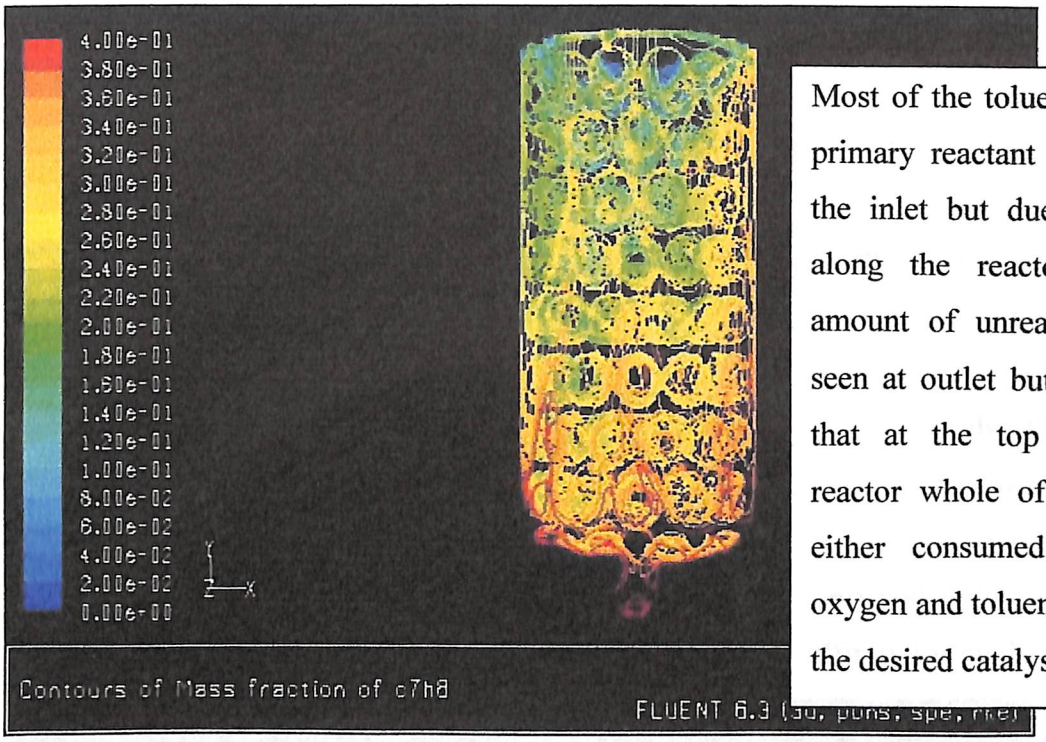

Most of the toluene which is the primary reactant is consumed at the inlet but due to channeling along the reactor walls some amount of unreacted toluene is seen at outlet but it is also seen that at the top centre of the reactor whole of toluene fed is either consumed or channeled oxygen and toluene does not meet the desired catalysts. .

Figure 08-25: Contours of mass fraction of toluene.

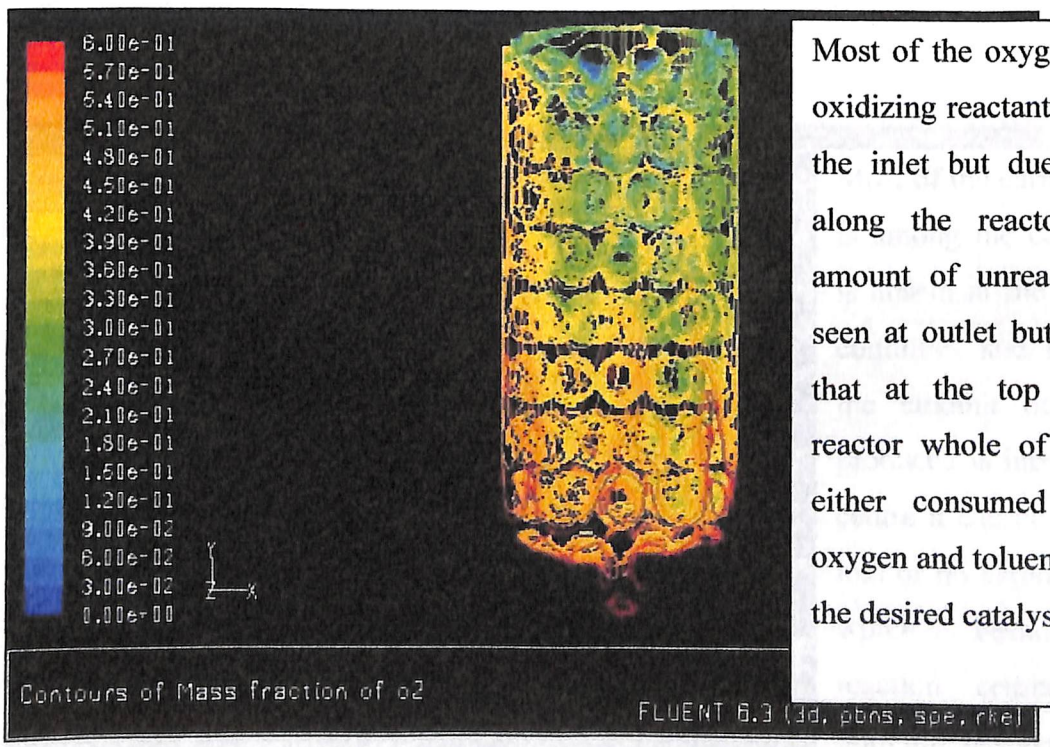

Most of the oxygen which is the oxidizing reactant is consumed at the inlet but due to channeling along the reactor walls some amount of unreacted oxygen is seen at outlet but it is also seen that at the top centre of the reactor whole of oxygen fed is either consumed or channeled oxygen and toluene does not meet the desired catalysts.

Figure 08-26: Contours of mass fraction of oxygen.

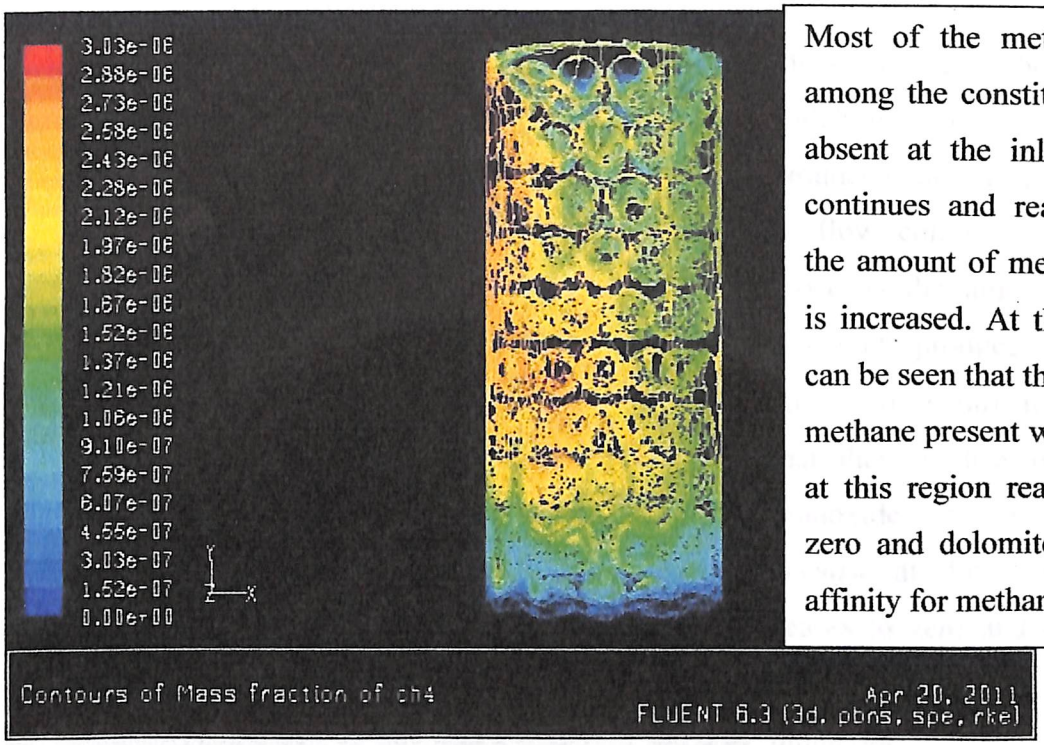

Most of the methane which is among the constituent product is absent at the inlet but as flow continues and reaction proceeds the amount of methane produced is increased. At the top centre it can be seen that there is less or no methane present which is because at this region reaction ceases to zero and dolomite has very less affinity for methane.

Figure 08-27: Contours of mass fraction of methane.

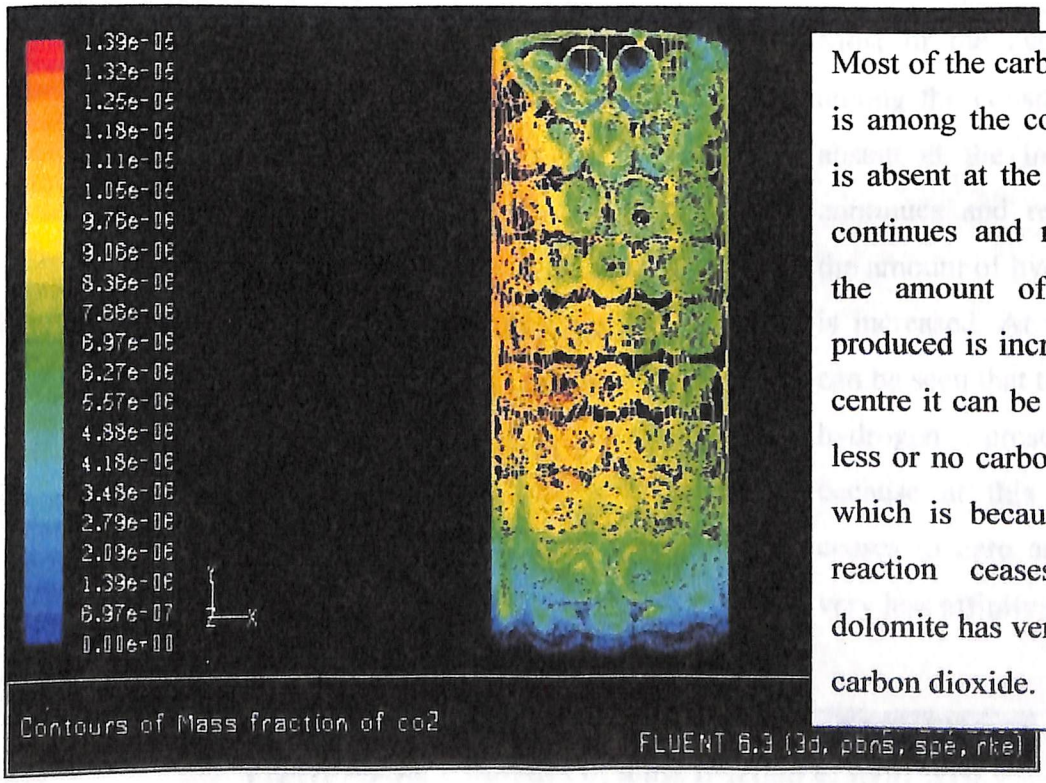

Most of the carbon dioxide which is among the constituent product is absent at the inlet but as flow continues and reaction proceeds the amount of carbon dioxide produced is increased. At the top centre it can be seen that there is less or no carbon dioxide present which is because at this region reaction ceases to zero and dolomite has very less affinity for carbon dioxide.

Figure 08-28: Contours of mass fraction of carbon dioxide.

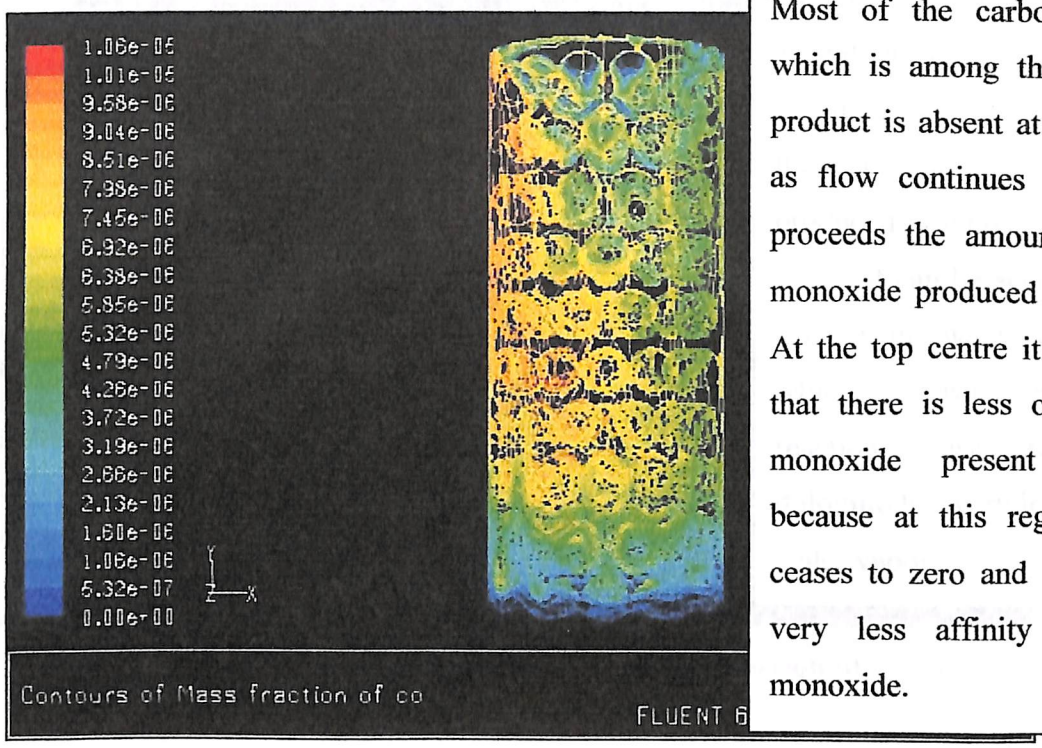

Most of the carbon monoxide which is among the constituent product is absent at the inlet but as flow continues and reaction proceeds the amount of carbon monoxide produced is increased. At the top centre it can be seen that there is less or no carbon monoxide present which is because at this region reaction ceases to zero and dolomite has very less affinity for carbon monoxide.

Figure 08-29: Contours of mass fraction of carbon monoxide.

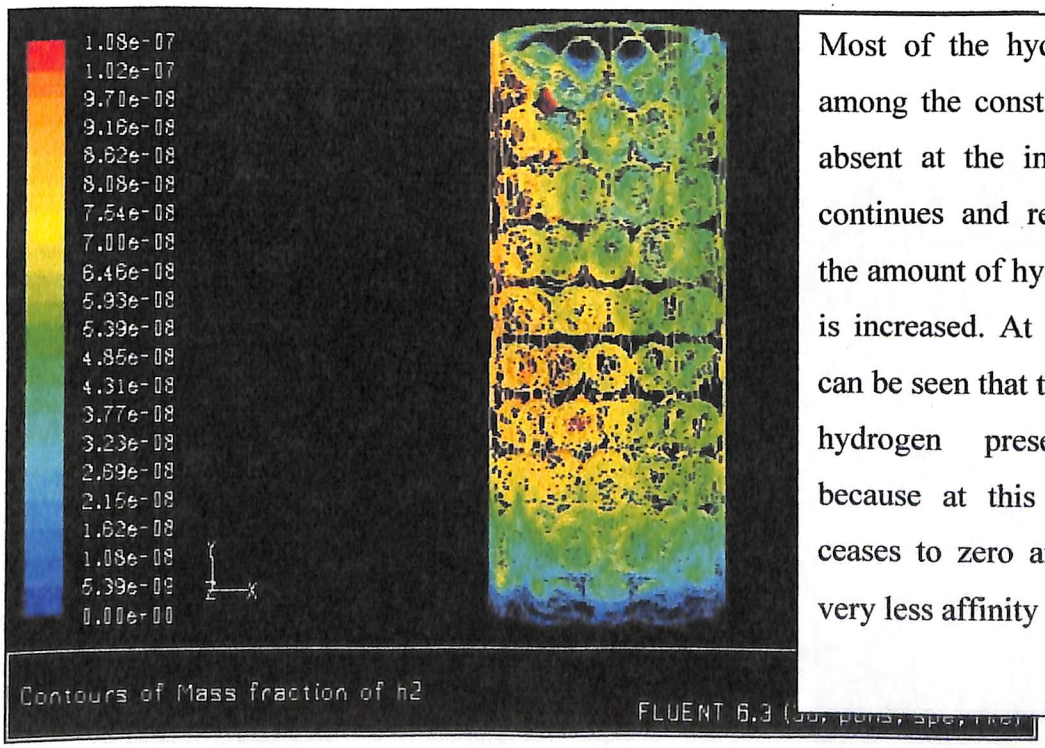

Most of the hydrogen which is among the constituent product is absent at the inlet but as flow continues and reaction proceeds the amount of hydrogen produced is increased. At the top centre it can be seen that there is less or no hydrogen present which is because at this region reaction ceases to zero and dolomite has very less affinity for hydrogen.

Figure 08-30: Contours of mass fraction of hydrogen.

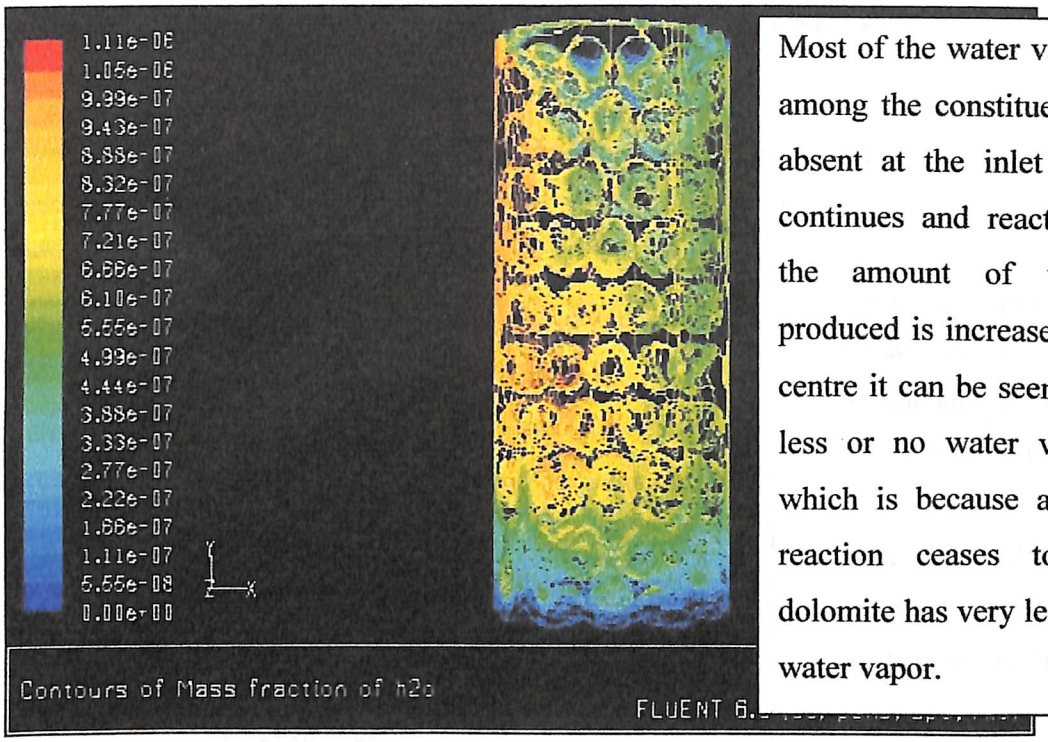

Most of the water vapor which is among the constituent product is absent at the inlet but as flow continues and reaction proceeds the amount of water vapor produced is increased. At the top centre it can be seen that there is less or no water vapor present which is because at this region reaction ceases to zero and dolomite has very less affinity for water vapor.

Figure 08-31: Contours of mass fraction of water.

CHAPTER 09. CONCLUSION

Table 09-1: Conclusion for 2D model

MODEL	REMARKS	RECOMMENDATIONS
2D	1. Linear reaction model. 2. Simple first order reaction considered. 3. Single overall reaction considered. 4. Linear profile of parameters like temperature, pressure and mass fractions observed. 5. Parameters used are all literature based and some on assumptions. 6. Single homogeneous phase considered for solid and gas.	1. Should incorporate other parallel or any side reactions. 2. Should analyze it for time unsteady model to get accurate results. 3. Variations in diameter and length of the reactor be done to analyze any influencing effects

Table 09-2: Conclusion for 3D model

MODEL	REMARKS	RECOMMENDATIONS
3D	1. Heterogeneous phase model considered. 2. Structured arrangement of packing considered. 3. Channeling effect observed. 4. Time steady model with reaction model same as 2D. 5. Non-linear variation in parameters observed but it is fair enough to reach a conclusion 6. Active reaction zone almost limited to the couple of inches from inlet. 7. arried out until trends were established.	1. Study is to be done for arrangement of catalysts inside the cylinder. Efforts are taken to reduce channeling to nil. 2. Should incorporate other parallel or any side reactions. 3. Should analyze it for time unsteady model to get accurate results. 4. If 3D study based on homogeneous 2D model than changes be made in mass-flow rate and feed concentration.

For the system stated above changes in trends will be observed, if:

1. **Change in flow rate:** Increasing the mass flow rate will increase the channeling effects but it will also shift the reaction zone, which is concentrated more near the inlet towards the centre of the reactor. Moreover, we may also observe increase concentration of reactants in outlet. In addition, since dolomite has high attrition rate, so that higher flow rates will increase the rate of attrition of the catalysts particles and in turn cause product contamination. Whereas, decreasing the mass flow rate would cause faster reaction and would raise questions regarding the length and diameter of the reactor. Hence, for the particular model in this study, it is recommended that the flow rates are kept the same.
2. **Change in inlet mass fraction:** In the above study, O_2 concentration in feed is 0.3 and rest is toluene (C_7H_8). On varying the mass fraction, concentration will reasonably show changes in the product concentration, but there must be at all times sufficient oxygen to for toluene cracking as insufficient oxygen will inversely affect the product concentration, affect catalysts loading and reduce the overall affectivity and efficiency of the reactor.
3. **Change in feed temperature:** The feed temperature in this study is around 700^0C (973.15K), Rath et al, 2001. The feed temperature has immense control on the rate of reaction. It is this feed temperature that controls product concentration, rate of cracking reaction and catalysts selectivity and reactivity. As, the catalysts used is dolomite which also has high attrition rate, so feed temperature is an important control element in this study. Literature shows feed temperature as high as 900^0C; but for categories of tar with higher complex nature. In thermal cracking, literature reports temperature as high as 1500^0C.

Although, there are many more factors which control and affect the packed bed reactor but those stated above are the most important of them.

The work stated here is nascent in nature and was primarily literature based. It was carried out with the purpose of opening the gateway to analyze complex chemical phenomena using CFD. Hope that work is carried forward and for better results experimental study is highly recommended. I hope that my work would pioneer the way for further studies in this particular field.

CHAPTER 10. BIBLIOGRAPHY

1. Anderson J. D (1995); *Computational Fluid Dynamics: The Basics and Applications*; Mc-Graw Hill Publications.
2. *Fluent 6.3 User Guide*; chapter 7,8,14 September 2006.
3. *Gambit User Guide*; March 2005.
4. Dr. U Guven, Goswami S, Kumar P. K, *Gambit & Fluent Tutorials,* February 2011
5. Binlin Dou, Jinsheng Gao, Xingzhong Sha, Seung Wook Baek (December 2003), *Catalytic cracking of tar component from high-temperature fuel gas,* Applied Thermal Engineering, Volume 23, Issue 17, Pages 2229-2239.
6. A. Donnot, P. Magne, X. Deglise (December 1991), *Kinetic parameters of the cracking reaction of tar from wood pyrolysis; comparison of dolomite with industrial catalysts,*

   Journal of Analytical and Applied Pyrolysis, Volume 22, Issues 1-2, Pages 47-59.
7. Johannes Rath, Gernot Staudinger (August 2001), *Cracking reactions of tar from pyrolysis of spruce wood*, Fuel, Volume 80, Issue 10, , Pages 1379-1389.
8. Jaime M. Faúndez, Ximena A. García, Alfredo L. Gordon, *A kinetic approach to catalytic pyrolysis of tars* , Fuel Processing Technology, Volume 69, Issue 3, March 2001, Pages 239-256.
9. Morf, P., Hasler, P., and Nussbaumer, T. (2002); *Mechanisms and kinetics of homogeneous secondary reactions of tar from continuous pyrolysis of wood chips.* Fuel,

   81 (7): 843–853.
10. Sjostrom, K., Taralas, G., and Liinanki, L. Sala, (2003); *Dolomite-catalysed conversion of tar from biomass pyrolysis*, In *Research in Thermochemical Biomass Conversion*; Bridgwater, A.V. and Kuester, J.L. (eds.); Elsevier Applied Science: London, 1993, 974–986.
11. Gil, J., Caballero, M.A., Martin, J.A., Aznar, M.-P., and Corella, J. (1999); *Biomass gasification with air in a fluidized bed: effect of the in-bed use of dolomite under different operation conditions*. Ind. Eng. Chem. Res., 38 (11): 4226–4235.
12. Devi, L., Ptasinski, K.J., and Janssen, F.J.J.G. (2003); *A review of the primary measures for tar elimination in biomass gasification processes*. Biomass Bioenerg., 24 (2): 125–140.

13. Coll, R., Salvado ′, J., Farriol, X., and Montane ′, D. (2001); *Steam reforming model compounds of biomass gasification tars: Conversion at different operating conditions and tendency towards coke formation.* Fuel Processing Technology, 74 (1): 19–31.
14. Dou, B., Zhang, M., Gao, J., Shen, W., and Sha, X. (2002); *High-temperature removal of NH3, organic sulfur, HCl, and tar component from coal-derived gas.* Ind. Eng. Chem. Res., 41 (17): 4195–4200.
15. Zhang, R., Brown, R.C., Suby, A., and Cummer, K. (2004) *Catalytic destruction of tar in biomass derived producer gas.* Energy Convers.Mgmt., 45 (7–8): 995–1014.
16. Corella, J., Toledo, J.M., andMolina, G. (2006); *Calculation of the conditions to get less than 2 g tar/Nm3 in a fluidized bed biomass gasifier.* Fuel Processing Technology, 87: 841–846.
17. Nikola Sundac. (2007); *Catalytic cracking of tar from biomass gasification.* Department of Chemical Engineering, Lund University, Sweden.
18. Taralas, G., Kontominas, M.G.,Chen, G.; *Olive-oil industry: mathematical modelling of tar cracking in pyrolysis of by-products for bioenergy*; Laboratory of Food Chemistry and Technology, Department of Chemistry, University of Ioannina, Ioannina, Greece. Department of Chemical Engineering and Technology, Royal Institute of Technology, Stockholm, Sweden.
19. Simell, P.A., Hirvensalo, E.K., Smolander, V.T., and Krause, A.O.I. (1999); *Steam reforming of gasification gas tar over dolomite with benzene as a model compound.* Ind. Eng. Chem. Res., 38: 1250–1257.
20. Marco Baratieri, Elisa Pieratti, Thomas Nordgreen, Maurizio Grigiante (2010); *Biomass gasification with dolomite as catalyst in a small fluidized bed experimental and modeling analysis.* Waste Biomass Valor (2010) 1:283–291.
21. Ragnar Warnecke (2000*); Gasification of biomass: comparison of fixed bed and fluidized bed gasifier.* Biomass and Bioenergy 18:489-497.
22. Ajay Kumar, David D. Jones and Milford A. Hanna (2009); *Thermochemical biomass gasification: a review of the current status of the technology.* Energies 2:556-581.
23. Zhang Xiaodong (2003); *The mechanism of tar cracking by catalyst and the gasification of biomass.* The dissertation of Zhejiang University (China).

APPENDICES

PHYSICAL AND THERMODYNAMIC PROPERTIES

Methane (CH_4) Gas Properties

1. **Molecular Weight**

   Molecular weight: 16.043 g/mol

2. **Solid phase**

   Melting point: -182.5 °C

   Latent heat of fusion (1,013 bar, at triple point): 58.68 kJ/kg

3. **Liquid phase**

   Liquid density (1.013 bar at boiling point): 422.62 kg/m^3

   Liquid/gas equivalent (1.013 bar and 15 °C (59 °F)): 630 vol/vol

   Boiling point (1.013 bar) : -161.6 °C

   Latent heat of vaporization (1.013 bar at boiling point): 510 kJ/kg

4. **Critical point**

   Critical temperature: -82.7 °C

   Critical pressure: 45.96 bar

5. **Gaseous phase**

   Gas density (1.013 bar at boiling point): 1.819 kg/m^3

   Gas density (1.013 bar and 15 °C (59 °F)): 0.68 kg/m^3

   Compressibility Factor (Z) (1.013 bar and 15 °C (59 °F)): 0.998

   Specific gravity (air = 1) (1.013 bar and 21 °C (70 °F)): 0.55

   Specific volume (1.013 bar and 21 °C (70 °F)): 1.48 m^3/kg

   Heat capacity at constant pressure (Cp) (1 bar and 25 °C (77 °F)): 0.035 kJ/(mol.K)

   Heat capacity at constant volume (Cv) (1 bar and 25 °C (77 °F)): 0.027 kJ/(mol.K)

   Ratio of specific heats (Gamma:Cp/Cv) (1 bar and 25 °C (77 °F)) : 1.305454

   Viscosity (1.013 bar and 0 °C (32 °F)): 0.0001027 Poise

   Thermal conductivity (1.013 bar and 0 °C (32 °F)): 32.81 mW/(m.K)

6. **Miscellaneous**

   Solubility in water (1.013 bar and 2 °C (35.6 °F)): 0.054 vol/vol

   Autoignition temperature: 595 °C

Toluene (C_7H_8) Gas Properties:

Property		Value
Mol wt		92.14
Freezing pt, ^0C		-94.965
Boiling pt, ^0C		110.629
Density , g/cm^3		
At 25^0C		0.8623
At 20^0C		0.8667
Critical properties		
Temperature, ^0C		318.64
Pressure, Mpa (atm)		4.109(40.55)
Volume, L/mol		0.316
Heat of combustion, at 25^0C constant		3910.3(934.5)
At bp		37.99(9.080)
Heat capacity, J/(g.K)(cal/g.K))		33.18(7.931)
Ideal gas		
Liquid at 101.3kPa(1atm)		1.125(0.2688)
Surface tension at 25^0C, mN/m		1.970(0.4709)
(=dyn/cm)		27.92
	Gas	Liquid
heat of formation, ΔH^0_f, kJ/mol	50.00 (11.950)	12.00(2.867)
(kcal/mol)		
entropy, S0, kJ/K (kcal/K)	319.7 (76.42)	219.6(52.48)
free energy of formation, $\Delta H^0_{f,kJ/K}$	93.00 (22.228)	114.1(27.282)
(kcal/K)		